CHALMERS

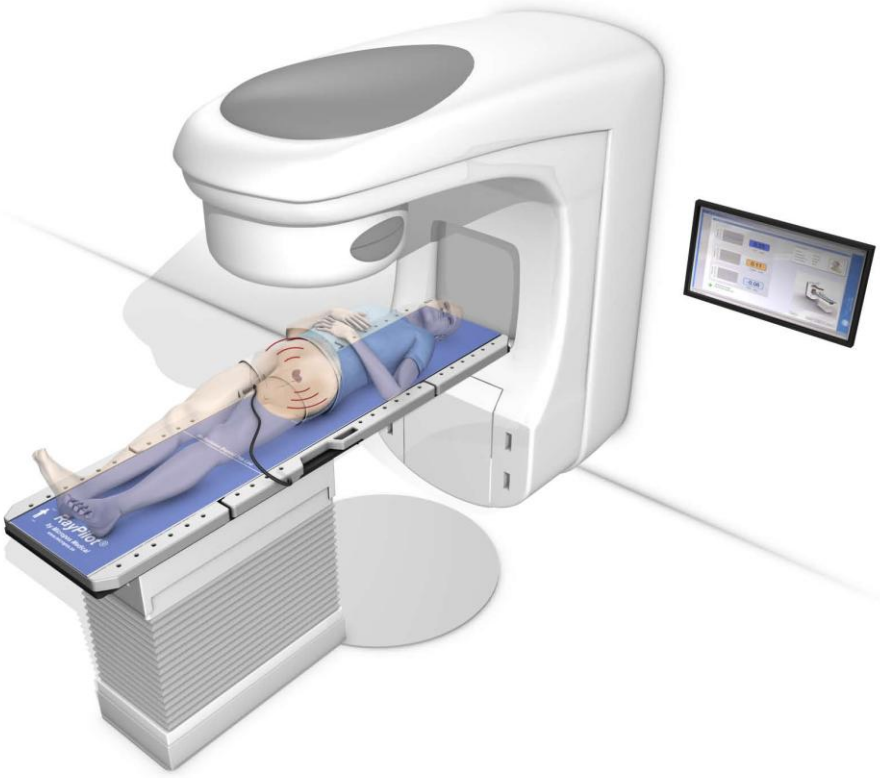

Design of 3D Magnetic Sensor Array for Medical Applications

Master of Science Thesis in Electrical Engineering

ANDERS TORSTENSSON

Department of Signals and Systems
Division of Biomedical Engineering
CHALMERS UNIVERSITY OF TECHNOLOGY
Göteborg, Sweden, 2010
Report No. EX075/2010

Design of 3D Magnetic Sensor Array for Medical Applications
Anders Torstensson

Technical report no EX075/2010
Department of Signals and Systems
Division of Biomedical Engineering
Chalmers University of Technology
SE-412 96 Göteborg
Sweden
Telephone +46 (0)31-7721000

Cover: Model of Micropos Raypilot© system, picturing patient with implant during radiology treatment.

TeknologTryck
Göteborg, Sweden 2010

Design of 3D Magnetic Sensor Array for Medical Applications
ANDERS TORSTENSSON
Department of Signals and Systems
Division of Biomedical Engineering
Chalmers University of Technology

Abstract

When treating tumours with radiotherapy an exact positioning of the organ in question is important in order to minimize damage to adjoining tissue. This thesis was performed at Micropos Medical, a med-tech company situated in Göteborg that has developed an electromagnetic positioning system for real-time positioning inside the human body.

The goal of this project was to test and evaluate an industrially manufactured 3D-antenna. Studies have been made to determine if the 3D-antenna can be used to replace the hand wired antenna used today in the system's antenna array and further to evaluate if the 3D-antenna can be used to increase the measurement volume. Different geometries of the 3D-antennas have been tested to collect data and determine precision of the system. The tests show that the primary coil of the 3D-antenna can be used with a mean error radius of 0.63 mm and a standard deviation of 0.47 mm. For 2000 evaluated points 98% of the tested points lie within a 2 mm error margin which is acceptable according to the requirements set by Micropos Medical.

The 3D-antennas secondary coils can be used to acquire position, however further testing and development of the algorithm will be needed before it might be possible to use these coils to increase the measurement volume.

Table of Contents

1. Introduction

The ability to track moving objects is developing rapidly with modern techniques. In medical applications the advantages of being able to track different objects of interest can be substantial.

Micropos Medical, a med-tech company located in Gothenburg is developing future products for precision radiology. The basic concept of the product is to track the tumour inside the body, making it possible to concentrate the radiation and minimize the damage of adjoining tissue. This is accomplished by placing an implant in the tumourous organ. The implant transmits signals which are received by sensors located outside the body. The transmitted information is used to determine the exact position of the implant and the organ in real-time.

1.1 Background

The positioning system developed by Micropos Medical is originally designed to be used for prostate cancer as it is one of the most common forms of cancer. In the future the system will be used for other forms of cancer as well. About 10000 cases of prostate cancer are discovered in Sweden every year. This form of cancer is very unusual in men under 40 years of age and more than half of all cases are found in patients over 70 years.

The prostate is a gland located directly beneath the bladder and in front of the rectum, see figure 1. When treating prostate cancer different treatments can be of interest. If the cancer is detected in its early stages there are three common methods of treatment, namely radiotherapy, operation and watchful waiting. Prostate cancer often develops slowly which means many of the old patients die for other reasons before the cancer has to be treated and many patients declines treatment in order not to be subjected to negative side effects. For patients choosing treatment the chance of being cured by radiotherapy or operation is considered equal. Often the choice is made depending on what the risks of side effects are. [4]

The movement of the organs makes it necessary to add a margin, often of 2 centimeters around the prostate gland, when treating the tumour with radiation. [13]

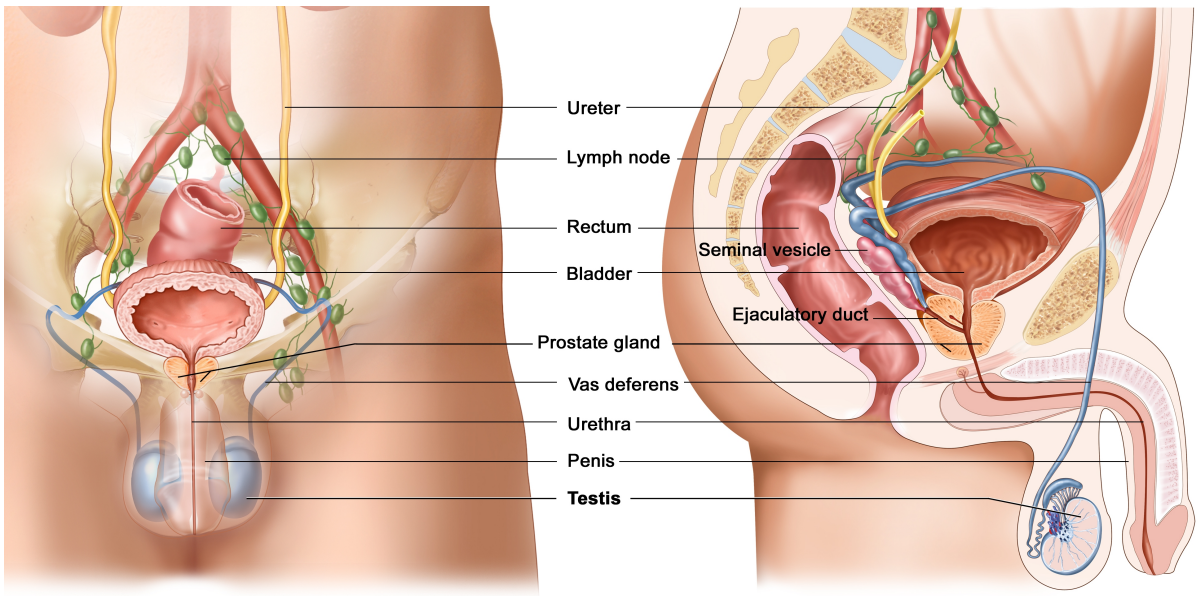

Figure 1: The male reproductive system [16]

Common side effects from radiotherapy are diarrhea, rectal bleeding, urinary incontinence and impotence. Although symptoms tend to improve somewhat over time the side effects

discourages many from subjecting themselves to treatment. With a positioning system the margin can be made smaller, hence diminishing the side effects. A smaller radiation volume means the intensity can be increased which makes it possible to diminish the treatment period, benefiting both patient and clinic. [4]

1.2 Micropos system

1.2.1 Overview

The basic principle of the Micropos system involves a transmitter inserted within the body and 16 receiving sensors placed in the treatment table. By testing and collecting data from different positions the Micropos software creates a model which can be used determine the position of the transmitting implant in real-time.

1.2.2 Antennas / Sensors

The system designed by Micropos Medical uses search coil magnetometers since this kind of sensors are well documented and exists in many different applications. In the current system the signal is transmitted from a small coil and received by 16 hand wired coils placed in rows with 4 coils on each row, see figure 14.

1.3 Aim of this thesis

This project aimed to define the geometry for a 3D magnetic sensor array for medical applications. Standard commercially available 3D magnetic sensors were used. The 3D sensors were tested and compared to the original sensors to determine if they could enhance the performance of the system.

The main purpose of this project was to test if 3D-antennas can replace and enhance the performance of the positioning system developed at Micropos Medical. Tests were designed to answer the following main questions:

- How do the 3D sensors compare to the hand wired sensors regarding the sensors' ability to receive signals in a distance test?
- How is the 3D sensors affected by mutual coupling from closely placed antennas?
- How good is the sensitivity of the 3D antenna compared to the hand wired antenna?
- How good precision can be achieved using the 3D sensors?
- How should the sensors be placed to achieve maximum precision?
- Can the hand wired antennas be replaced by standard component sensors?
- Can coil 1 and 2 of the 3D sensors be used to calculate position?

1.4 Overview of the report

To make the experiment and results easier to follow the disposition was altered from the standard. The content of the different chapters is as follows:

1. Introduction. Provides background and basic operations of the system as well as the main aim of this study.

2. Theory. Presents a brief background theory concerning electromagnetic fields and sensor operation. For more electromagnetic theory, see [15].

3. Sensor tests. Presents setup, results and discussion concerning the sensor tests.

4. System tests. Presents setup, results and discussion concerning the system tests.

5. Conclusions. Presents conclusions and an outlook for future studies.

Appendix A. MQ/Error radius calculation.

Appendix B. Error distribution plots.

Appendix C. MSAT plots.

2. Theory

Since the system tested in this project is built of transmitters and receivers an introduction to basic concepts in wireless engineering is needed to grasp the principles of the system. On certain occasions the system has been described as a GPS within the body which is a analogy not entirely accurate although it has some points. While the two systems function in different ways and in different media both systems share the goal of delivering accurate real-time positioning.

2.1 Maxwells equations

Maxwell's equations is a set of equations that is fundamental when studying the behavior of electric and magnetic fields. The four equations describe different effects and are presented below in differential form:

$$\nabla \cdot \vec{D} = \rho_f, \qquad (1)$$

$$\nabla \cdot \vec{B} = 0, \qquad (2)$$

$$\nabla \times \vec{E} = -\frac{\partial \vec{B}}{\partial t}, \qquad (3)$$

$$\nabla \times \vec{H} = J_f + \frac{\partial \vec{D}}{\partial t}. \qquad (4)$$

$\vec{E} = electric\ field$	$\vec{H} = magnetizing\ field$
$\vec{D} = electric\ displacement\ field$	$J_f = free\ current\ density$
$\vec{B} = magnetic\ field$	$\rho_f = free\ charge\ density$

Equation (1) is also known as Gauss' law and shows how an electric field is generated by electric charges. This equation is followed by Gauss' law for magnetism (equation (2)) which states that no magnetic charges exists. Equation (3) is Faraday's law of induction and describes how a varying magnetic field can induce an electric field. The last of Maxwell's equation, equation (4) is called Ampere's law with Maxwell's correction and describes how a magnetic field can be created either by electrical currents or by changing electric fields. [15]

Interesting properties when studying wave propagation through the human body is e.g. permittivity, conductivity and loss factor. The permittivity of a material describes the ability of the material to polarize in response to an electric field and therefore relates to the ability of the material to transmit (permit) an electric field. Another important parameter is conductivity which describes the ability of the material to conduct current. The loss tangent is a quantity that describes the power losses of a propagating wave through a conducting material.

Compared to air or vacuum a lossy media has a higher relative permittivity and a conductivity larger than zero. For air the relative permittivity $\varepsilon_r = 1$ ($\varepsilon = \varepsilon_0\varepsilon_r = \varepsilon_0 = 8.854*10^{-12}$ F/m) and the conductivity is close to zero.

2.2 The near and far fields

Maxwell's equations describes the propagation of electromagnetic waves. As the waves behave differently depending on the distance to the source the wave pattern is often divided into two regions: the non-propagating near field and the propagating far field. The far field is characterized by a planar wave front, which means that the electric field $\vec{E}$ and the magnetic field $\vec{H}$ are in phase and the ratio of E and H is close to the characteristic impedance of free space. The wave is free to propagate and in diffraction terms this zone is

called the Fraunhofer region. In the near field the $\vec{E}$ and $\vec{H}$ components are out of phase and the ratio $\vec{E}/\vec{H}$ is not matched to the impedance of free space. This mismatch of impedance results in the wave being reflected back toward its source which means it does not propagate. In terms of diffraction the near field corresponds to the Fresnel zone.

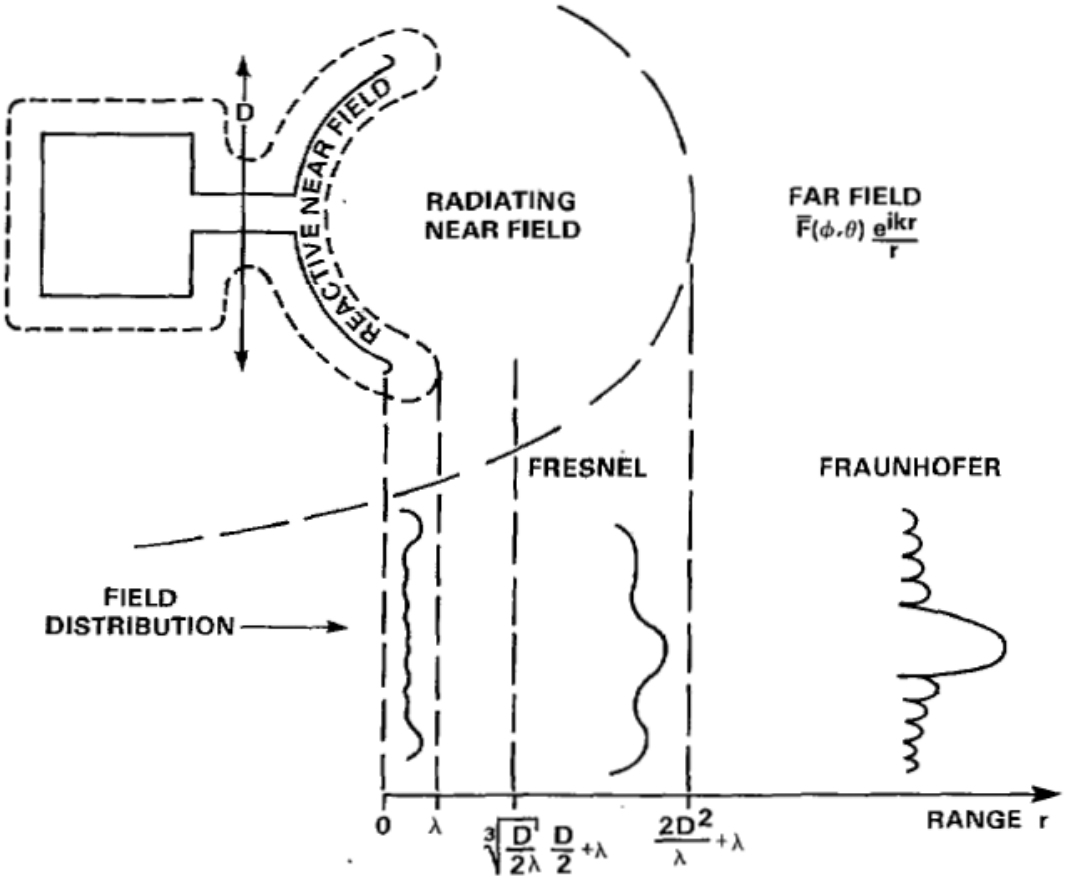

Figure 2: Propagation regions of a transmitting antenna [18]

Figure 2 illustrates a commonly used model that divides the field of an antenna into different regions. The antenna considered here is assumed ordinary in the sense that it is not an extraordinarily highly reactive radiator and the antenna radiates into free space with the single-frequency time dependence of exp(-iωt). The far-field region is described as extending to infinity. [18] In this region the electric and magnetic fields vary approximately as

$$\frac{e^{(ikr)}}{r}. \quad (5)$$

Today the magnetic part of the near field is used by applications in many different fields. Shop security tags and contactless key systems are good examples of common utilizations of the technique. Although the use of the magnetic near field within the body is relatively young, the interest in this field of research is increasing. [17]

2.3 Magnetic fields

To study the techniques used to measure magnetic field strength basic knowledge of magnetic fields is important. The most commonly known source of a magnetic field is probably the bar magnet. Magnetic field, $\vec{H}$, is a vector quantity which means it has both a magnitude and a direction. Figure 3 illustrates a solenoid with its surrounding field lines.

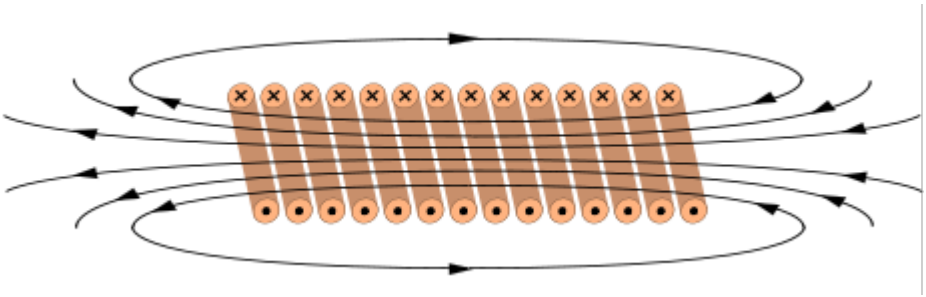

Figure 3: A solenoid with field lines [14]

The strength or intensity of a magnetized object is called its magnetization M and is defined as the magnetic dipole moment per unit volume:

$$\vec{M} = \frac{\vec{m}}{volume}. \quad (6)$$

Analogously with the magnetic field the magnetization is a vector quantity. The magnetization is a material property derived from either internal magnetic sources or induced by a magnetic field. Magnetic properties are described with a third vector quantity $\vec{B}$ called magnetic induction or flux density. In free space magnetic field and magnetic induction are proportional to one another by a constant factor μ_0 .

$$\vec{B} = \mu_0 \vec{H}. \quad (7)$$

Magnetic fields are strongly linked to electrical fields. Örstedt discovered that a current through a wire could make a compass needle rotate and later Faraday found that it was possible to generate electricity by moving a magnet through a loop of wire. This discovery led to the induction or search coil sensor. [2]

Faraday´s law of electromagnetic induction is representated by the equation (3) in chapter 2.1, describing how a changing magnetic field can create an electric field.

2.3.1 Magnetic field-sensors

Today magnetic sensors are used everyday in numerous applications. Since the sensors can be made both durable and reliable they have found use in for example cars, airplanes and factories where high reliability is of importance. [1]

One interesting property concerning magnetic sensors as opposed to other sensors is that they do not directly measure the physical property of interest. While a device measuring flow or temperature for example gives a direct output of the desired parameter the output from a magnetic sensor requires some signal processing before it is translated into a suitable parameter. Although magnetic sensors might be more difficult to use they can offer good measuring capabilities without physical contact. [3]

There is a wide assortment of different sensors today which makes it important to categorize them in varying ways. Sensors can measure either the vector or scalar quantity and different sensors have different properties.

Magnetic sensors are often classified into low-, medium- and high-field sensitivity range to sort the sensors for different applications. See [1] for a more detailed overview of magnetic sensors existing today.

2.3.2 The search-coil magnetometer

The principle behind the search-coil magnetometer is Faraday's law of induction which states that if the magnetic flux through a coiled conductor changes, a voltage proportional to the rate of change of the flux is generated between its leads. The law is described by formula (8), where ϵ is the induced electromotive force and Φ is the magnetic flux. [19]

$$\epsilon = -\frac{d\,\phi}{dt} \quad (8)$$

The flux experienced by the coil will change if the magnetic field changes with time, if the coil is rotated in an uniform field or if the coil is moved through a non-uniform field. To enhance the capacity of the coil a rod of ferromagnetic material is often placed inside the coil. The rod gathers the surrounding magnetic fields and increases the flux density.

There are several factors that affects the search-coil magnetometer's ability to detect a signal; the permeability of the core material, the area of the coil, the number of turns and how the magnetic flux through the coil varies. The ratio between the coil's resistance and its inductance will determine how fast the induced current dissipates when the external magnetic field is removed, which determines the frequency response of the sensor. (See formula (9), (10) and (11) in the following section). The current dissipates faster with reduced resistance or increased inductance. Sometimes the inter-winding capacitance can also limit the frequency response whereas in practice often the voltage readout electronics can limit the frequency response as well as the sensitivity of the sensor.

The search-coil sensor can detect fields as weak as 20 fT and there is no upper limit for their sensitivity. This type of sensors is useful for frequencies between 1 Hz and 1 MHz. The sensor requires 1-10 mW of power which is consumed in the readout electronics. [1]

2.4 Resonant circuits and Q value

Resonant circuits are commonly used to filter out signals of desired frequencies and suppress signals of other frequencies. [10] If the frequency response of the circuit is more narrowly peaked around the chosen frequency the circuit is said to have a higher selectivity which can be described by the quality factor, Q. A circuit with high Q factor is more selective than a circuit with low Q factor. Figure 4 shows the frequency response for a resonant circuit, illustrating that a higher Q makes the bandwidth more narrow as the frequency response plot becomes more sharply peaked. The Q factor can be of interest when comparing the antennas since a high Q makes it very important to center the frequency correctly as a small deviation in frequency may cause big change in output. The resonant frequency ω_0 and Q factor for a parallel circuit are defined as follows:

$$\omega_0 = 2\pi f_0 = \frac{1}{\sqrt{LC}}, \quad (9)$$

$$Q = R\sqrt{\frac{C}{L}}. \quad (10)$$

At $\omega = \omega_0$ the impedance Z = R which means it carries no capacitive or inductive components. For frequencies higher or lower than the resonant frequency the impedance will increase. The quality factor controls how rapidly |Z| increases. [11]

A general definition for the Q value is stated in formula (11).

$$Q = 2\pi \frac{(Energy\ stored)}{(Energy\ dissipated\ per\ cycle)}. \quad (11)$$

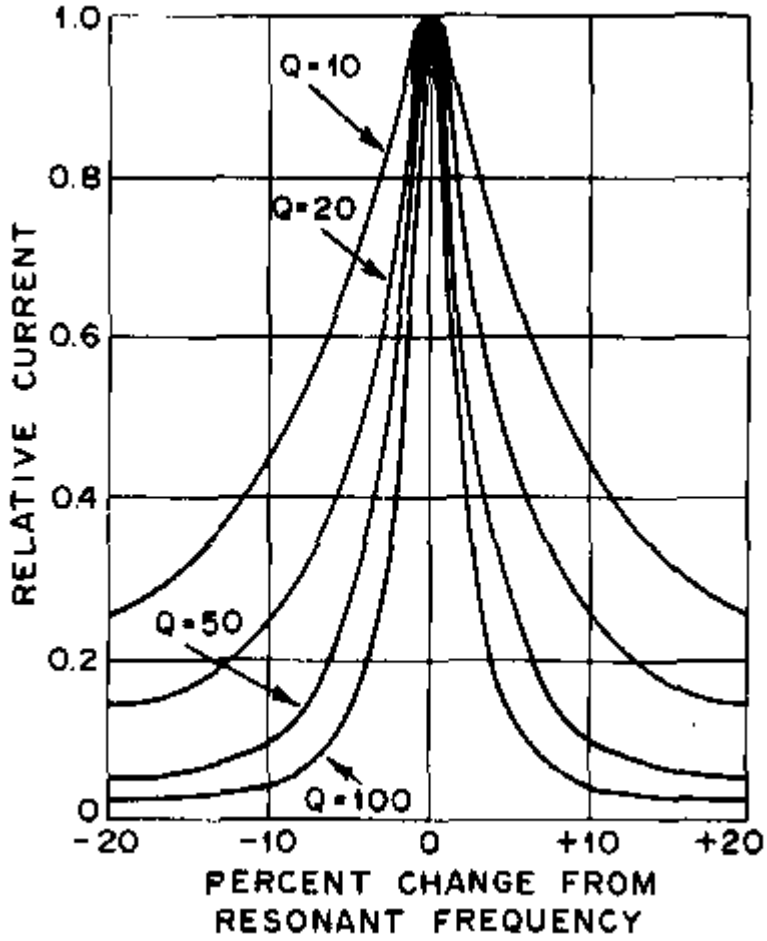

Figure 4: Relative current vs. percent change from resonant frequency. [12]

2.5 Sensitivity

The sensitivity parameter describes how well a transponder coil can receive a transmitted signal. A higher sensitivity means that the receiving coil can receive weaker signals at the design frequency which means that the reading distance is increased. Important to note is that sensitivity only is one of many factors that affects reading distance. The design of the PCB (Printed Circuit Board) and specifically the composition, placement and orientation of the different components also determines what the actual read distance will be.

Different ways to measure the sensitivity give different results and in order to make a fair comparison between the sensors the method of measuring sensitivity must be consistent. The setup used in this project is presented in section 3.4.1. [6]

2.5.1 Helmholtz coils

A common way to measure sensitivity is to use Helmholtz coils. This device is composed of a pair of thin, parallel and identical coils separated by a distance equal to their radius. These coils are mainly used to generate small and highly uniform magnetic fields in the space between the coils. Figure 5 displays the cross-section of a Helmholtz coil with a test object placed in the middle.

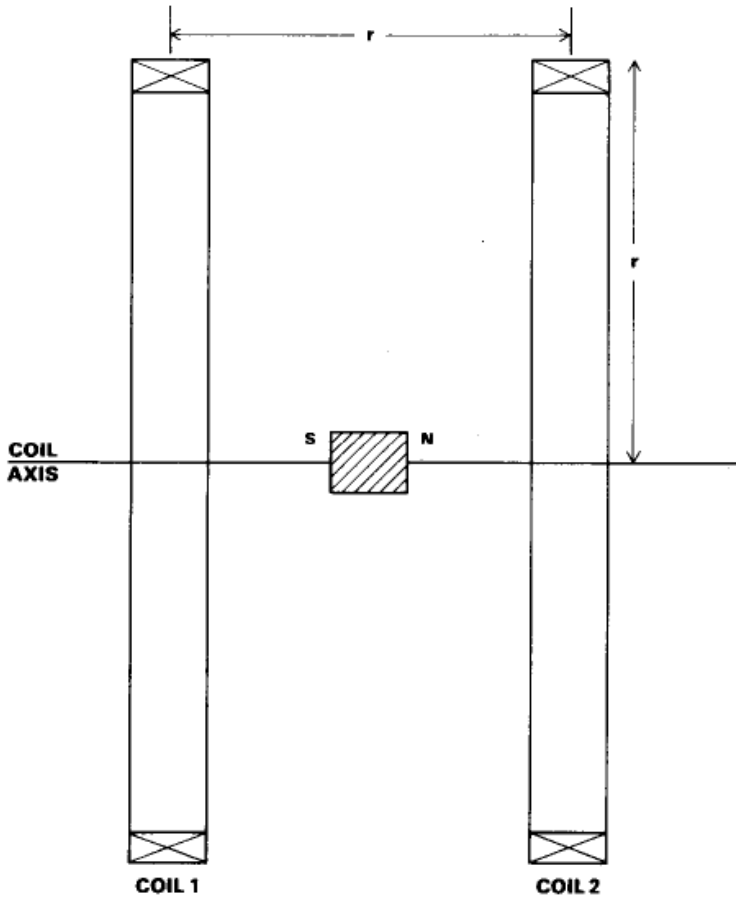

Figure 5: Cross-section of Helmholtz coils [5]

With the aid of the uniform magnetic field created by the Helmholtz coil it is possible to calculate a sensitivity for the device under test.

The sensitivity of a transponder coil is defined by the following equation:

$$Sensitivity = \frac{V_{DUT}}{I * K}, \quad (12)$$

where V_{DUT} is the voltage across the device under test, I is the current through the coils and K is the Helmholtz constant. The Helmholtz constant is different for different coils. If the Helmholtz constant is unknown it can be established using a DUT (Device Under Test) with given sensitivity combined with the following formula (12). [6]

3. Sensor tests

3.1 Background

The antennas used in the Micropos system today consists of 150 turns of hand wired copper wire. Although the hand wired antennas used today deliver reliable positioning the manufacturing process is somewhat tedious. Wiring 150 turns of wire is time-consuming and the process of wiring the exact number of turns demand high accuracy. To make mass-production of the system possible one solution can be to purchase standard antennas from an established manufacturer.

The sensors tested during this project are two different industrially manufactured antennas, the z-antenna and the 3D-antenna, and the hand wired antenna designed by Micropos. Since the hand wired antenna is wired directly on a circuit card a replica of the antenna has been built for certain experiments. The replica is made of 150 turns of 0,15 mm copper wire wound around a 50*35 mm block of insulating material which makes it similar to the original antenna. Figure 6 shows the z-antenna, the 3D-antenna and the replica of the hand wired antenna.

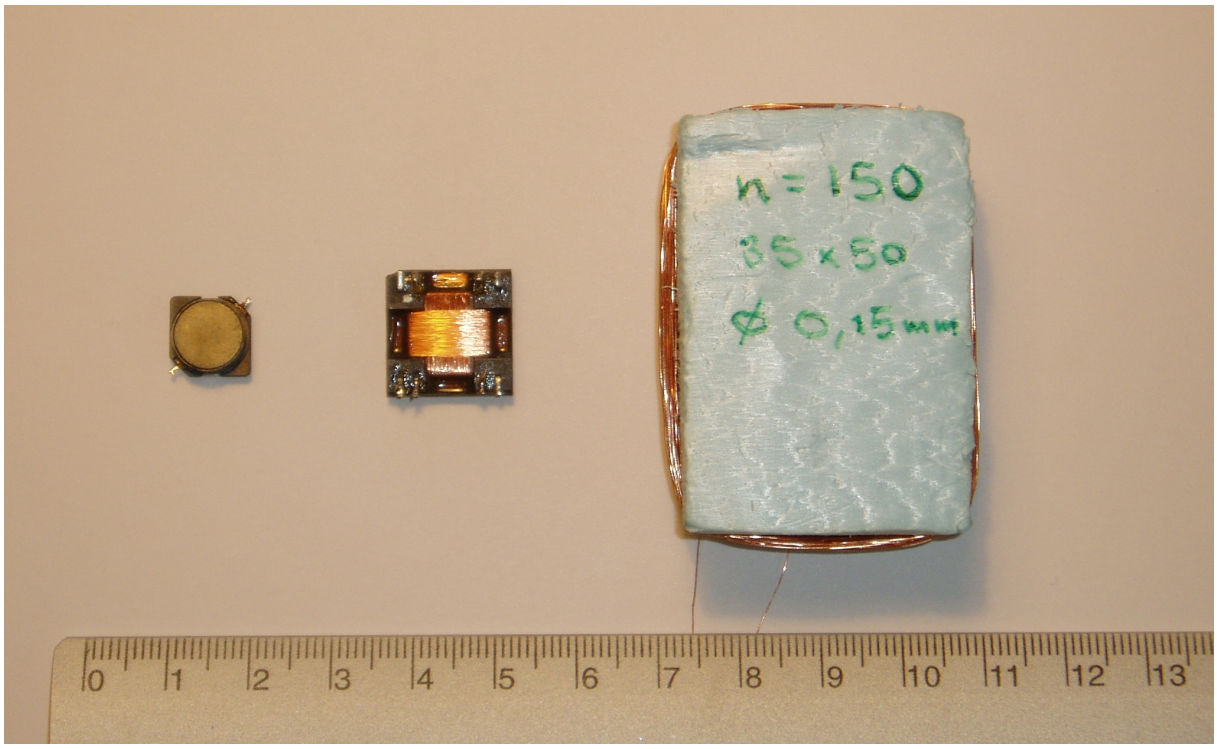

Figure 6: From the left: Premo Z-antenna, Neosid 3D-antenna and the hand wired antenna.

Different data of the antennas has been collected from data sheets from the manufacturers and from measurements conducted during the project. Interesting parameters from the manufacturers regarding the commercially available antennas are presented in table 1 :

	Antenna			
Parameter	Premo Z-antenna	3D-antenna Neosid 3D15a		
		Coil 1	Coil 2	Coil 3
Dimension	10x10x3 mm	4x15mm	4x15mm	15x15mm
L @125kHz	9mH ±5%	4.7mH±5%	4.7mH±5%	4.7mH±5%
Q unloaded	90±10%	≥14	≥14	≥26
DC resistance	57Ω ±10%	≤140Ω	≤140Ω	≤115Ω
Self resonant frequency	≥800 kHz	≥260 kHz	≥240 kHz	≥700 kHz
Sensitivity	43.67mV/A/m	no info.	no info.	no info.

Table 1: Antenna characteristics from the manufacturers' data sheets.

While the Premo Z-antenna is tested mainly as a reference the 3D-antenna was tested in the Micropos system. The 3D-antenna is illustrated in figure 7 with the different coils marked as n1, n2 and n3.

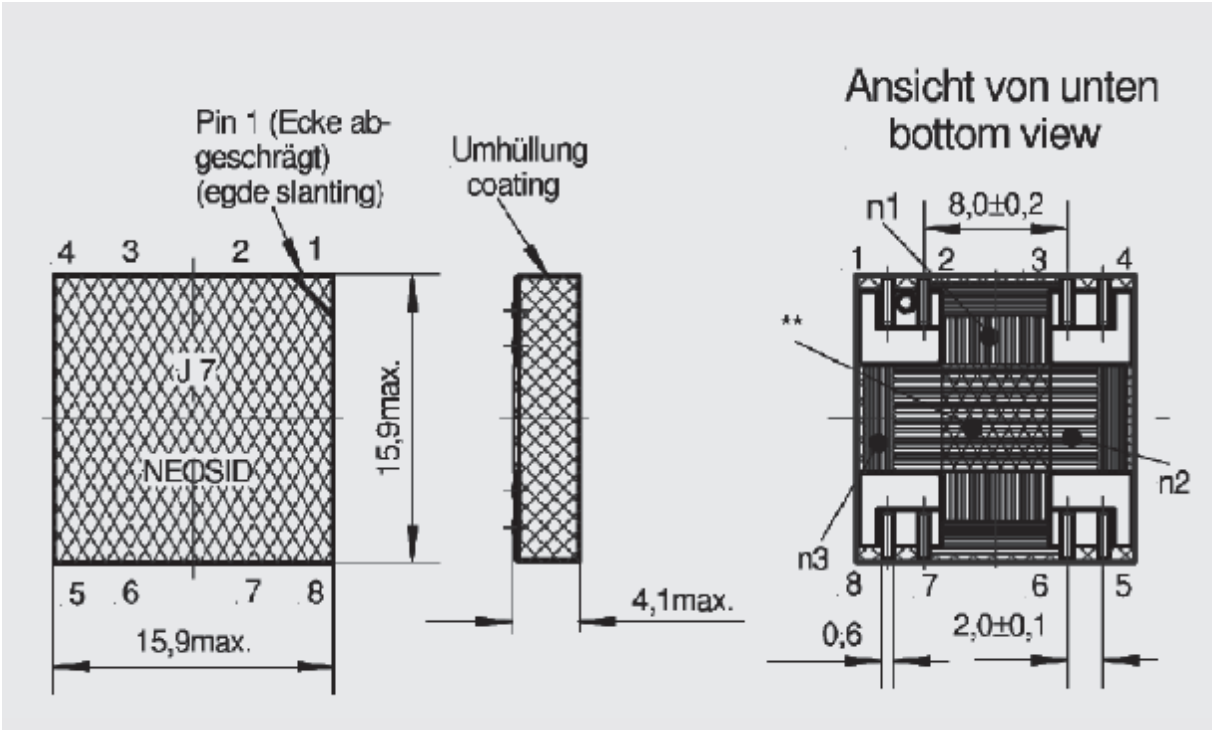

Figure 7: The Neosid 3D-antenna. [8]

3.2 Distance test

3.2.1 Method

To compare the sensors' ability to receive signals a simple test was constructed as shown in figure 8.

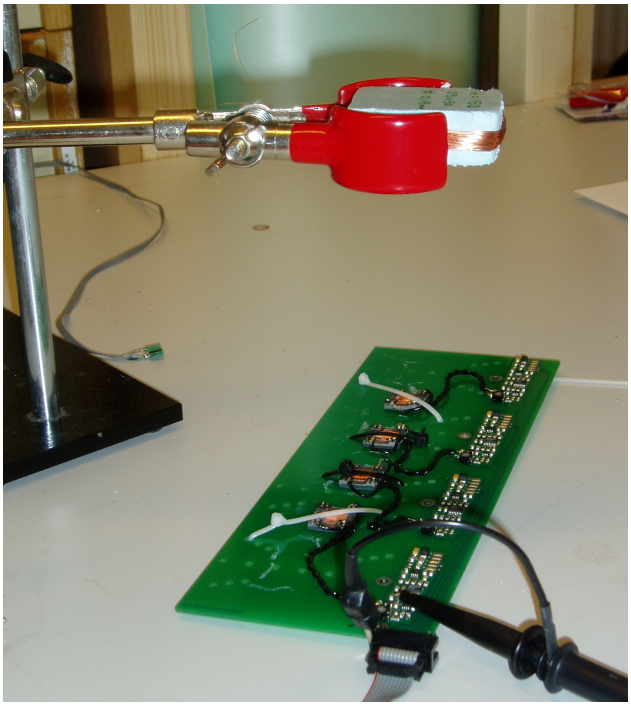

Figure 8: Distance test setup.

A hand wired coil is connected to a signal generator delivering a fixed signal set to the frequency 123 kHz. The transmitted signal is received by the tested antenna which is connected to a circuit board (Micropos RecBoard14a) that filters and amplifies the signal to a chosen level. This experiment was performed by testing the distance required to generate an induced voltage of 1,5 Volt which is used as reference voltage by Micropos. The transmitter consists of 30 turns of 0,40 mm copper wire connected to a signal generator and wired around a 65x45 mm piece of insulating material. The transmitter is connected to Marconi Instruments Signal Generator 2024 that generates a sinusoidal signal with the RF level set to -20dBm.

3.2.2 Results

The results are presented in table 2.

Antenna	Distance
Hand wired	42 cm
Z-antenna	15 cm
3D-antenna Coil 1	23 cm
3D-antenna Coil 2	23 cm
3D-antenna Coil 3	24 cm

Table 2: Distance test results.

In this test the hand wired antenna performs significantly better than the other tested antennas.

3.3 Mutual coupling / Disturbance test

3.3.1 Method

Mutual induction is a term used to describe how coils interact with each other, see [11].

This test was performed by measuring output voltage from an 3D-antenna with fixed position beneath a transmitting antenna with fixed height. The frequency of the transmitting antenna was set to 123 kHz and the distance between the antennas was adjusted to receive an output voltage of 1,5 volt from the receiving antenna. While continuously measuring the output voltage different conditions were changed to determine which aspects affects the 3D-antenna. In the first test an adjacent antenna was moved around the tested antenna, in the second test the circuit board was moved below the tested antenna and in the third test an antenna was placed above the antenna under test. Figure 9 and 10 illustrates two tested placements of the antennas.

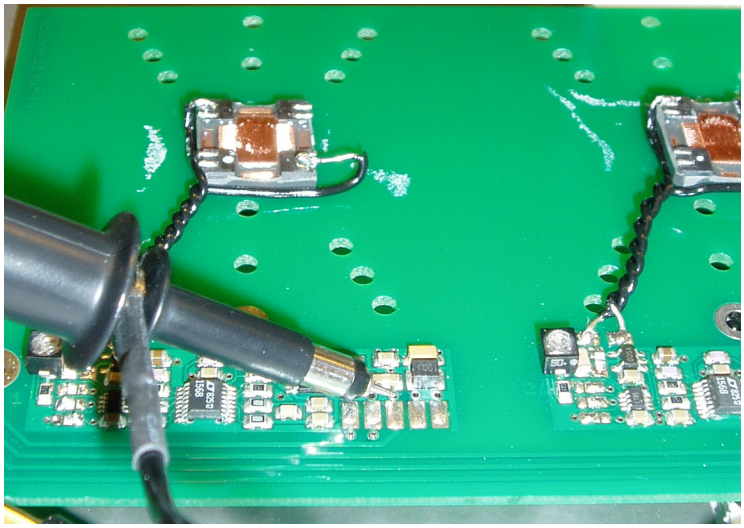

Figure 9: Mutual coupling test: Ordinary antenna position.

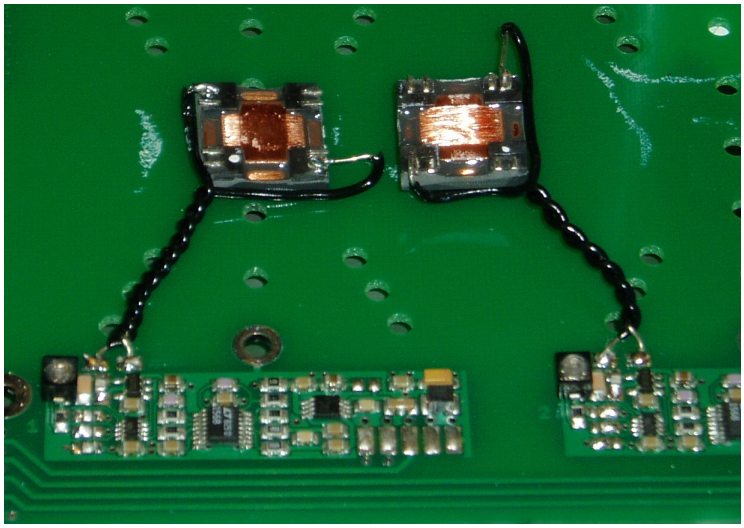

Figure 10: Mutual coupling test: Right antenna moved toward left antenna.

3.3.2 Results

The first test was conducted by moving an adjacent receiving antenna around the device under test (DUT). During this experiment both antennas were orientated flat against the circuit board. In this test the output voltage of the DUT was not changed.

In the second test the DUT was fixed in space while the circuit board was moved under the device. This resulted in a fluctuating output voltage when the electrical components of the card came within a 2-3 cm radius of the DUT.

A third test was conducted by keeping the device under test fixed and placing a receiving 3D-antenna above the DUT. This procedure increased the output voltage, probably due to the ferrite core inside the 3D-antenna. By performing the same test while arranging the disturbing antenna perpendicularly compared to the DUT the output voltage was decreased.

The results of the tests above imply that some caution is advisable when placing the receiving antennas. It is possible to place them close to other receiving antennas but they should not be placed closer than 3 cm to the electronics.

3.4 Sensitivity test

3.4.1 Method

Each antenna is designed with an individual sensitivity which is a quantity that can be measured with the aid of a Helmholtz coil, see chapter 2.5.1. With the setup shown in figure 11 the sensitivity of different sensors has been measured and compared.

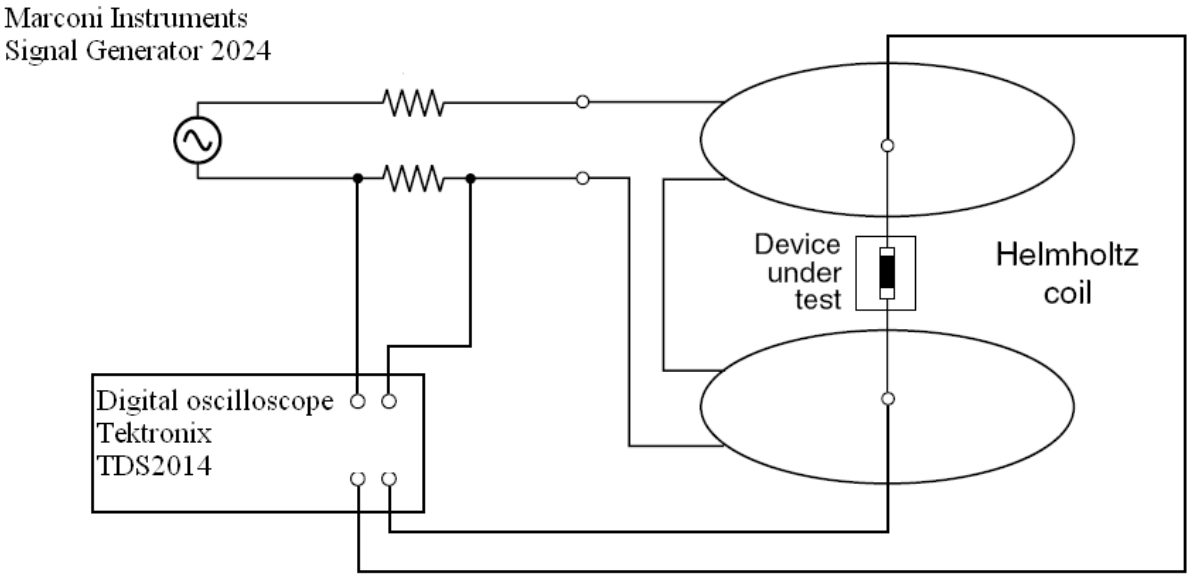

Figure 11: Sensitivity test setup. [6]

Using an antenna with given sensitivity the Helmholtz constant of the coils used was calculated with formula (12). The setup consists of a Marconi Instruments Signal Generator 2024 connected to a set of resistors and the Helmholtz coil being tested. The current is established by measuring the voltage drop over one of the resistances and then calculating the current according to Ohm's law.

The DUT is connected to a digital oscilloscope which makes it possible to measure the induced voltage of the DUT and according to formula (12) the sensitivity can be computed.

3.4.2 Results

As shown in table 3 the hand wired antenna has higher sensitivity than the other tested antennas.

Antenna	Sensitivity (mV/A*m)
Z-antenna	43,67 (from manufacturer)
Hand wired	202
3D-antenna Coil 1	70.3
3D-antenna Coil 2	76.2
3D-antenna Coil 3	68.2

Table 3: Sensitivity test results.

3.5 Discussion

Since the tests implemented in the previous sections was conducted primarily to get a rough comparison of the different sensors no calculation of measurement uncertainties have been

made. While this makes the result inexact it can still be used to get an idea of the different antennas' sensitivity.

Concerning the distance test the hand wired antenna performed substantially better than the two industrially manufactured antennas. This was probably due to to the bigger cross-section of the hand wired antenna.

According to the mutual coupling test the antennas did not disturb each other when attached flat against the circuit board as displayed on figure 9 and 10. This was an expected result as the antennas were receiving and not transmitting during the test. Some unexpected results were found when an antenna was placed over another antenna. These effects are probably explained by the ferrite core placed inside each antenna. Depending on orientation the ferrite core can collect or disperse the magnetic field lines and enable a higher or lower current to be induced. Thus, the detected variations are most likely explained by the ferrite core and not by the different coils inside the antennas.

The tests also showed that the output voltage was disturbed when the antenna under test was placed close to the electrical components of the circuit card. A possible explanation of this result can be that the electrical components generates an magnetic field that disturbs the measurements from the antenna.

For the sensitivity tests a Helmholtz coil with unknown Helmholtz constant was used. Since the constant was calculated using the Premo Z-antenna a first prerequisite for this test is that the sensitivity stated from the manufacturer is correct. Another important thing to note is that when using Helmholtz coils a 100-ppm homogeneity is achieved only within a cylinder that has 10% dimension of the coils [7] which in this experiments means a cylinder with diameter 1,5 cm and the same height. This means that parts of the antennas has been outside the most homogeneous magnetic field of the Helmholtz coil during the test. Based on this only two significant numbers should be taken into consideration when studying table 3.

The given circumstances makes the result of the test somewhat unreliable although it can be used as a rough comparison of the sensors.

4. System tests

4.1 Background

The system used today consists of 16 hand wired antennas placed according to figure 14. In order to test precision and other factors of the system a test setup has been designed prior to these experiments.

The test setup involves an implant cable with a coil of wired copper that transmits at chosen frequency and voltage. To test different positions the implant is attached to a motorized coordinate machine that moves around in five dimensions, x,y,z positions and v_y, v_x angles, and acquires actual position of the implant. The signal from the transmitting antenna will be received by the 16 sensors where a current is induced. When this signal has been processed and amplified to a certain level it is ready to be used by the software that establishes a calculated position of the implant. Then the calculated position of the implant can be compared with the real position and the calculation error and various statistics can be determined.

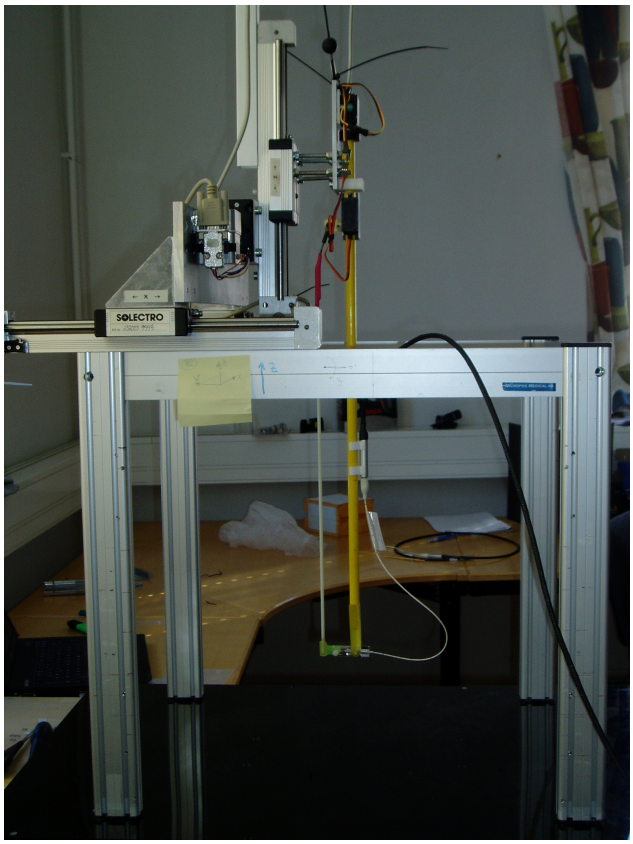

Figure 12: Coordinate machine test setup.

Fig. 12 shows the system in use with the implant cable (the white cable in the picture) attached to the coordinate machine and the antenna cards concealed under the casing. With the assistance of the coordinate machine the implant is moved 100 mm in all directions with the center (x, y, z) being 90, 90, 80 from a chosen center point which is placed in the middle of the two antenna cards closest to the middle. For each point in space the implant can be tested in different angles.

4.2 Aim

These tests were designed to test how the system is affected when changing from the hand wired antenna to the 3D-antenna. Can the 3D-antenna replace the hand wired antenna and how good precision can be achieved? How should the 3D-antennas be placed to provide a reliable positioning?

4.3 Method

To test the system with the 3D-antennas some alterations of the circuit cards were made. To adjust the resonant frequency of the receptive coil the capacitors connected to it were changed to 356 pF. The replacement capacitance was derived from formula 13:

$$\omega_{SRF} = \frac{1}{\sqrt{LC}} \Rightarrow C = \frac{1}{(\omega^2 L)} = \frac{1}{((2\pi f)^2 L)}. \quad (13)$$

Choosing a trim capacitor as one of the resulting capacitors made it possible to adjust the capacitance in order to maximize the output voltage. This was achieved by adjusting the trim capacitor while the antenna is broadcasting. Output voltage was measured with a voltmeter and this procedure was repeated on each antenna to trim and achieve the correct resonant frequency and yield the highest output level for each sensor.

The tests described in this report have been made with the 3D-antenna flat on the circuit card as pictured in figure 13. The sensors were attached to the circuit card by double sided adhesive tape and, after the first run, additional cable ties to prevent the sensors from moving during database collection.

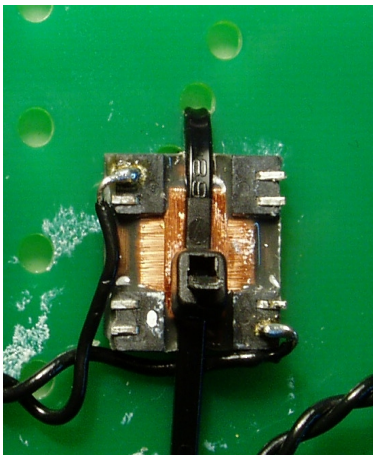

Figure 13: 3D-antenna attached to circuit board.

This placement of the antenna means that the third coil will have the same orientation as the original antenna while coil 1 and 2 will be orientated perpendicularly to each other and the circuit card.

Initial testing began by placing the center of the 3D-antenna on the same place as the former center of the hand wired antennas. A sketch of the placement is shown in figure 14. The Z axis begins close to the table and increases with height.

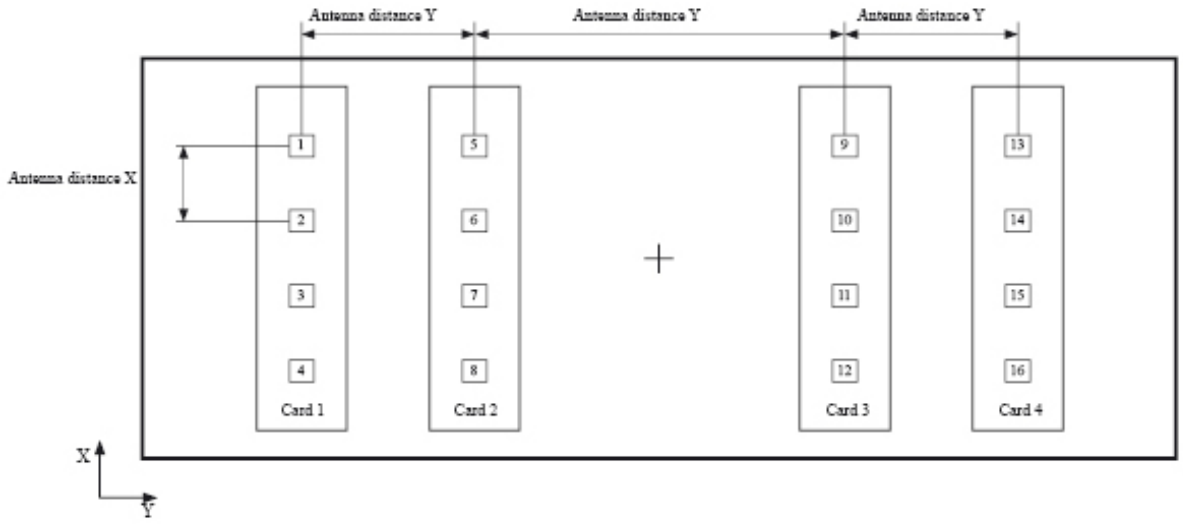

Figure 14: Antenna placement.

During the first test run three of the sensors taped to the board lost their placement which gave significantly big errors. Cable ties were used to attach the sensors to prevent this from happening in subsequent tests. By studying the levels of output voltage and comparing with those for the hand wired antenna, a decision was made to change the amplification of the cards. Only the four most centered antennas (no. 6,7,10,11 in figure 14) were left unaltered since their output voltage was considered sufficient. An overview of the tested geometries is presented in table 4 along with the chosen attenuation for the antennas.

X Antenna distance (mm)	Y Antenna distance (mm)	Comment	Antenna attenuation
60/60/60	100/260/100	Original setup	Card 1,4: 10V/V card 2,3: 5V/V
60/60/60	100/260/100	Original setup	Card 1,4:20V/V | no. 5,8,9,12:10V/V no. 6,7,10,11:5V/V
40/40/40	90/240/90	Moved in Y, closer to center	Unchanged
40/40/40	90/240/90	Same geometry as previous	Unchanged
40/40/40	90/240/90	Same geometry as previous	Unchanged
40/40/40	90/240/90	Same geometry as previous	Unchanged
40/40/40	65/240/65	Antennas on card 1, 4 moved closer to center in Y	Unchanged
40/40/40	65/240/65	Same geometry as previous	Unchanged
Card 2,3:40/40/40 Card 1,4:35/35/35	75/240/75	Antennas on outer cards moved closer in X	Unchanged
40/40/40	90/240/90	Same geometry as DBA003	Unchanged
40/40/40	115/215/90	Antennas on card 3 moved closer to center in Y axis	Unchanged
40/40/40	115/190/115	Antennas on card 2 moved closer to center in Y axis	Unchanged
40/40/40	90/240/90	Antennas 1,4,13,16 tow ard center 15 mm in X, 5 mm in Y	Unchanged
40/40/40	90/240/90	Same geometry as DBA003	Unchanged
40/40/40	90/240/90	Same geometry as DBA003	Unchanged

Table 4: Tested geometries.

In the experiments performed during this project two different test strategies were used. For making fast evaluations a database was generated by using a step size of 33,33 mm/13,33° and testing 4 points in each direction which in combination with 4 angle alternatives for up/down and left/right respectively give 4^5=1024 points. After the data has been collected

from the antennas a model is made by Micropos' software that uses the method of least squares to fit polynomials of chosen order to the measured data and make a model that gives the implant position as a function of antenna data. For small databases third order polynomials are preferred when generating the model. Polynomials of fourth order are used when using a big database which consists of 6 points in every direction, yielding 6^5=7776 points, a step size of 20 mm and an angle step of 8°. The bigger database together with the fourth order model increases reliability of the system but was considered too time-consuming to be used for all experiments.

To test the system the coordinate machine is programmed to place the implant in different positions within the measurement volume while the antenna output voltage is recorded. These values are collected in a database used to make a model file in Matlab that calculates a position based on the different antenna values. In the last step the calculated values for each position is compared with the actual value of the coordinate machine. This comparison yields a error radius for each test point as well as the mean and the standard deviation of the error radii. Additionally, for each point a measurement quality, MQ, value is computed. The MQ value gives a measure of the quality of the calculation performed by the algorithm and can warn users if something disturbs the system. When comparing different geometries it can be used to evaluate how well the calculated model can describe the real system. A system with low MQ is considered a more stable system. For details considering calculation of the MQ value see Appendix A1.

4.4 Results

4.4.1 Mean error radius, MQ and standard deviation

Table 5 shows the different test runs for the system. The table presents the date for the runs as well as different valuable parameters, including the voltage gain (Vg) of the transmitting antenna as well as order which concerns the polynomials used by the algorithm.

Date	Run	Coil	Vg	DB Size	Order	Eval. points	Mean error radius	Std. Dev.	Points within 2mm error
20090225	DBA001	3	2.0	7776	4		Not noted due to antenna displacement		
20090226	DBA002	3	2.0	7776	4	500	7.723	9.023	17.4%
20090226	DBA003	3	1.9	7776	4	500	2.039	0.781	58.2%
20090302	DBA004	3	1.8	7776	3	500	0.628	0.398	98.8%
20090302	DBA005	3	1.8	7776	4	500	0.690	0.339	98.1%
	Same DB, 2000 point evaluation					2000	0.631	0.471	
20090303	DBA006	3	1.7	7776	4	2000	0.729	0.453	98.9%
20090305	DBA007	3	1.8	7776	3	500	2.963	3.236	53.4%
20090305	DBA008	3	1.8	7776	4	500	1.469	1.926	84.8%
20090306	DBA009	3	1.8	7776	4	2000	0.891	0.870	95.5%
20090310	DBA010	3	1.8	1024	3	500	0.888	0.736	94.4%
20090310	DBA011	3	1.8	1024	3	500	6.221	8.511	23.2%
20090311	DBA012	3	1.8	1024	3	500	6.055	9.054	36.8%
20090311	DBA013	3	1.8	1024	3	500	2.419	4.225	74.2%
20090312	DBA014	1	1.8	1024	3	500	83.247	25.972	0.0%
20090313	DBA015	2	1.8	1024	3	500	21.368	14.609	8.0%

Table 5: Test run results.

According to specifications made by Micropos 95% of the points in a 2000-point evaluation must be within a 2 mm error radius for the system to be accepted. During the tests conducted within this project such accuracy was achieved for three of the databases. Note that since the

2000 point evaluation is time-consuming it was only performed on geometries showing promising results although some of the other geometries might produce results matching the specifications. As seen in table 5 DBA005 has a mean error radius of 0,63 mm and a standard deviation of 0,47 mm. Of the 2000 tested points 98,05% of the points lie within the 2 mm error margin. DBA006 shares the same geometry but was tested with a lower Vg (voltage gain) which affects the result in collaboration with other factors. For DBA006 98,9% of the points lie within the limit while the mean error radius is slightly higher than DBA005. DBA009 has a different geometry and has 95,45% of the points within the 2 mm limit. An overview of the best run with the 3D-antenna compared to a run from the hand wired antenna is shown in figure 14. The figure illustrates the error radius of the runs as well as the MQ for each point.

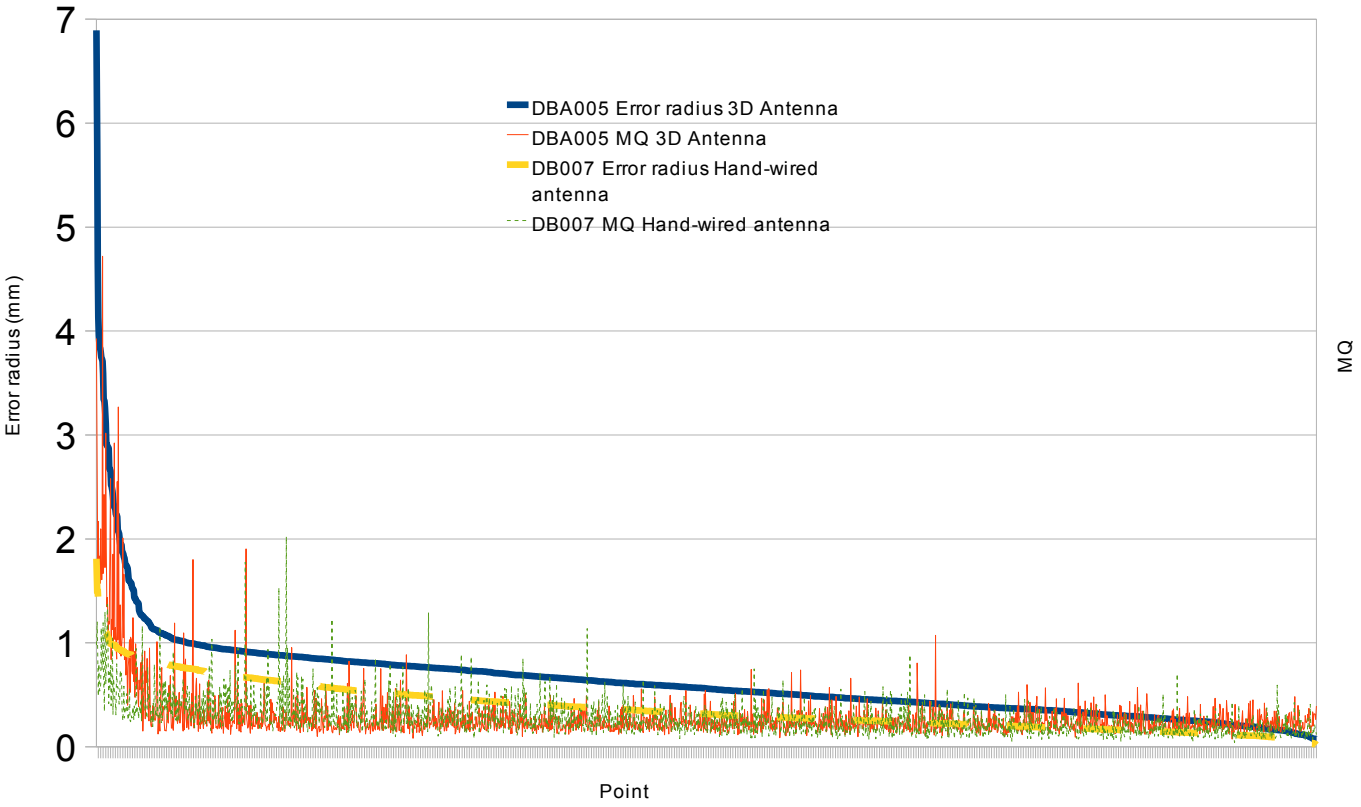

Figure 14: Test results, 3D-antenna vs. hand wired antenna.

The collected databases can be compared with MDB007 which was collected from a test run of one of the accepted systems at Micropos Medical. MDB007 has a mean error radius of 0,38 and of the 2000 evaluated points all lie within the 2 mm limit. Figure 15 shows a comparison of the errors for DBA005, DBA006, DBA009 and MDB007 where the error is sorted to get the points with highest error to the left. The Y axis of the graph is scaled which means that some of the error points for DBA006 and DBA009 are missing. As seen in the figure 15 the results of these test runs is similar to each other although DBA006 shows a different characteristic in the beginning of the graph. DBA006 has less error points over 2 mm although most of the remaining error points show bigger error radius when compared to DBA005.

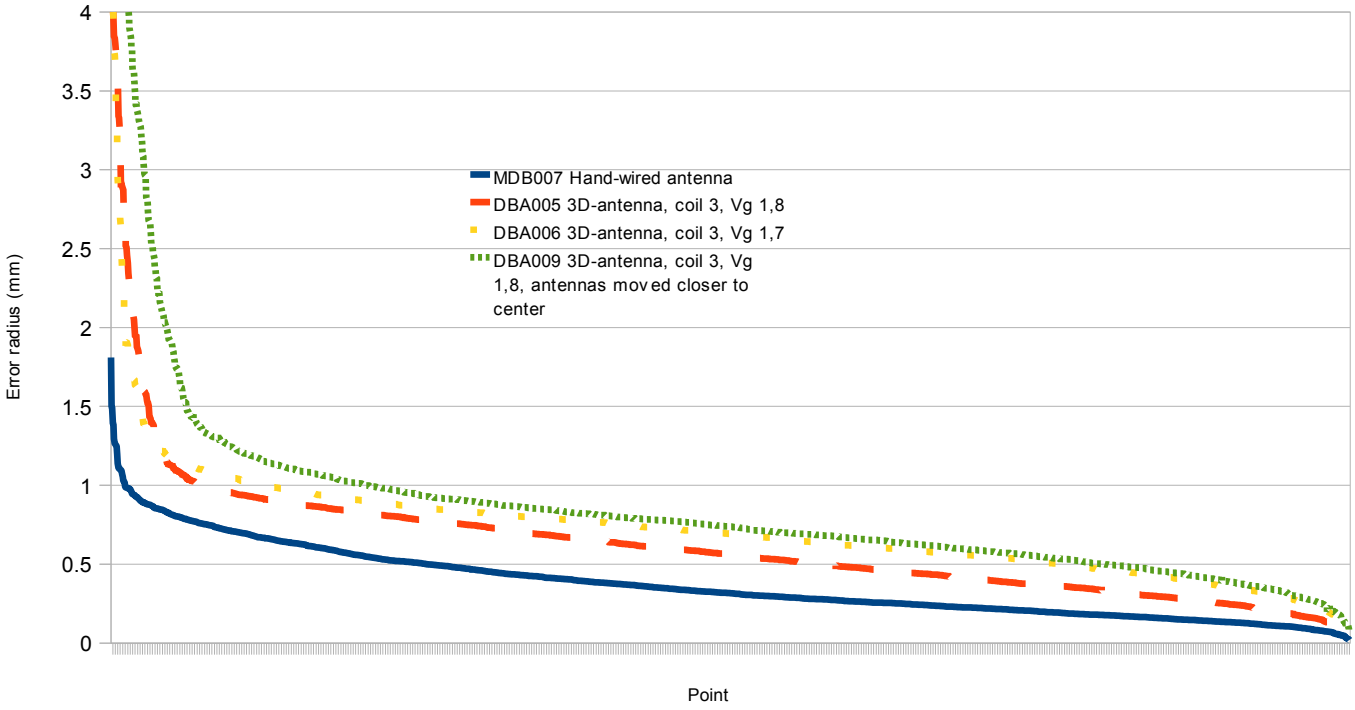

Figure 15: Error radius comparison. Note that some of the points fall above the plotted area.

Figure 16 illustrates the MQ for the different runs. Note that MDB007 from the hand wired antenna has a mean MQ of 0,27 while DBA005 from the 3D-antenna has a mean MQ of 0,29.

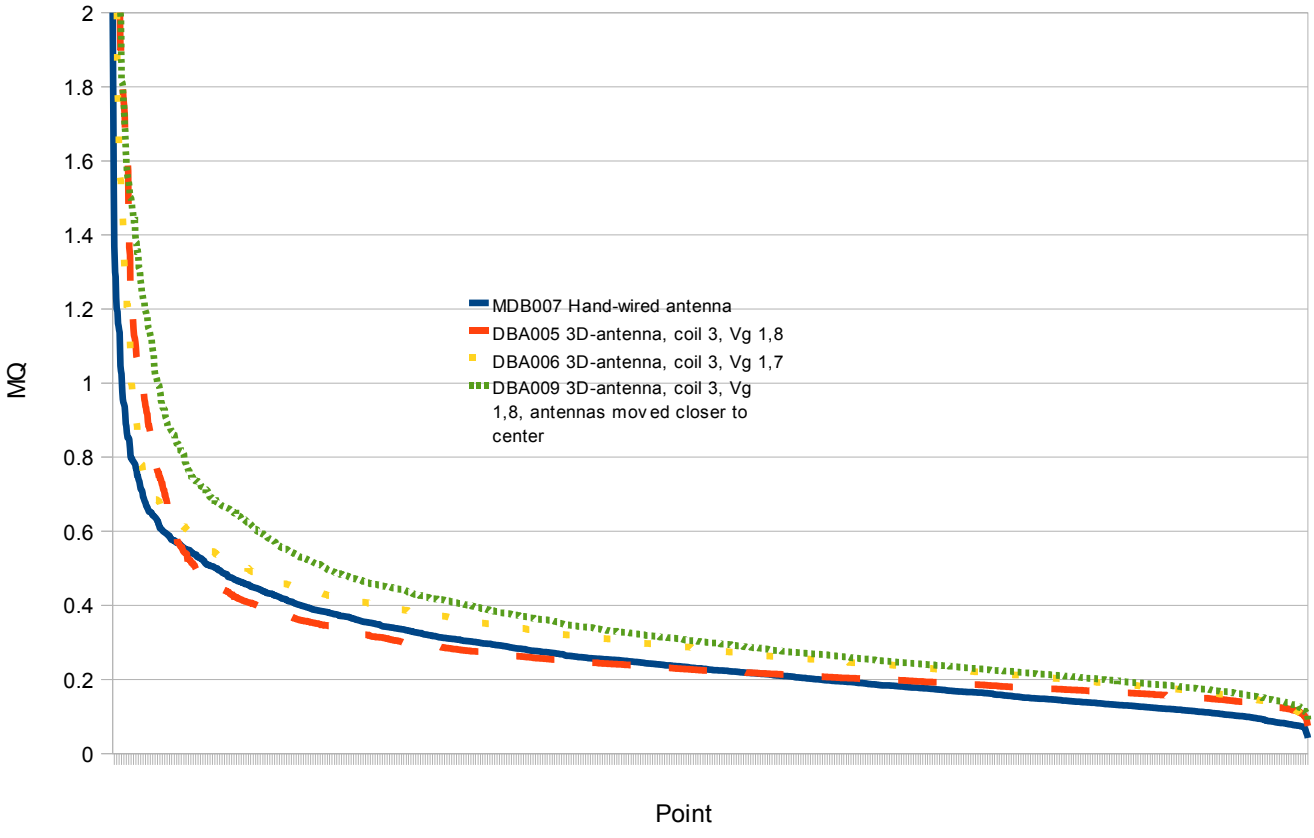

Figure 16: MQ value comparison.

Some of the databases are of particular interest for further evaluation. DBA005, DBA014 and DBA017 contains data collected from the 3D-antennas coil 3, 1 and 2 respectively. As pictured in figure 13 coil 3 lies flat on the table like the hand wired antenna while coil 1 is oriented with center axis along the table and coil 2 has its axis across the table. This means that coil 1 has the same orientation as the sending antenna which should mean that the induced current of these antennas become low.

Figure 17 provides an overview of the test runs evaluated for 500 points. By studying the diagram as well as the mean error radius presented in table 5 it is evident that the tests with coil 1 and 2 were less accurate than the tests with coil 3. DBA015 and DBA017 were sampled from coil 2 and can be used to illustrate the difference between using 1024 and 7776 evaluation points as well as polynomials of the third and fourth order where more points and higher order should provide a more reliable positioning. When comparing different setups it is important that the databases are of the same order since the effect of changing order is unpredictable.

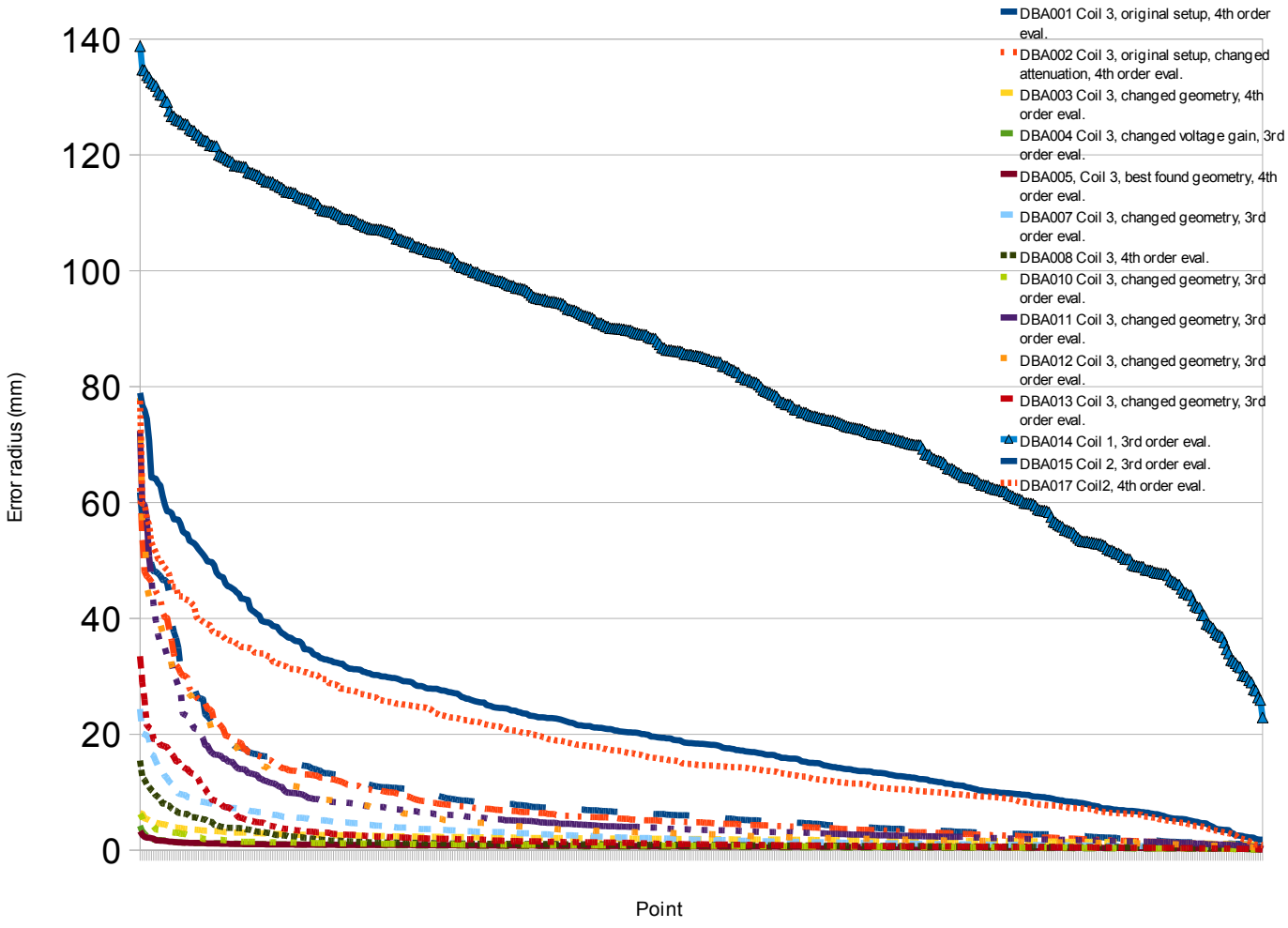

Figure 17: Test run overview.

4.4.2 Error distribution

With the acquired data it has been possible to test different aspects of the system. Plotting error radius and MQ vs. position (x,y, z) and angle (V_y and V_z) makes it possible to study where the accuracy of the system is high or low. The V_y angle is defined as the angle that tilts the implant up and down while the V_z angle turns the implant right or left. Important to note is that for the databases from the hand wired antenna V_y goes in the opposite direction

compared to V_y for the 3D-antenna databases. Plots from the databases MDB007, DBA005, DBA014 and DBA017 are presented in appendix A2. Note that the information from the other 4 dimensions are lost as each plot only concerns one dimension.

MDB007 is a database from the hand wired original system which makes it a good reference to the databases from the 3D-antenna. In the X axis plot the error is evenly distributed while some tendencies can be discerned in the Y-and Z-axis plots. High Y values as well as low Z values seem to result in a slightly higher error radius and MQ. Low V_z angle has the same effect. When studying the effect of the angle it can be noted that the error tend to be lowest when the angle is zero.

The plots from DBA005 are harder to analyze since the error distribution is quite even. Low Y axis values have slightly higher errors. In the plots for X and Z trends are hard to distinguish. As noted in MDB007 the error seem to increase when deviating from zero angle in both V_y and V_z. A high collection of errors are found for low values of V_z.

For DBA014 which was taken from the coil with the same orientation as the transmitting coil the accuracy is bad overall although some interesting trends can be noted. The plots for Y and Z shows that the error increases for higher Y and Z values. This is particularly obvious for the Z plot where the error increases significantly when the implant comes closer to the table.

From DBA017 sampled with coil 2 no significant accumulation of errors was detected.

4.4.3 MSAT Output voltage comparison

MSAT is a software developed by Micropos that can be used to visualize the behaviour of the antennas in different ways. One function of the program is to plot output voltage for each antenna against position in X, Y, Z and the two angles. While one dimension is plotted the other dimensions are in their respective center position. This function can be used to easily identify malfunctioning antennas. During this project the function has also been used to compare different tests of the 3D-antenna with the hand wired antenna. Since the algorithm is built for the hand wired antennas it is interesting to determine if the voltage characteristics are similar for the different coils of the 3D-antenna. Plots for chosen databases are attached in appendix A3.

A comparison between DBA005 from coil 3 of the 3D-antenna and the corresponding plots for the hand wired antenna shows that the antennas behave similarly although some differences can be noted. Concerning the X values the plots from DBA005 are more curved than the plots from the hand wired antenna, especially so for antennas 5,9,8 and 12. The Y plots are similar while the Z plots for the antennas on the outer cards are more curved. Regarding the angles the V_y plots are more curved while the V_z plots are more similar. The V_y plots are mirrored as mentioned in the previous section.

When comparing DBA014 from coil 1 with the hand wired antenna more differences are found. While the X and Z plot are quite similar, the Y plots are severely differing from the hand wired antenna antenna plots. The plots for V_y and V_z shows big differences where the V_z plots for the 3D-antenna are remarkably flat especially for antennas 10 and 11. These antenna plots are flatter in the X plots as well. Note also that DBA014 has a very high MQ value compared to the other databases.

The database from coil 2, DBA017, shows big discrepancies in the X plots compared to the hand wired antenna. The Y and Z plots are similar while the V_z plots differs much. Considering the V_y plots that are mirrored they seem to have similar characteristics for the two inner cards. The V_y plots for the outer cards goes in the opposite direction when compared to the hand wired antenna plots.

4.5 Discussion

4.5.1 Mean error radius, MQ and standard deviation

Using the same setup for the 3D-antennas as with the hand wired antenna resulted in poor accuracy. Establishing a plausible explanation for this is hard since many factors can affect the accuracy of the system.

During the first three tests concerning coil 3 of the 3D-antenna (the coil with same orientation as the hand wired antenna) the accuracy increased as the antennas were moved closer to the center. This may be explained by the smaller cross-section of the 3D-antennas compared to the hand wired antenna. The smaller cross-section means that the output voltage from the antennas will be lower. Possibly the outer 3D-antennas had difficulties establishing a correct voltage value which resulted in input values of lower quality to the algorithm. To make the algorithm function properly it is important that each position of the transmitting implant yields a unique set of antenna output values.

After DBA005, the database with the best tested geometry, more combinations were tested. The new geometries mainly tested moving the antennas closer to the center in different combinations which only resulted in poorer accuracy. Closely grouped antennas might have resulted in output values without the diversity needed for the algorithm to calculate a correct position.

As suspected the results for coil 1 and 2 were considerably less accurate than the results for coil 3. The least precise results came from the test with coil 1 which is the coil with the same orientation as the transmitting antenna. This can be expected as this orientation is the least favorable when related to the field from the transmitting antenna. Due to the bad reception angle the output voltage from coil 1 of the antennas was low and likely the diversity of the antenna values was not enough for the algorithm to function properly. Although the accuracy from the other coils can be enhanced by testing other geometries it is not likely that they will be as accurate as coil 3 under the given circumstances.

When comparing the results from the 3D-antenna to the hand wired antenna it is important to note that the tests are made with different coordinate machines. While the results recorded during this study are made with an older coordinate machine the results from the hand wired antenna comes from tests with a new and improved machine. Therefore it is likely that the accuracy of the 3D-antenna is somewhat better than the results presented in this report.

Concerning the results from the first two databases it should be noted that these databases were made without the cable ties that prevented the antennas from moving during data collection and evaluation. During these tests the antennas were attached to the circuit boards using only double adhesive tape which proved a insecure means of fastening.

4.5.2 Error distribution

By arranging the collected data from the databases in certain ways some interesting patterns can be discerned although no deeper investigation is presented in this report.

The results presented from the hand wired antenna suggests that the error is lowest when the transmitting antenna is placed as central as possible. A probable explanation for this is that the magnetic field becomes weak and the orientation bad when the implant is moved to the periphery of the system. Although such placement of the implant should benefit the antennas placed directly below the transmitting antenna this effect does not surpass the negative effect from the antennas placed far away from the transmitter.

To a lesser extent trends of the same character can be found when studying the plots for coil 3

of the 3D-antenna as well. Perhaps the lesser accuracy of the 3D-antenna is a factor that contributes to the more evenly distributed errors compared to the hand wired antenna.

The plot standing out most compared to the other plots is the z-axis plot from coil 1. Since this is the coil with the same orientation as the transmitting antenna the created magnetic field should be low overall for the receiving antennas and specifically so as the transmitter comes closer to the table. The bad orientation of the field makes it impossible for the system to accurately calculate position. Evidently the accuracy increases almost linearly with the height of the transmitter which shows a direct relation between transmitter position and accuracy.

4.5.3 MSAT Output voltage comparison

While the MSAT software can be used to visualize the output voltages in many different ways the analysis made in this thesis has been limited. One trend that seem obvious when studying the various graphs is that the plots from coil 3 are very similar to the plots from the hand wired antenna. When comparing these plots to the plots from coil 1 and 2 the similarities are much smaller and least so for coil 1. The distinguishable trends seem to suggest that the accuracy is higher when the plots are similar to the hand wired antenna plots. No more detailed analysis has been possible to make during this study.

5. Conclusions

5.1 Conclusions

During this project a 3D-antenna has been tested and compared with other antennas. The main interest has been to determine if a industrially manufactured antenna can replace the hand wired antenna used in the Micropos system today. Tests have been designed to evaluate certain properties of the antenna as well as the antenna´s performance when incorporated in the positioning system. Concerning the tests the following results were of main interest:

- The hand wired antenna performed significantly better in distance and sensitivity tests, probably due to the bigger cross-section of the hand wired antenna.
- Tests implicate that the 3D-antennas can be grouped close to each other without disturbance effects. Caution is advisable when placing the antennas close to electric components.
- The best geometry tested during this project was achieved by placing the 3D-antenna cards in rows at 90/240/90 mm with 40 mm between antennas on each card and using coil 3.

This yielded the results displayed in the table 6:

	Mean error radius (mm) + standard dev.	Mean MQ + standard dev.
3D-antenna	0.63 + 0.47	0.29 + 0.29
Hand wired antenna	0.38 + 0.23	0.27 + 0.18

Table 6: Comparison between 3D-antenna and Hand wired antenna.

This result means that the accuracy of coil 3 of the 3D-antenna fits the requirements decided by Micropos, i.e. more than 95% of 2000 tested points are within a 2 mm margin.

Coil 1 and 2 has mean errors of 83,3 and 17,9 mm respectively. This means that the algorithm used today cannot provide acceptable results using these coils which can be expected due to the geometry of these coils. Coil 1 which is orientated in the same direction as the transmitter yielded the worst results.

Important to note is that the test results from the hand wired antenna were made with a more exact coordinate machine than the older machine used for the 3D-antenna tests.

Brief investigations have been conducted to evaluate if the collected data can be used to analyze different aspects of the system. Two methods has been used to visualize collected data: error distribution plots and MSAT plots.

The plots showing error distribution show that measurement volumes with lesser accuracy can be discerned in some of the databases. Due to the complexity of the MSAT plots no thorough conclusions are presented within this project.

5.2 Future studies

With the results from this thesis project some suggestions for future studies are given below.

During this project the 3D-antennas have not been able to provide as good accuracy as the hand wired antennas. However, the 3D-antennas have provided acceptable results concerning one of the coils. These results should improve with the new, more precise, coordinate

machine. More testing should be able to increase the accuracy further considering the limited time spent testing different geometries. As mentioned in the previous section an interesting test would be to decide if the 3D-antennas were disturbed by the electronic components of the adjoining cards or if the decreased accuracy for certain geometries can be explained in some other way. Rotating the inner antenna cards 180 degrees might make it possible to move the antennas closer. Another interesting test can include equipping the sensors with longer cables, making it possible to distance the sensors from the electronics and possibly group the sensors and electronics separately. A problem with this approach is that the longer cables can result in disturbances and different coupling effects.

With aid from the MSAT software output voltage from the antennas can be visualized in plots. This information might be useful in some way to further enhance the precision of the system. Some information should be possible to extract by comparing the data from the 3D-antenna to the hand wired antenna. Perhaps the data from coil 1 and 2 of the 3D-antenna can be used for positioning somewhere in the measurement volume.

The error distribution plots can be interesting to study in order to decide where in the measurement volume the system has difficulties to decide position. Following that, it might be possible to determine why the system has difficulties in that position.

In order to use all the coils from the 3D-antennas more research will have to be done. Since the algorithm used today is developed to be used with the receiving coil flat on the table it might be possible to enhance positioning capabilities by altering the algorithm to use coil 1 and 2 as well. Coils 1 and 2 might be useful if the transmitting antenna changes orientation. Perhaps a sensor can be included in the implant to detect the angle between the implant and the receiving system. That information could then be used to decide when to use of coils 1 and 2.

Further tests can also include tests of other types of sensors. A more sensitive sensor might make it possible to determine position with higher accuracy.

Bibliography

[1] Lenz, James & Edelstein, Alan S (2006). *Magnetic Sensors and Their Applications.* Proc. IEEE, vol. 6, no. 3, pp. 631-649, Jun. 2006.

[2] Macintyre, Steven A (2000) *Magnetic Field Measurement.* [internet] Available at: <http://engineering.dartmouth.edu/dartmag/docs/macintyre.pdf> [Accessed 2008-11-13]

[3] Bratland, Tamara & Caruso, Michael J et. al. (1998) *A New Perspective on Magnetic Field Sensing.* [internet] <http://www.sensorsmag.com/articles/1298/mag1298/main.shtml> [Accessed 2008-11-14]

[4] *Om prostatacancer.* [internet] Available at: http://www.cancerfonden.se/upload/Dokument/Patientbroschyrer/prostatacancer_070806.pdf [Accessed 2008-11-24]

[5] Trout, S.R (1988) *Use of Helmholtz Coils for Magnetic Measurements* Proc. IEEE, vol. 24, no. 4, pp. 2108-2111, Jul. 1988

[6] *Measuring Sensitivity of Transponder Coils.* [internet] Available at: http://www.coilcraft.com/pdfs/Doc371_TCCoilSens.pdf [Accessed 2009-02-15]

[7] Ripka, Pavel (2001). *Magnetic Sensors and Magnetometers.* Boston: Artech House.

[8] *Inductors / Transformers.* [internet] Available at: http://www.neosid.de/DWL/Teil4/Seiten/440-442.pdf [Accessed 2009-01-22]

[9] Björkström, Jessica (2005). *Experimental Studies of Operating Near-field Antennas.* Göteborg: Chalmers University of Technology

[10] *Resonance.* [internet] Available at: http://hyperphysics.phy-astr.gsu.edu/HBASE/electric/serres.html [Accessed 2008-12-15]

[11] Dorf, C. Richard & Svoboda, A. James (2001). Introduction to Electric Circuits. New York: Wiley.

[12] *Relative current vs. percent change from resonant frequency.* [internet] Available at: http://tradcentral.com/ei6iz/Images/Q2.gif [Accessed 2008-12-15]

[13] Schoster, Carl & Syrén, Hanna (2005). *Integration of a realtime implant positioning system for 4D radiotherapy cancer treatment.* Göteborg: Chalmers University of Technology

[14] *Solenoidspole*. [internet] Available at: http://sv.wikipedia.org/wiki/Fil:Solenoidspole.svg [Accessed 2009-09-25]

[15] Cheng, David K (1992). *Field and wave electromagnetics.* New York: Addison-Wesley.

[16] Winslow, Therese (2005). *Anatomy of the male reproductive and urinary systems.* [internet] Available at: http://www.meb.uni-bonn.de/cancer.gov/Media/CDR0000457830.jpg [Accessed 2009-10-03]

[17] Evans-Pughe, Christine (2005). *Close encounters of the magnetic kind.* IEE Rev., vol. 51, iss. 5, p. 38-42, May 2005.

[18] Johnson, Richard C (1993). *Antenna engineering handbook. 3rd ed.*, New York: McGraw-Hill Inc.

[19] Nordling, Carl & Österman, Jonny (2006). *Physics Handbook for Science and Engineering.* Lund: Studentlitteratur.

Appendix

A1. MQ calculation

This section has been removed for confidentiality purposes.

A2. Error distribution plots

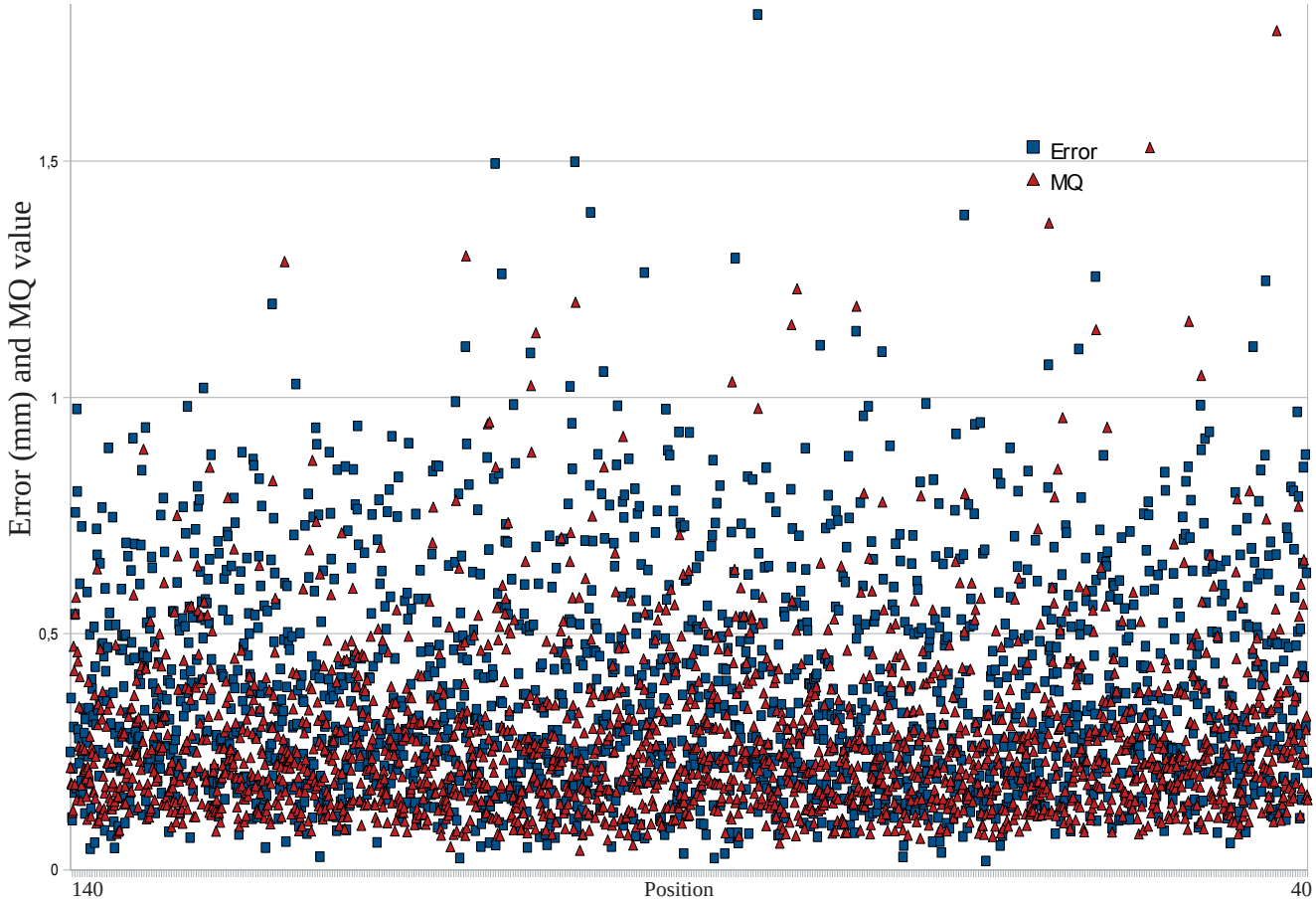

Figure 1: MDB007, Hand wired antenna, X position

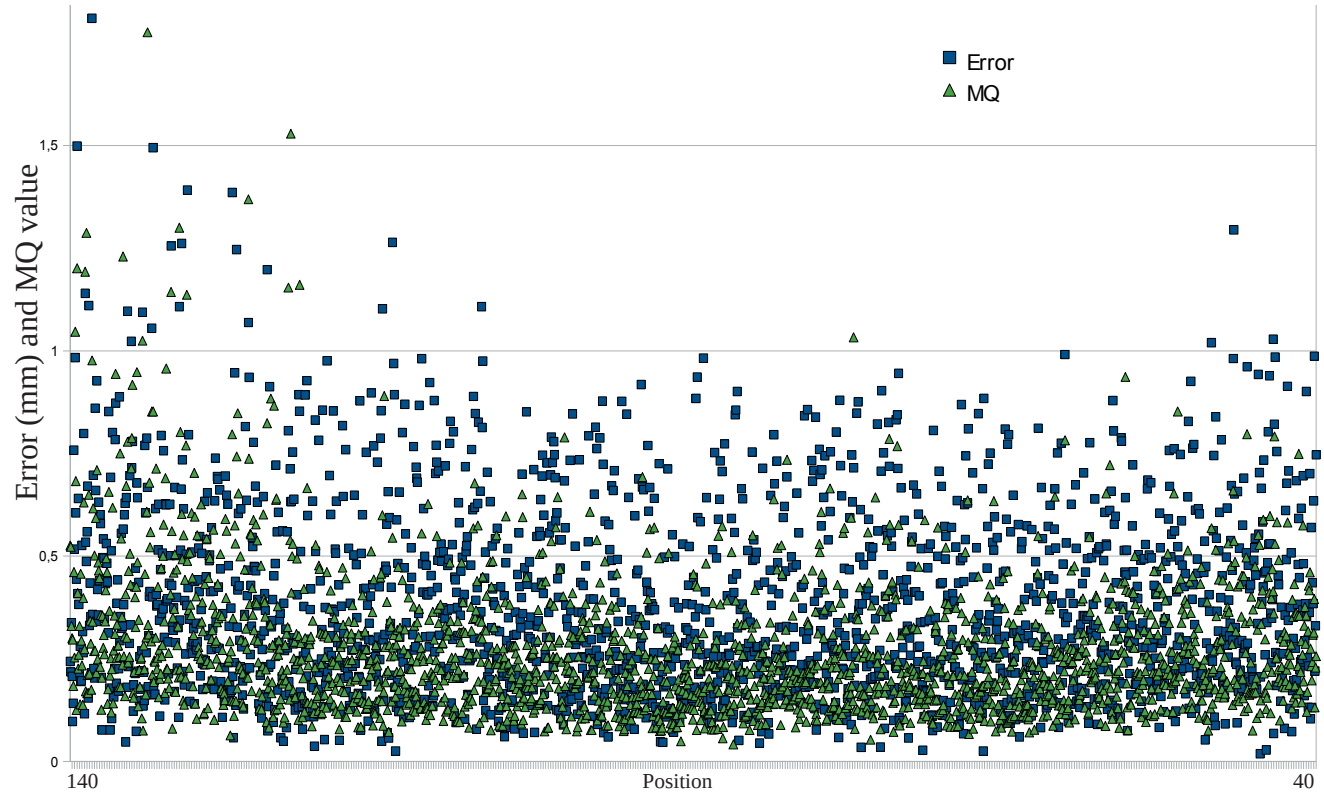

Figure 2: MDB007, Hand wired antenna, Y position

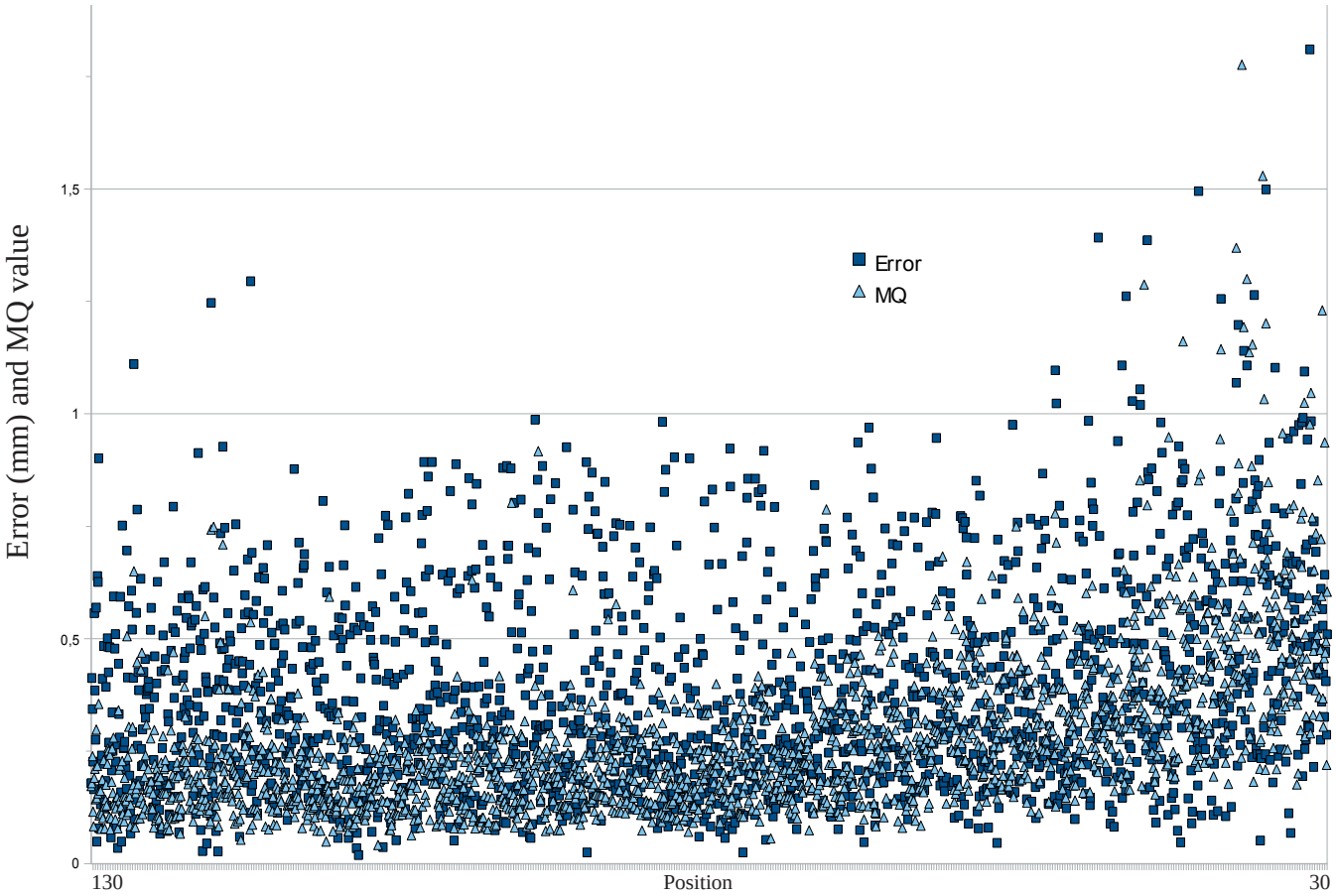

Figure 3: MDB007, Hand wired antenna, Z position

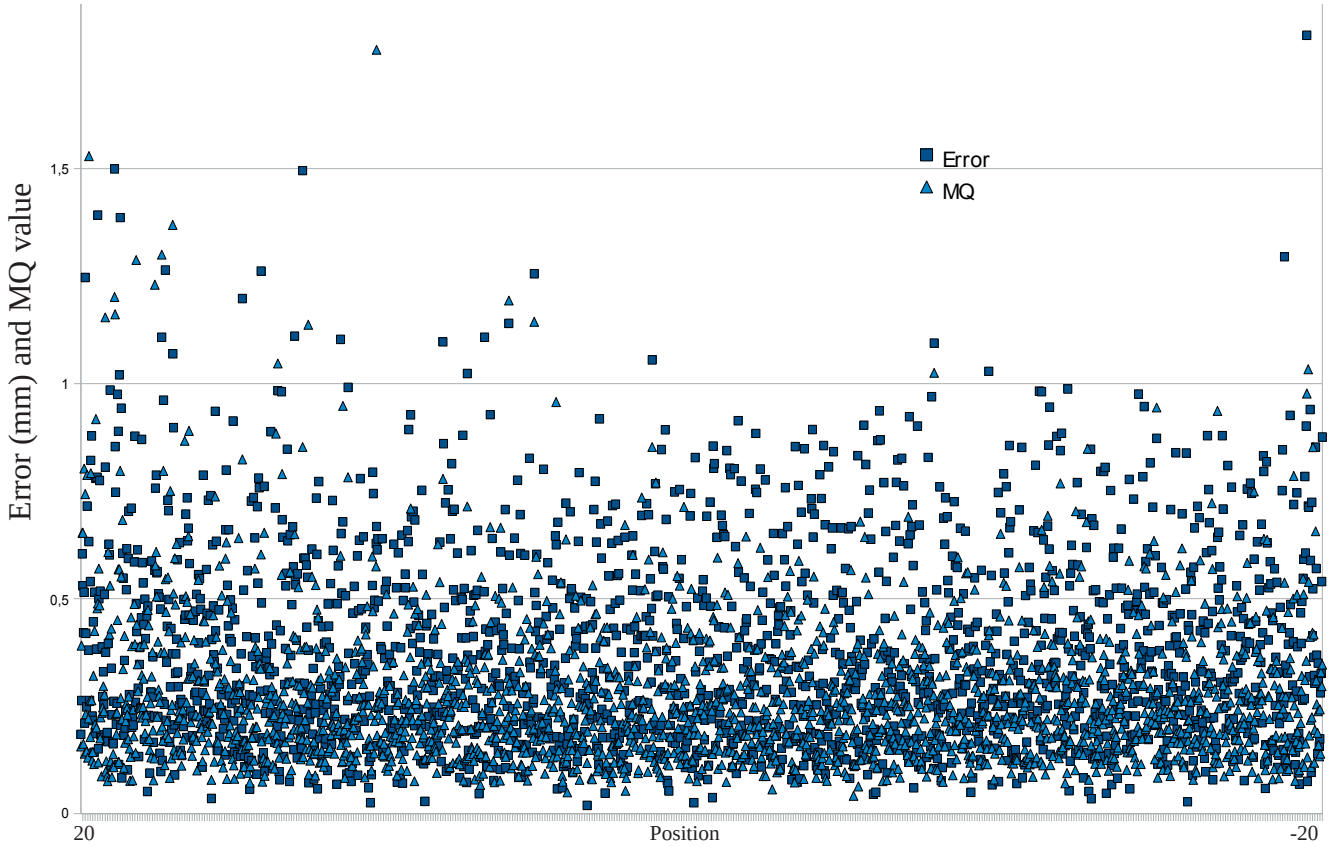

Figure 4: MDB007, Hand wired antenna, Vy angle

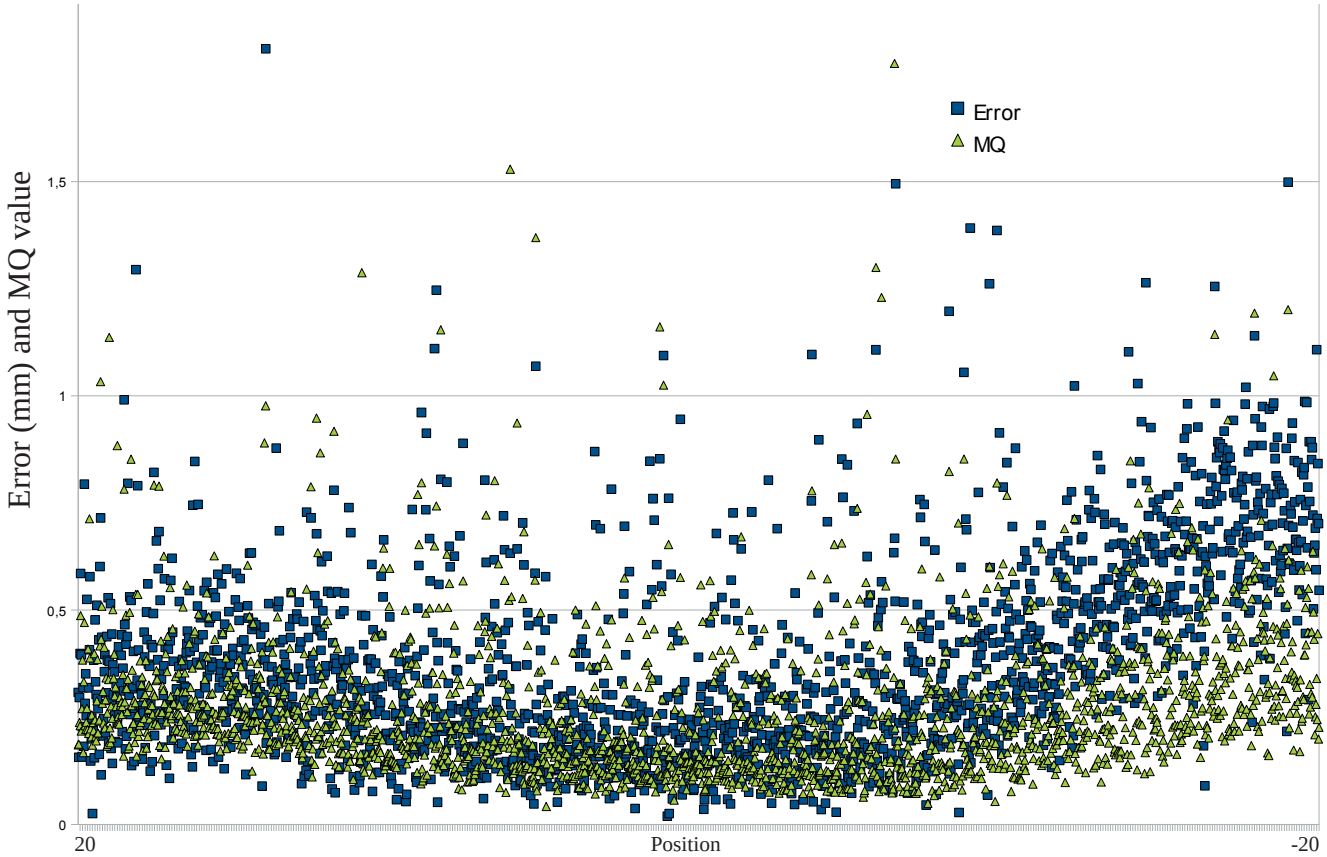

Figure 5: MDB007, Hand wired antenna, Vz angle

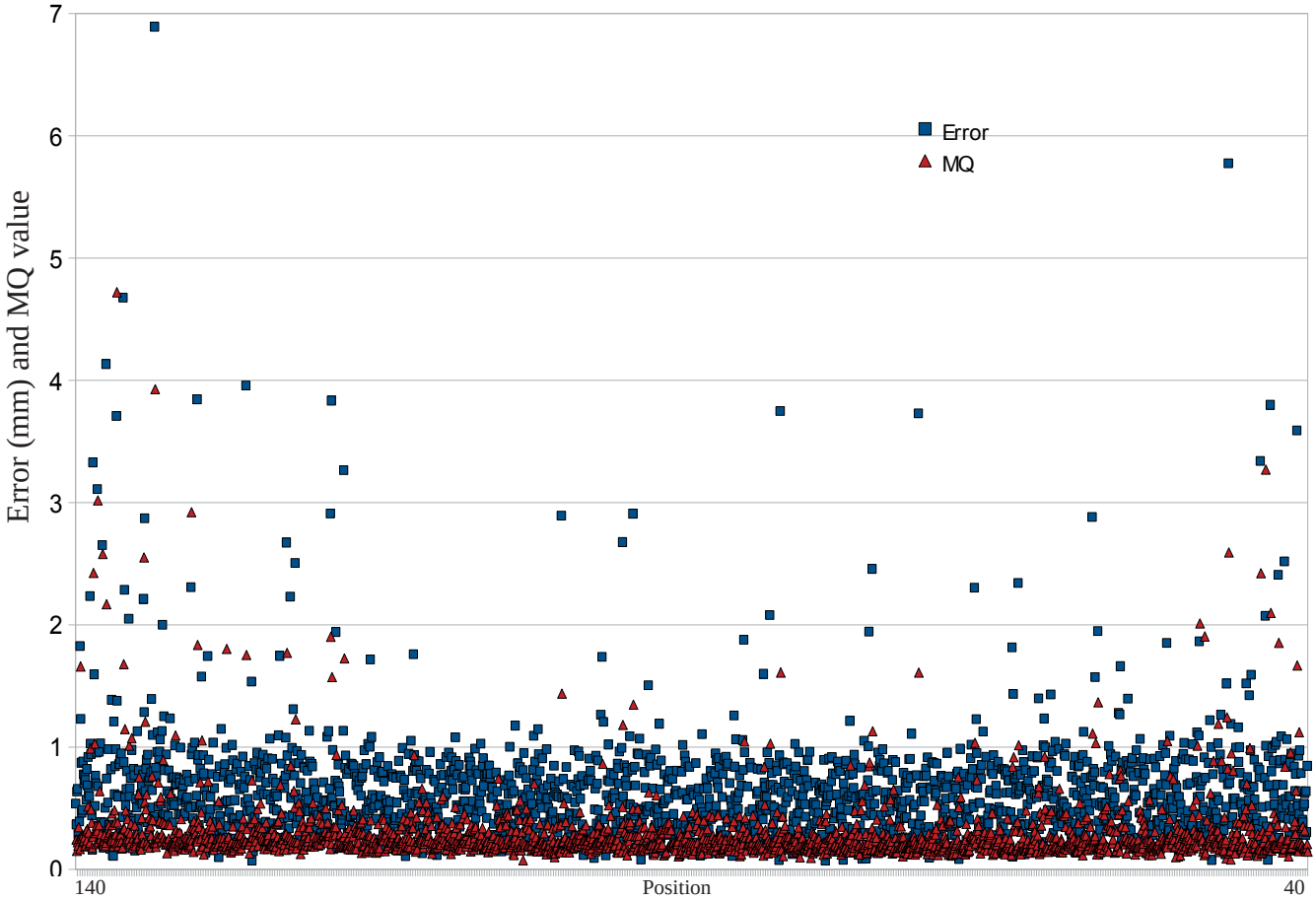

Figure 6: MDBA005, 3D antenna coil 3, X position

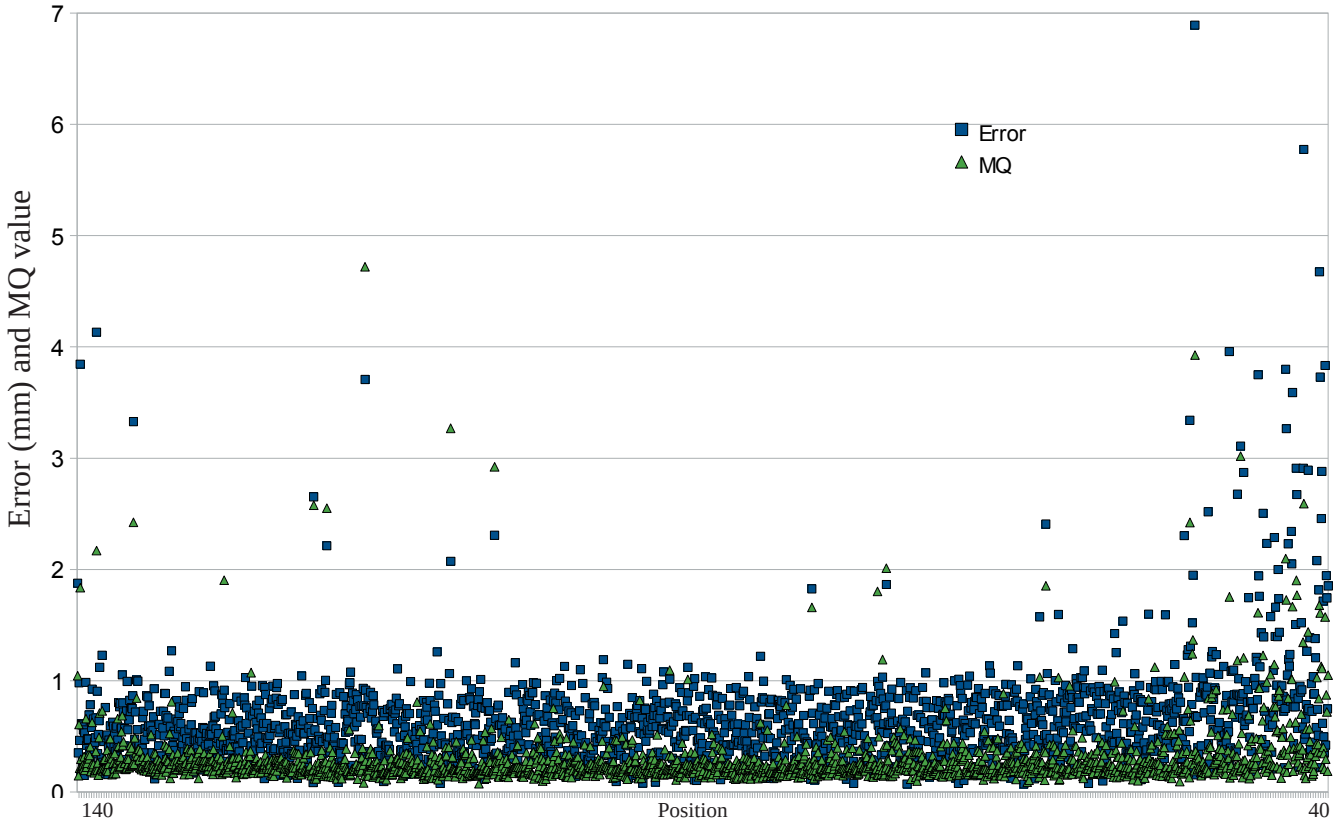

Figure 7: MDBA005, 3D antenna coil 3, Y position

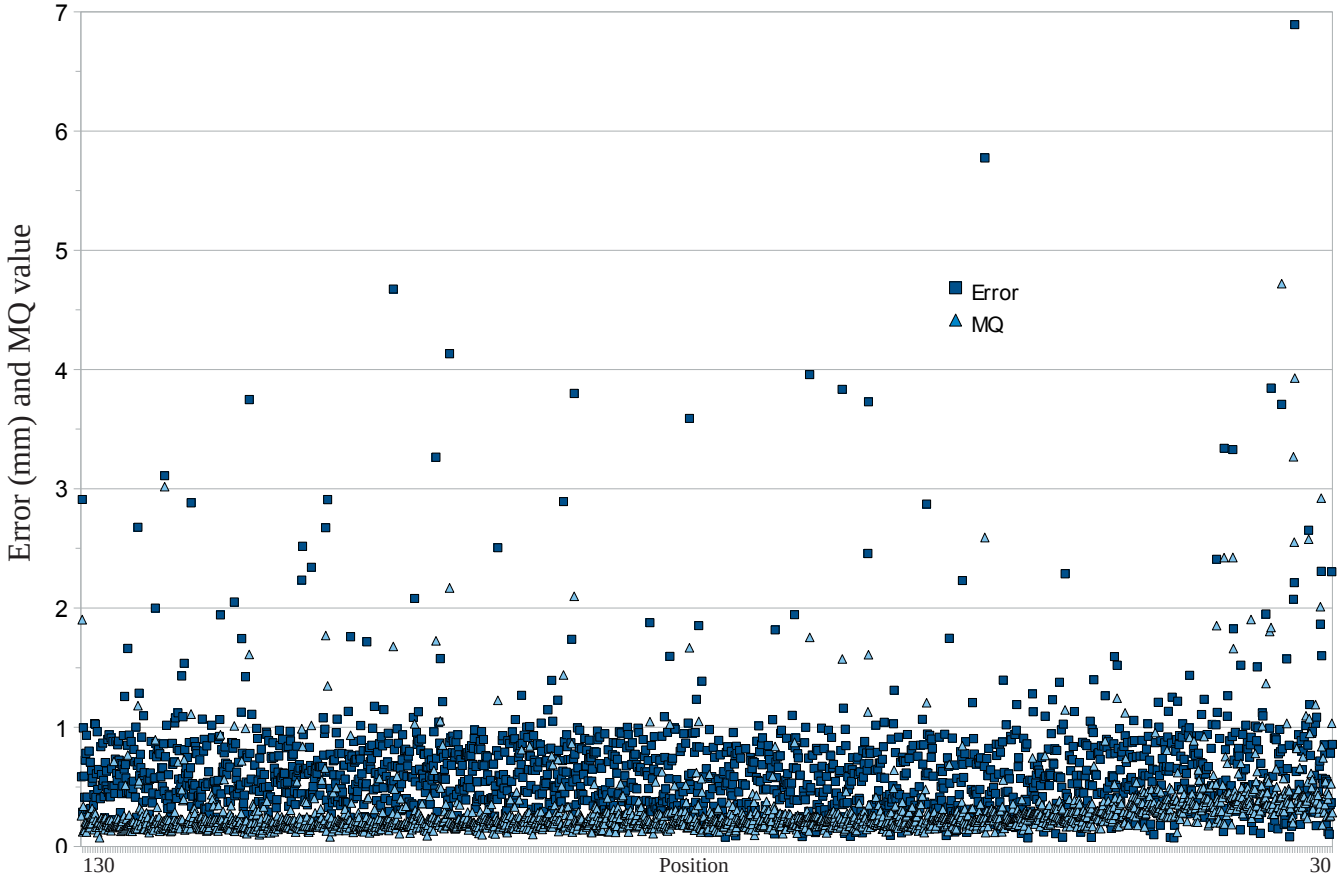

Figure 8: MDBA005, 3D antenna coil 3, Z position

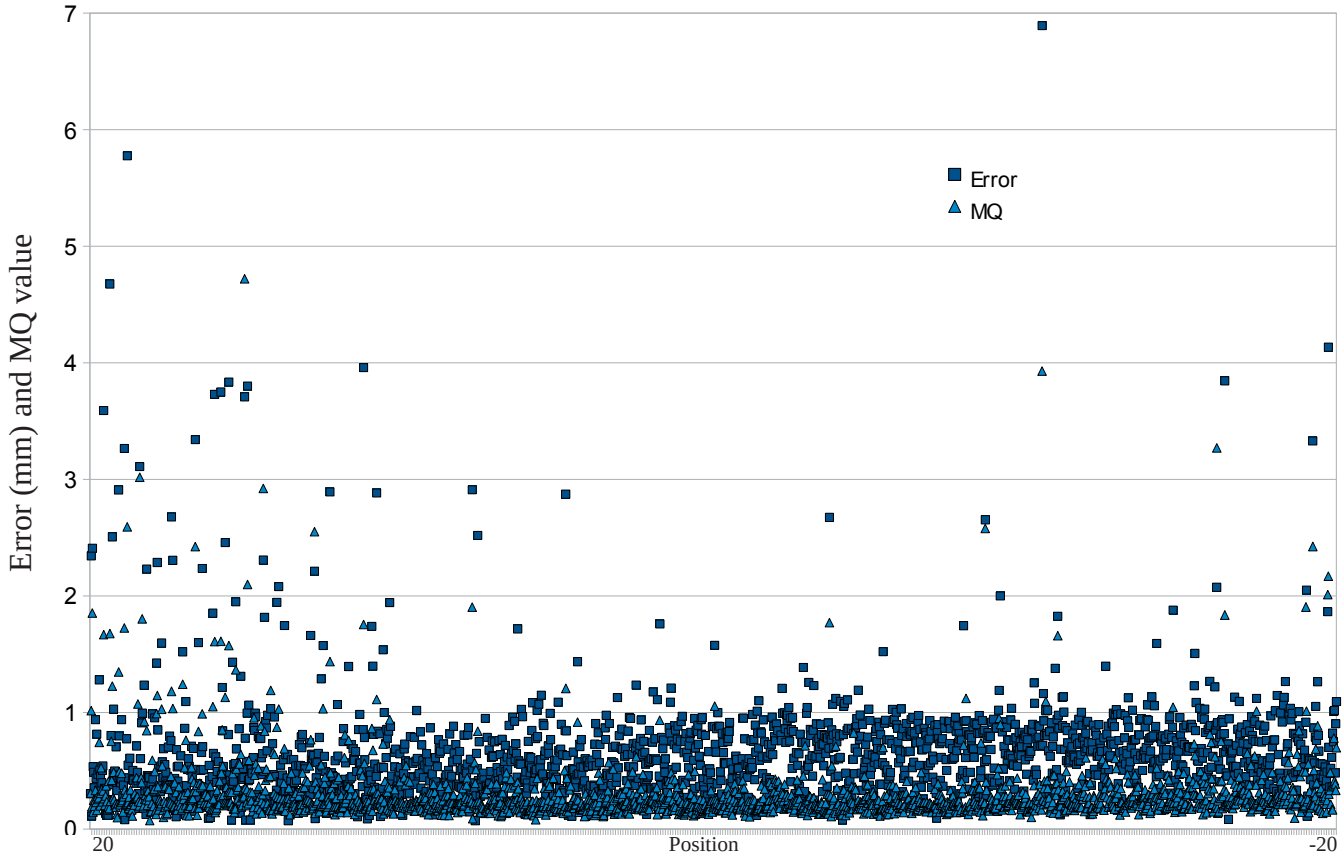

Figure 9: MDBA005, 3D antenna coil 3, Vy angle

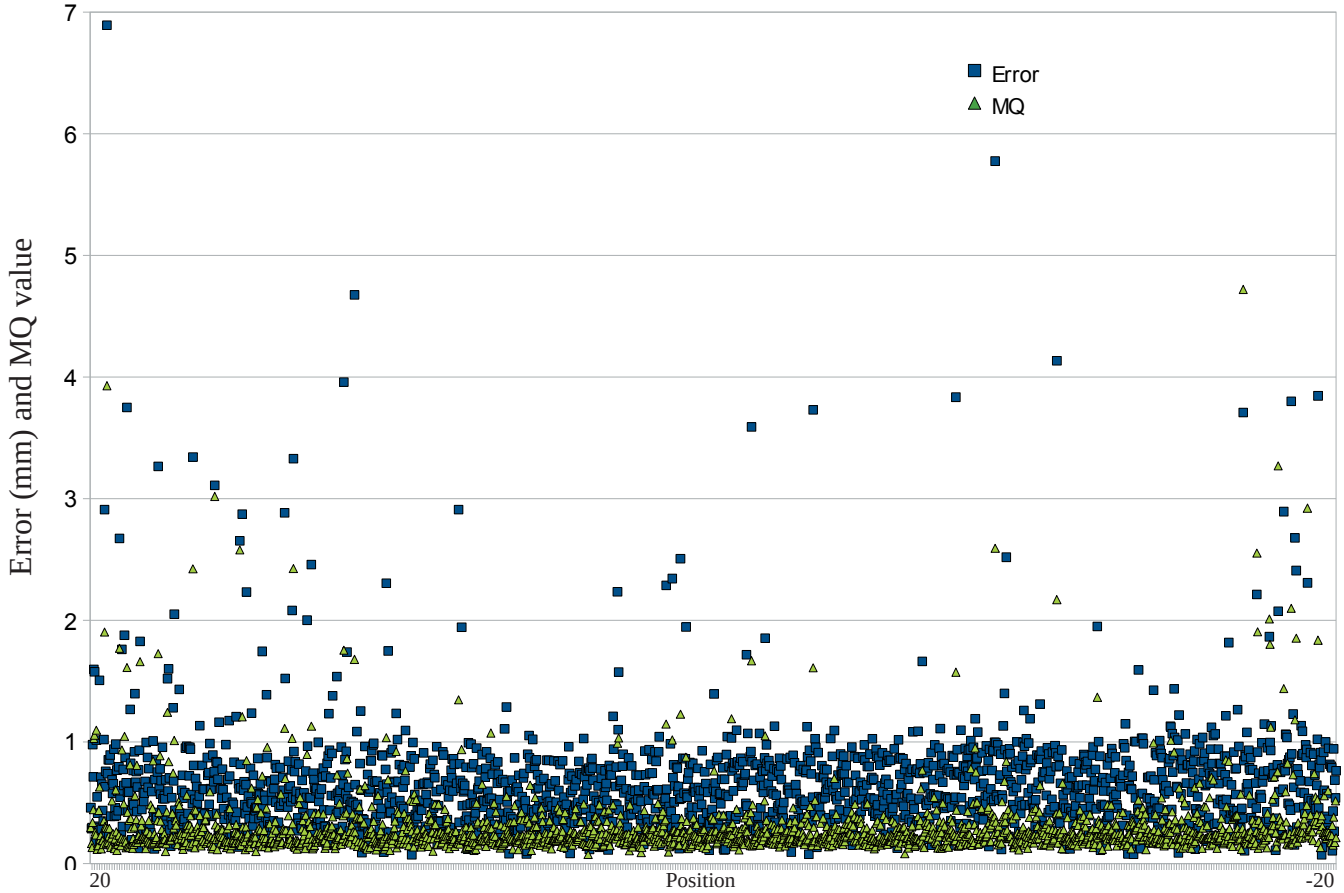

Figure 10: MDBA005, 3D antenna coil 3, Vz angle

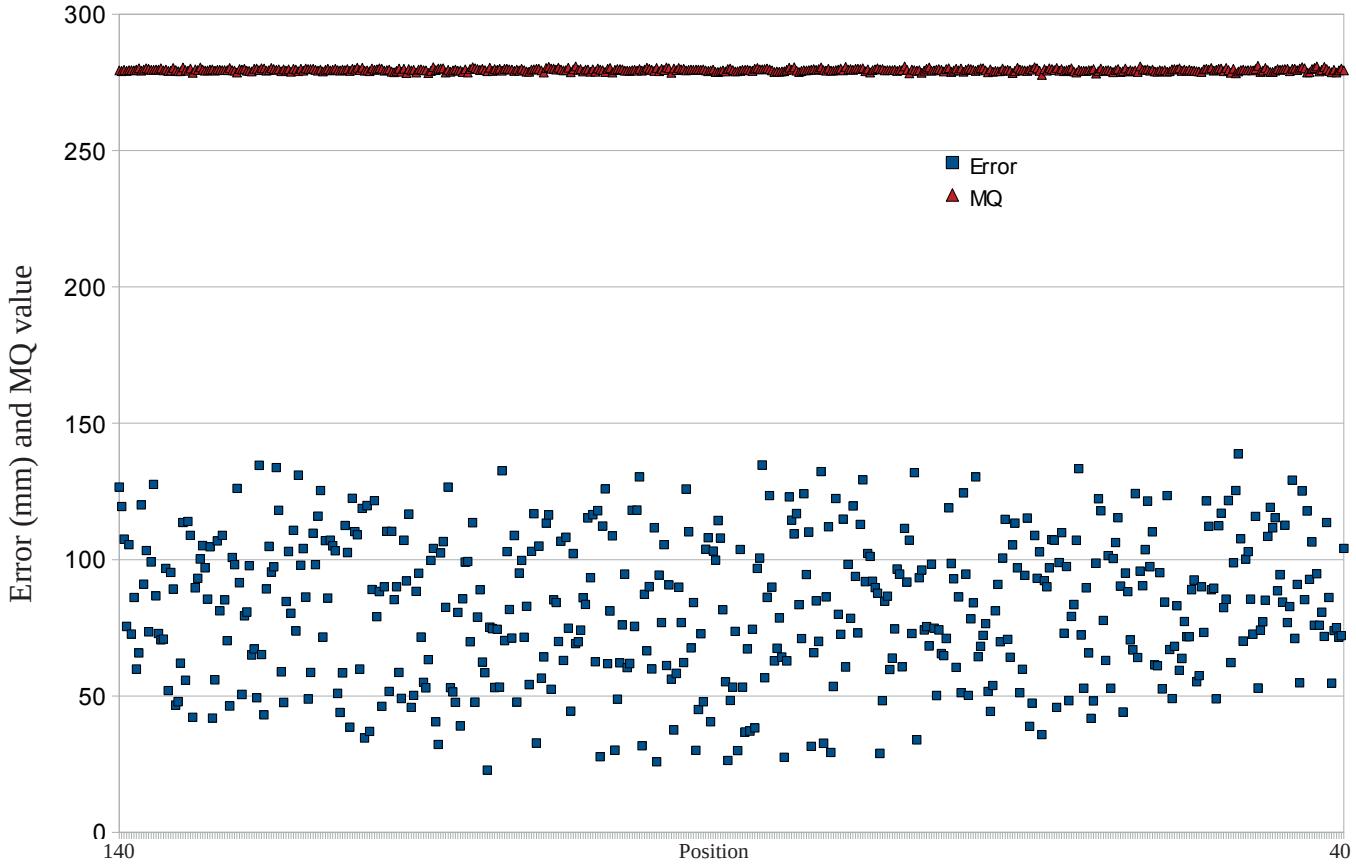

Figure 11: MDBA014, 3D antenna coil 1, X position

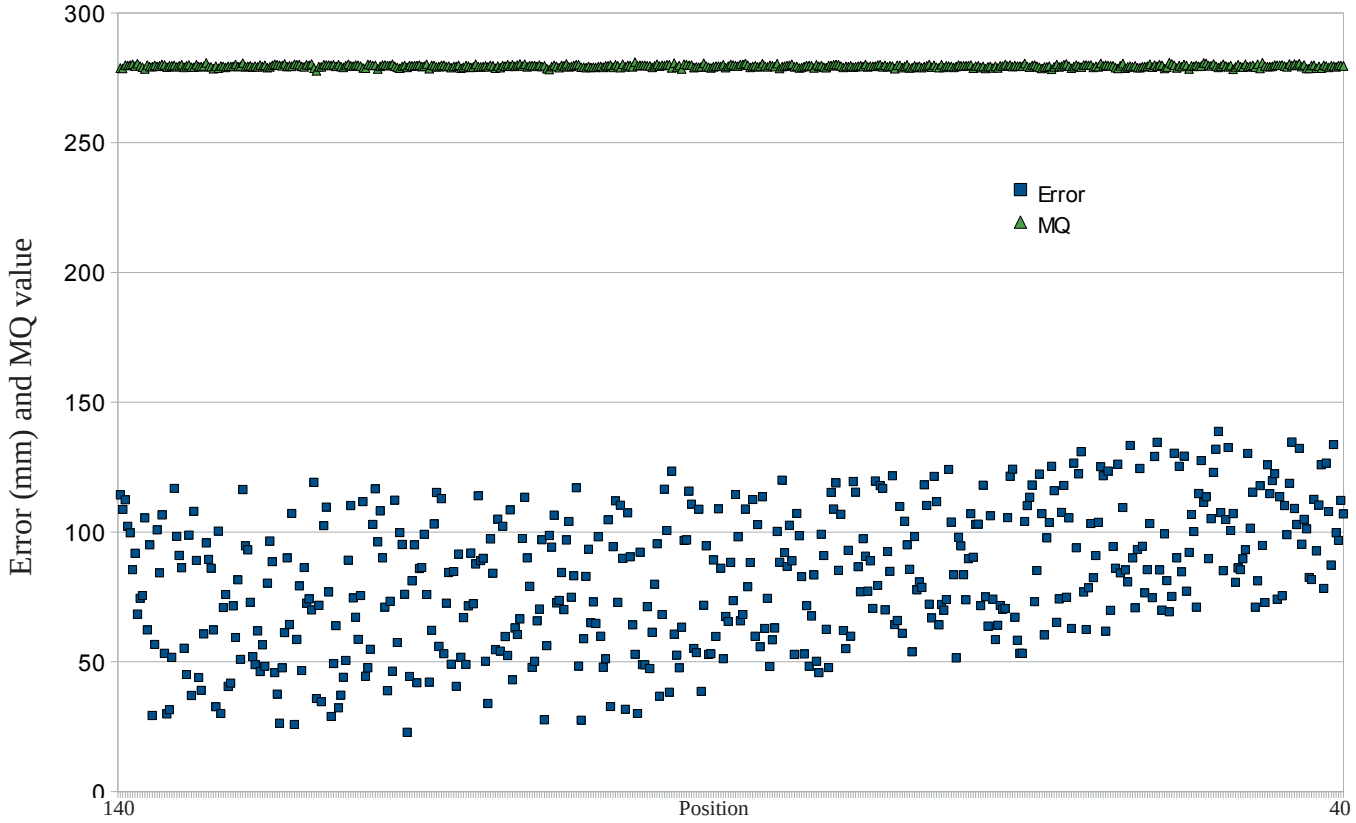

Figure 12: MDBA014, 3D antenna coil 1, Y position

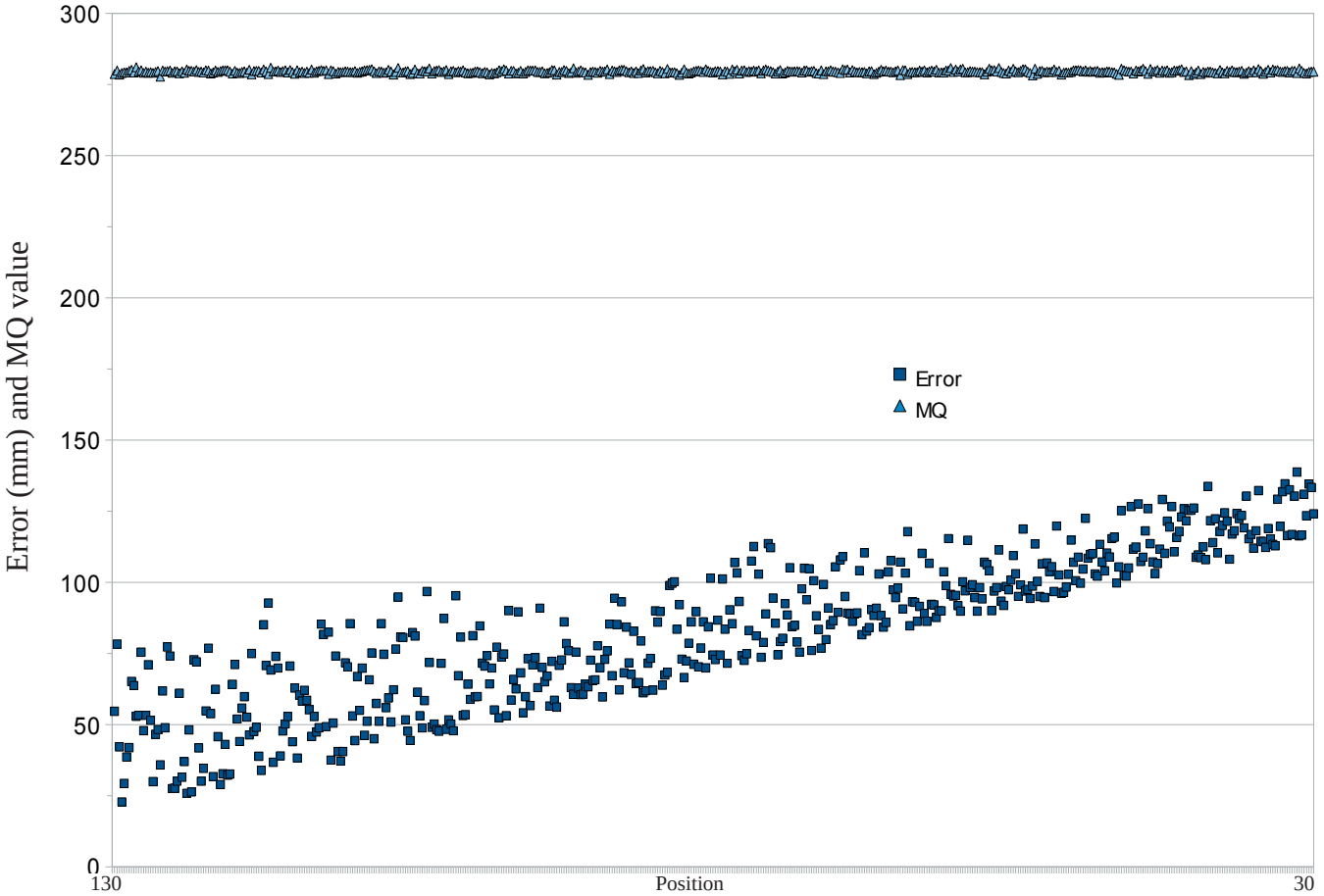

Figure 13: MDBA014, 3D antenna coil 1, Z position

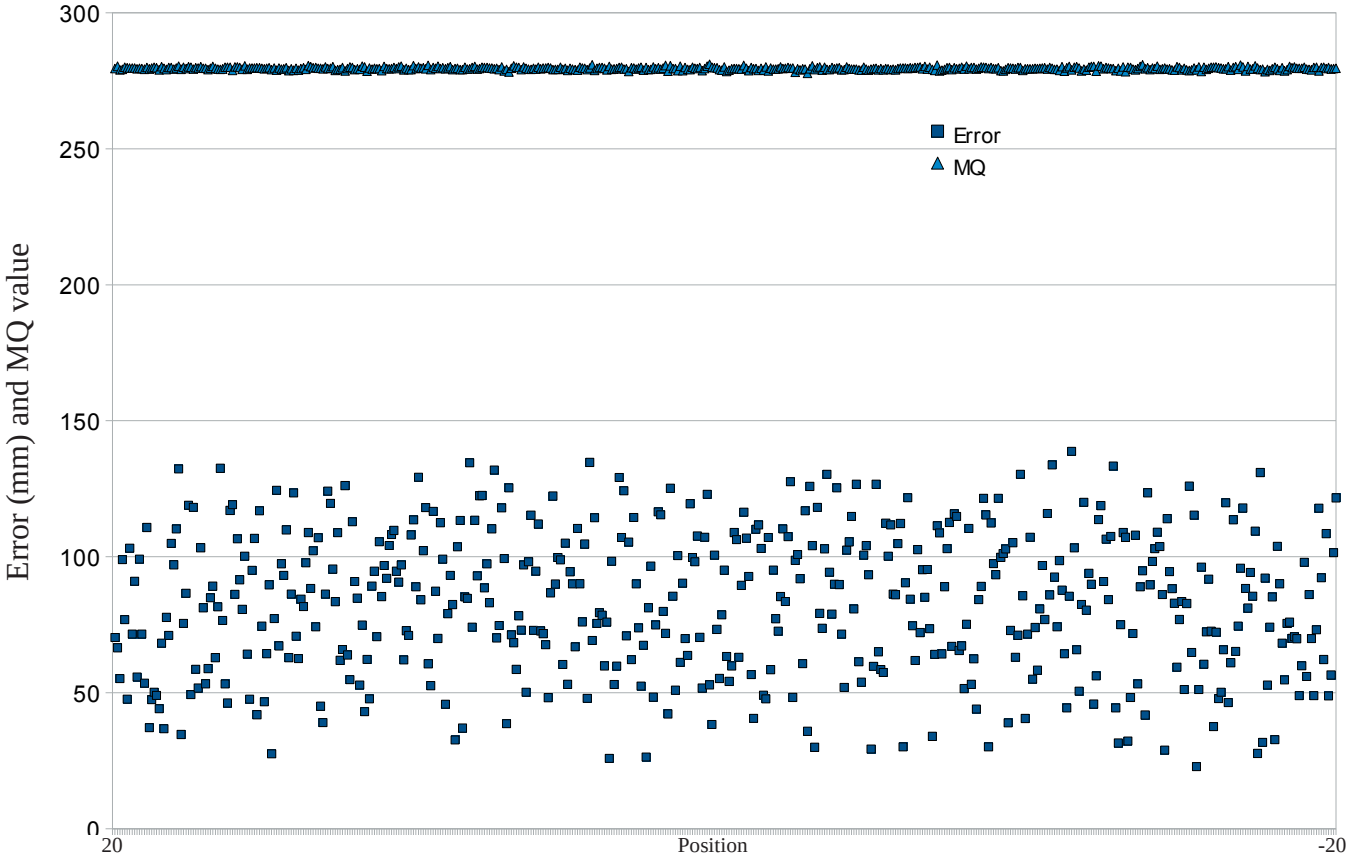

Figure 14: MDBA014, 3D antenna coil 1, Vy angle

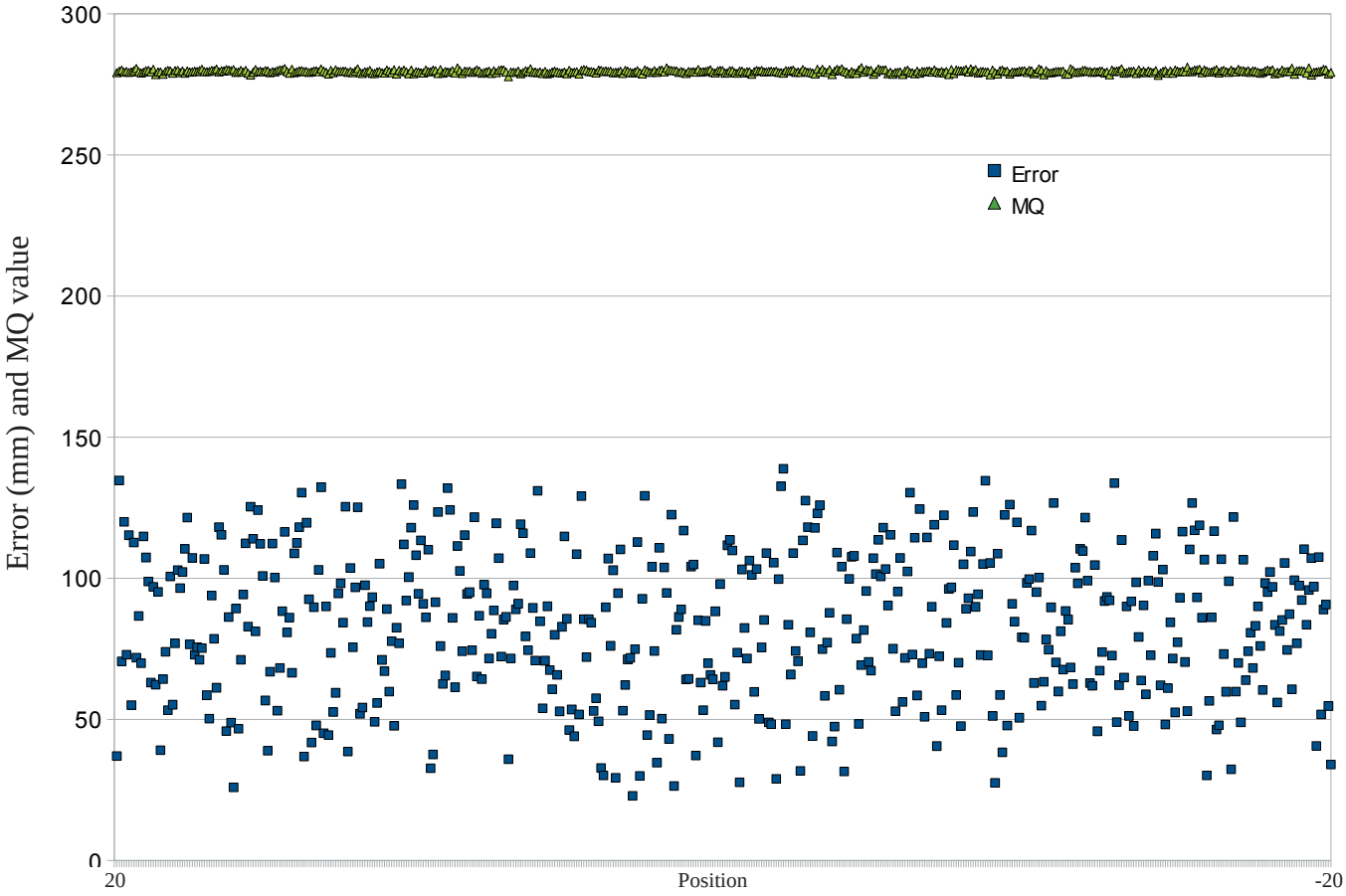

Figure 15: MDBA014, 3D antenna coil 1, Vz angle

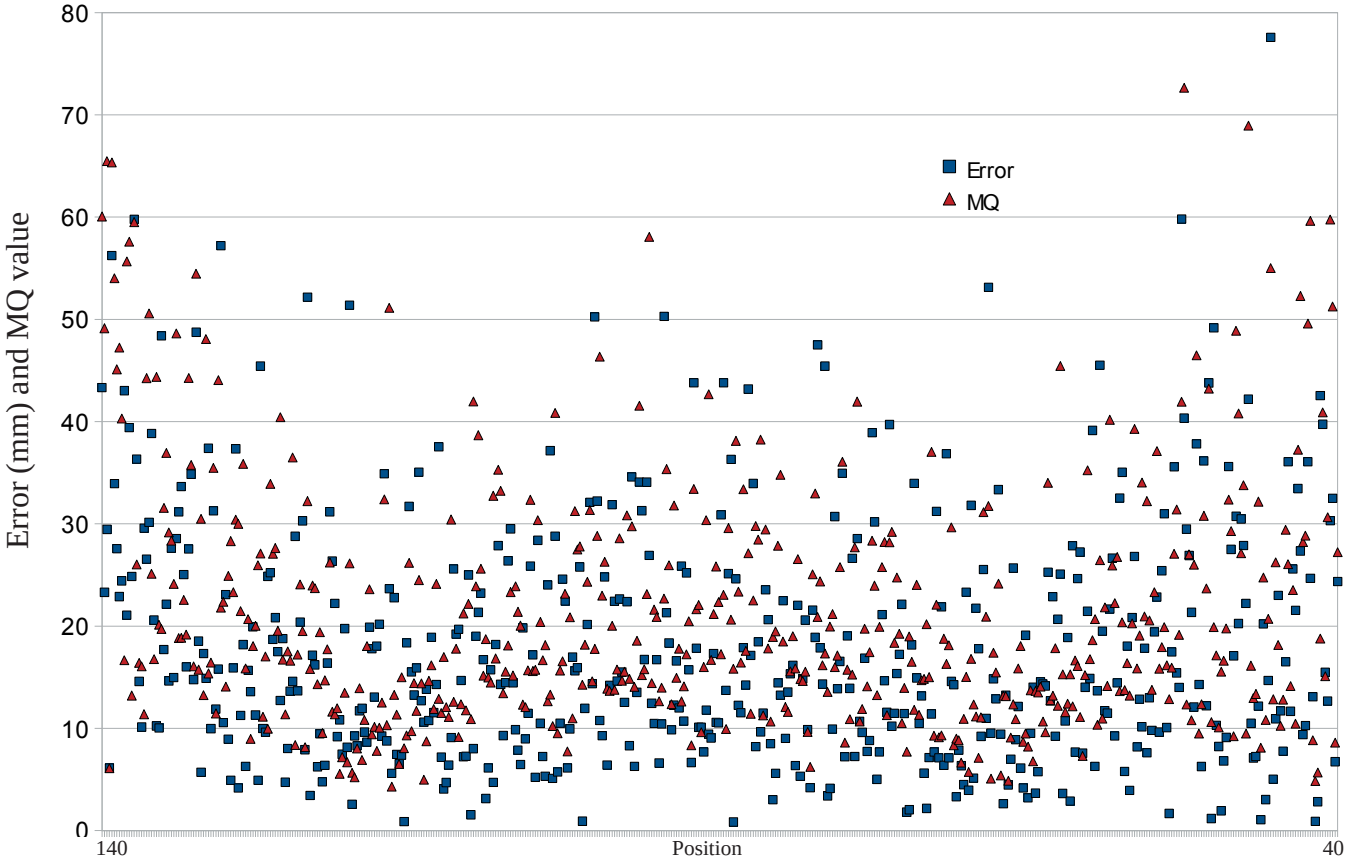

Figure 16: MDBA017, 3D antenna coil 2, X position

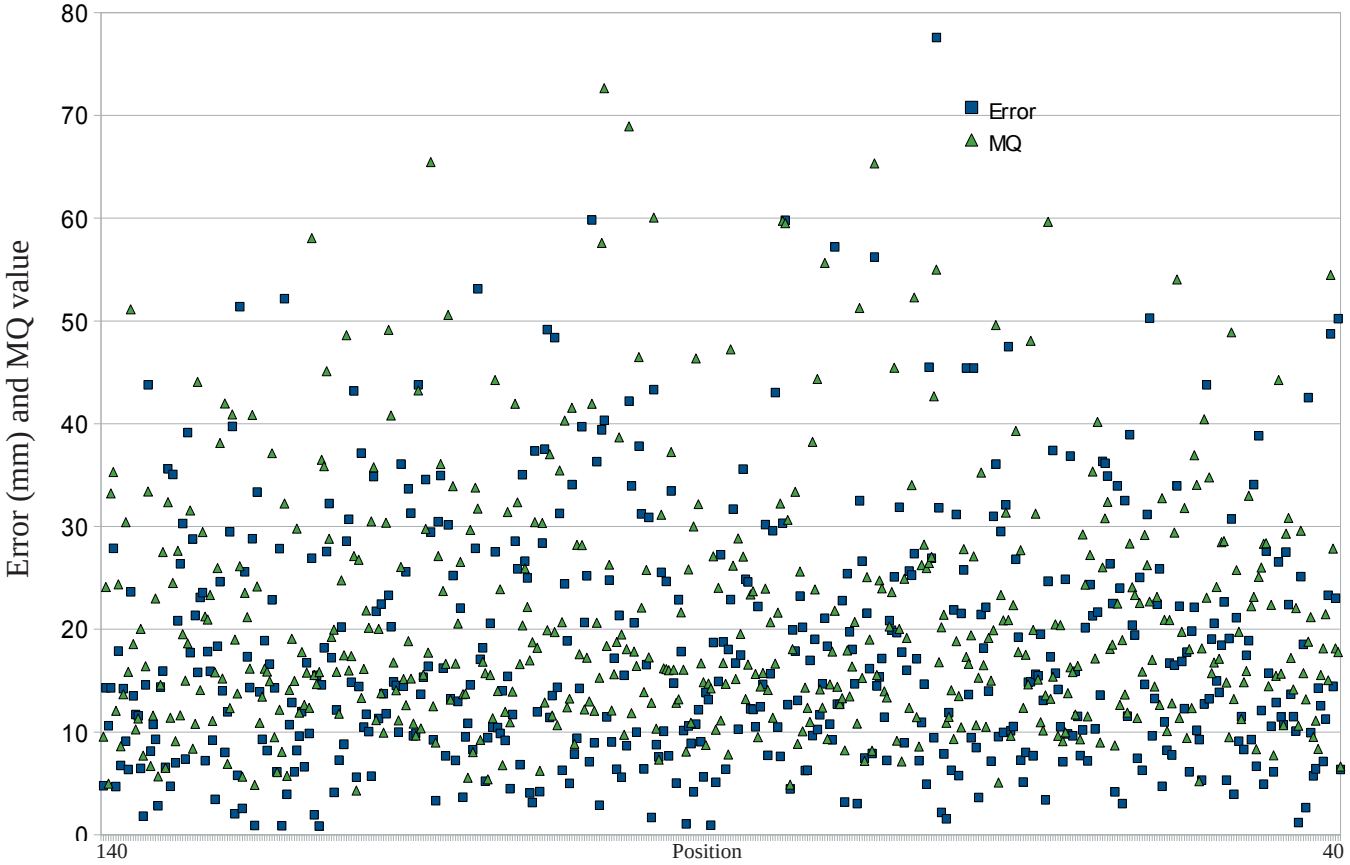

Figure 17: MDBA017, 3D antenna coil 2, Y position

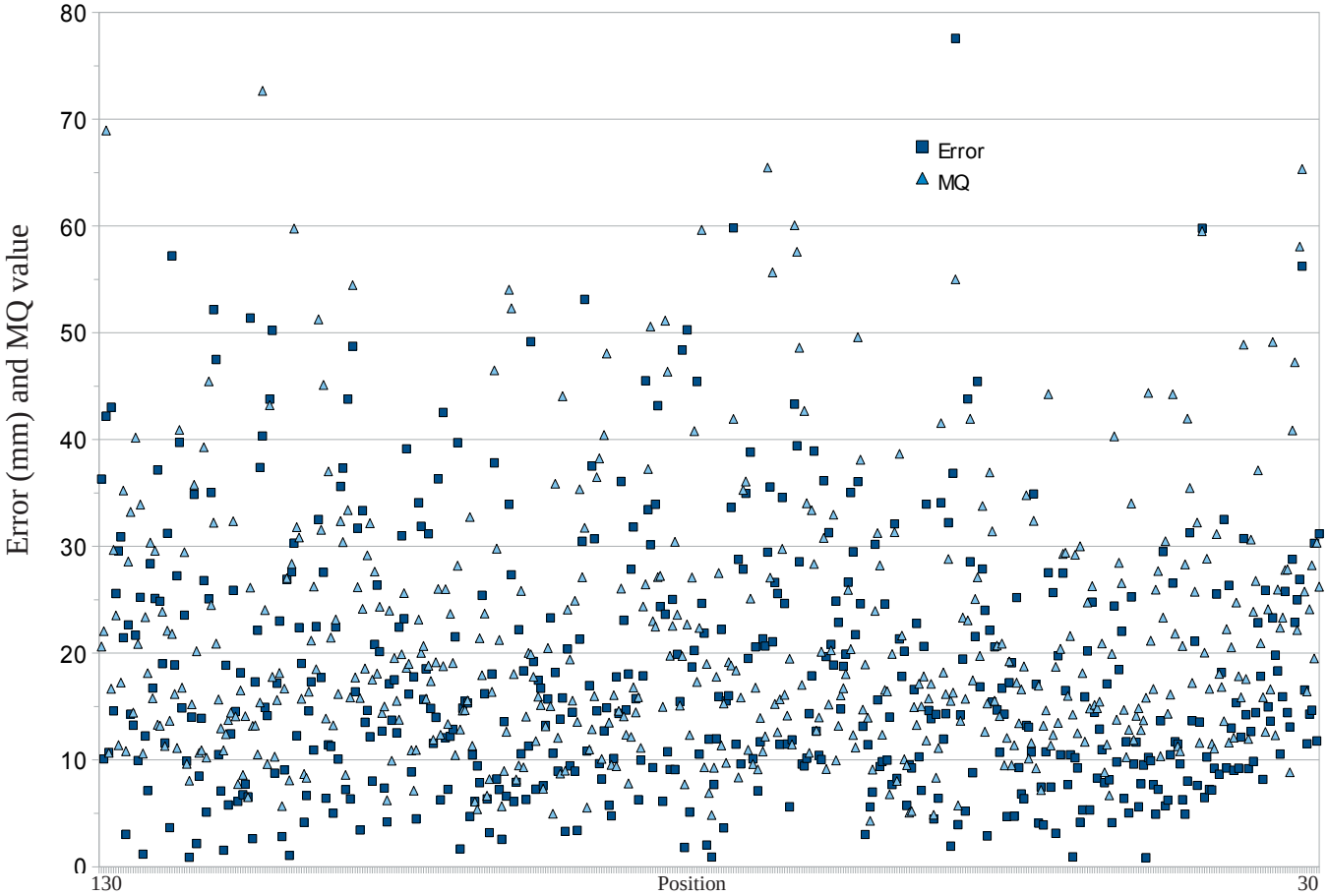

Figure 18: MDBA017, 3D antenna coil 2, Z position

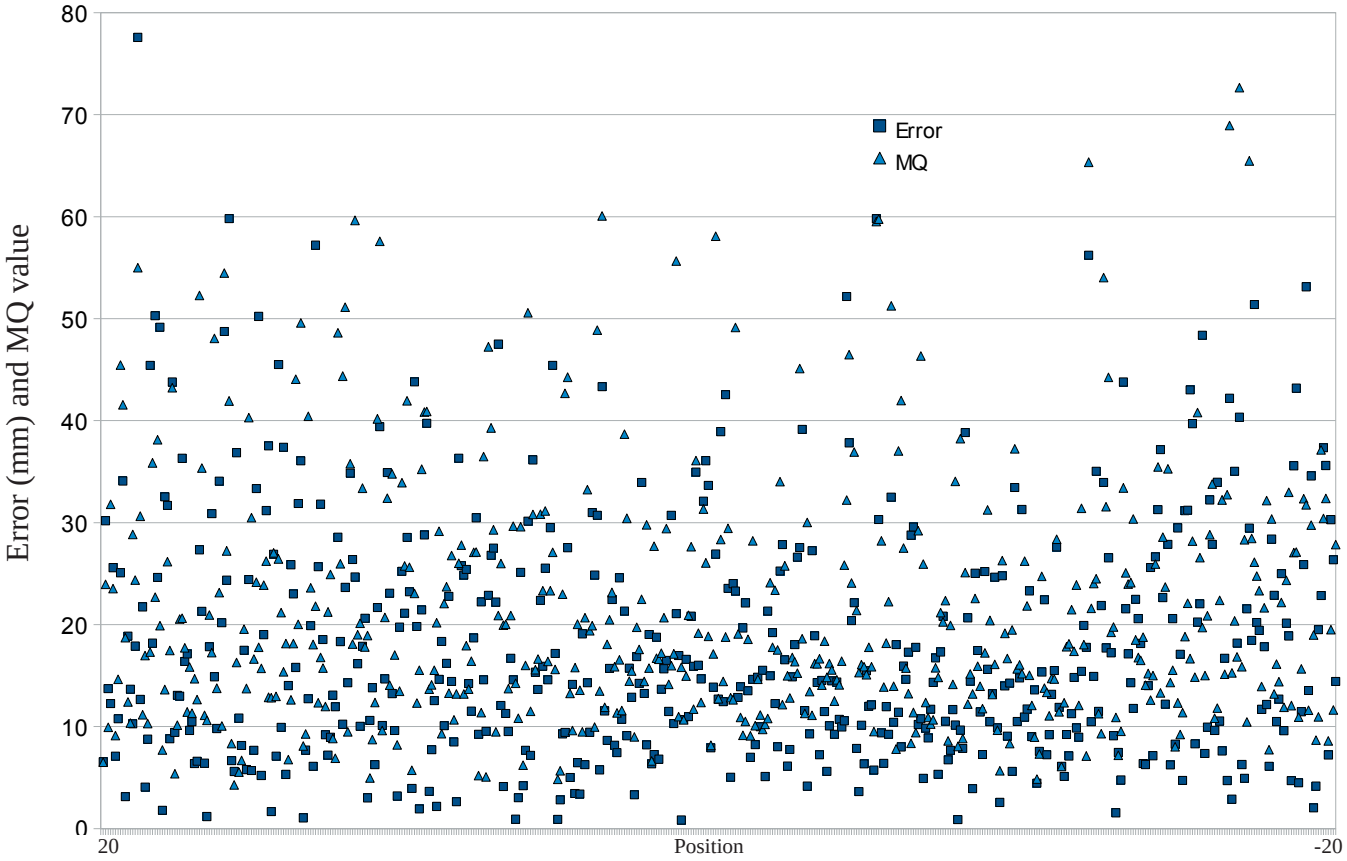

Figure 19: MDBA017, 3D antenna coil 2, Vy angle

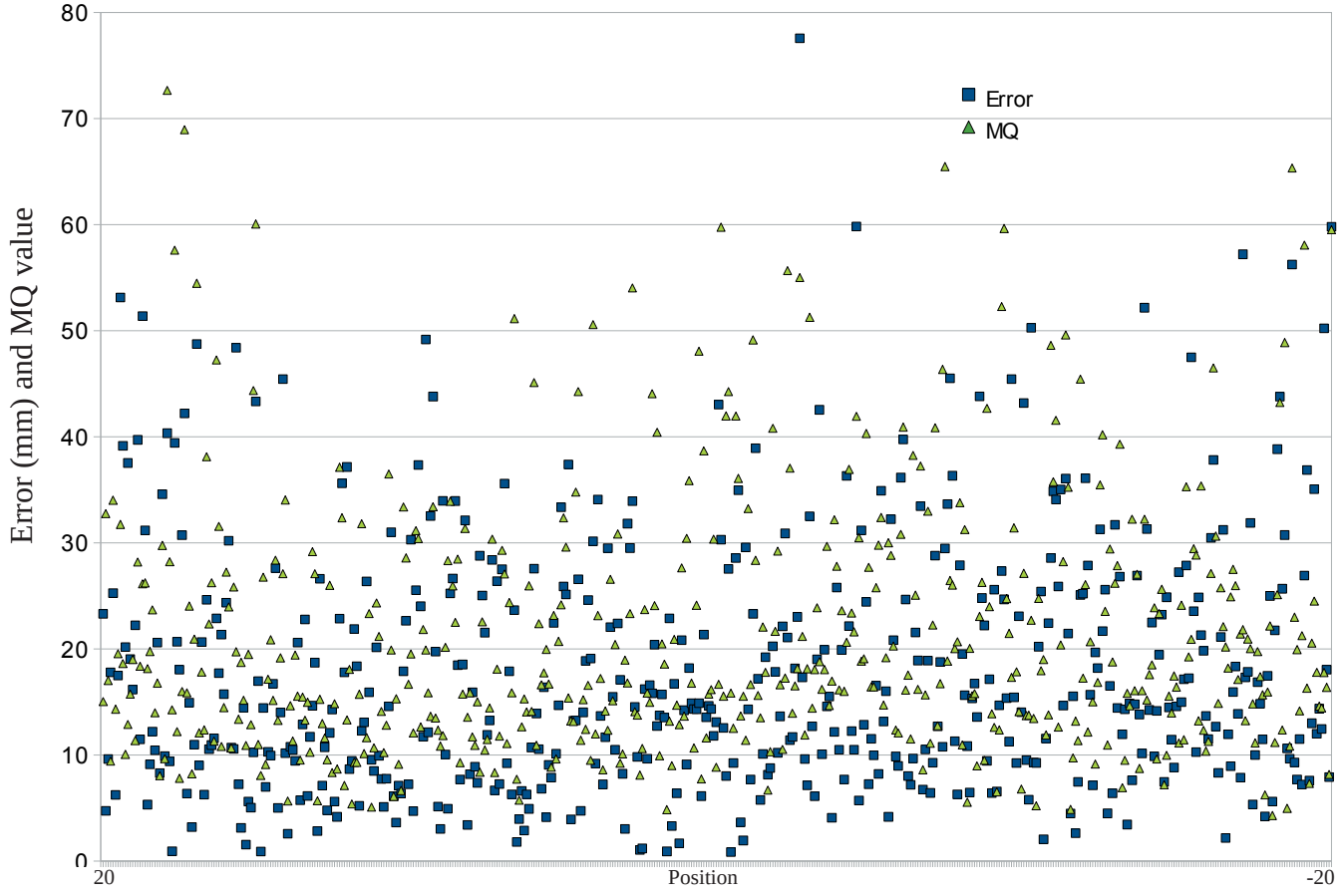

Figure 20: MDBA017, 3D antenna coil 2, Vz angle

A3. MSAT Plots

Y axis: Output voltage (V)
X axis: Variable X,Y,Z: distance (mm), variable Vy, Vz: angle (degrees)

A3.1 DB017, Hand-wired antenna

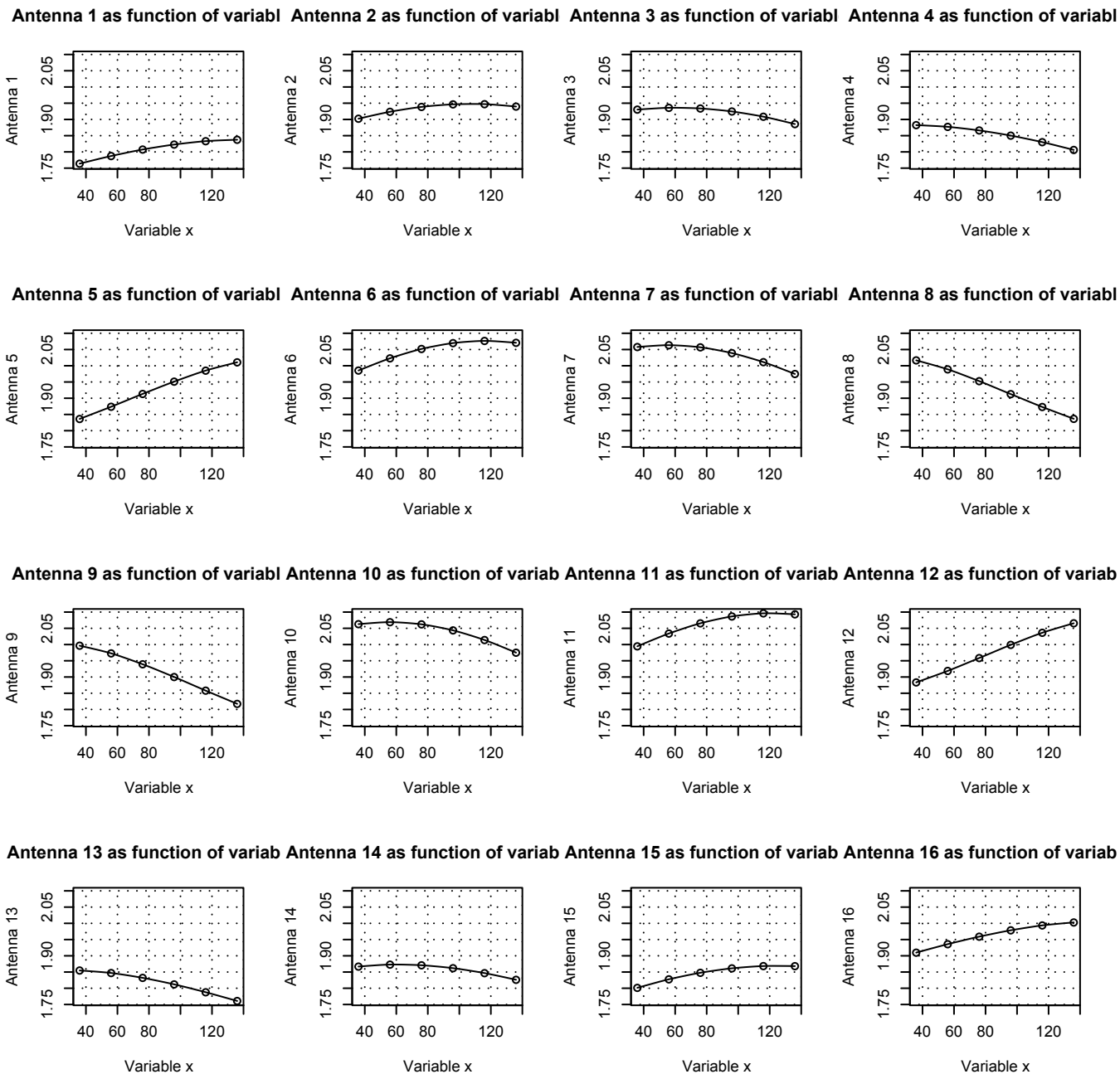

Antenna 1 as function of variabl

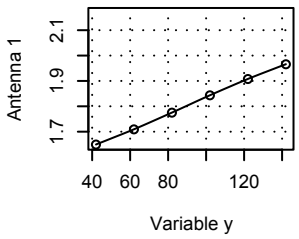

Antenna 2 as function of variabl

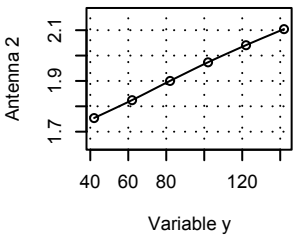

Antenna 3 as function of variabl

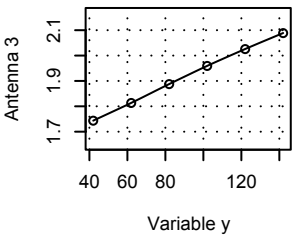

Antenna 4 as function of variabl

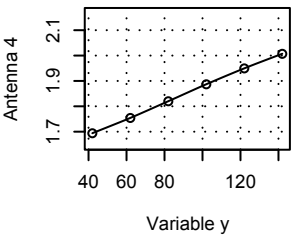

Antenna 5 as function of variabl

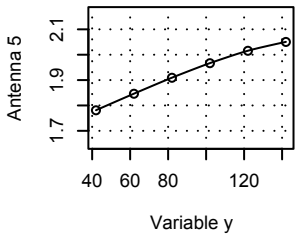

Antenna 6 as function of variabl

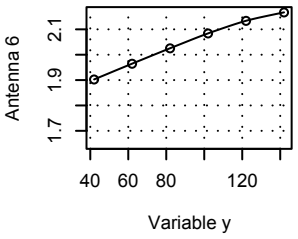

Antenna 7 as function of variabl

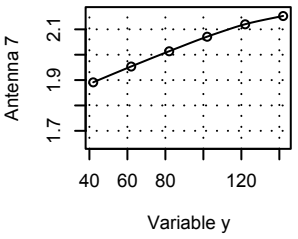

Antenna 8 as function of variabl

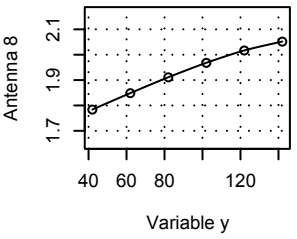

Antenna 9 as function of variabl

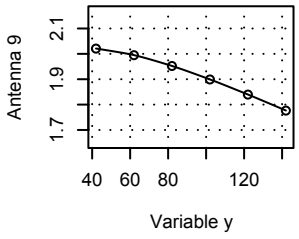

Antenna 10 as function of variab

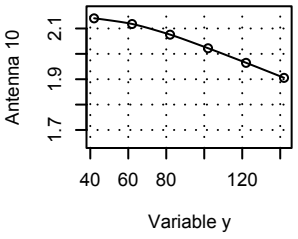

Antenna 11 as function of variab

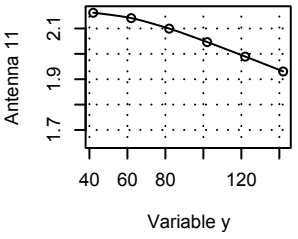

Antenna 12 as function of variab

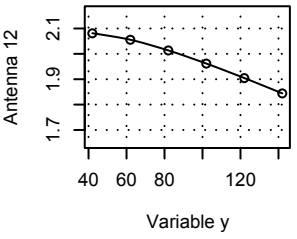

Antenna 13 as function of variab

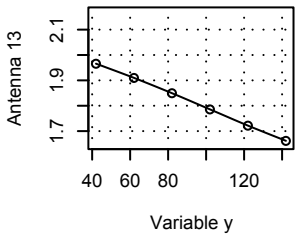

Antenna 14 as function of variab

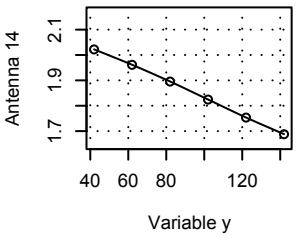

Antenna 15 as function of variab

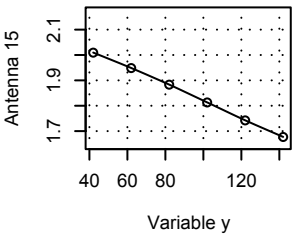

Antenna 16 as function of variab

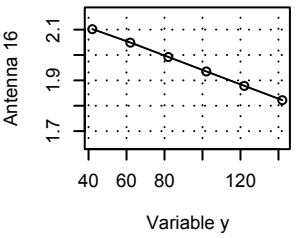

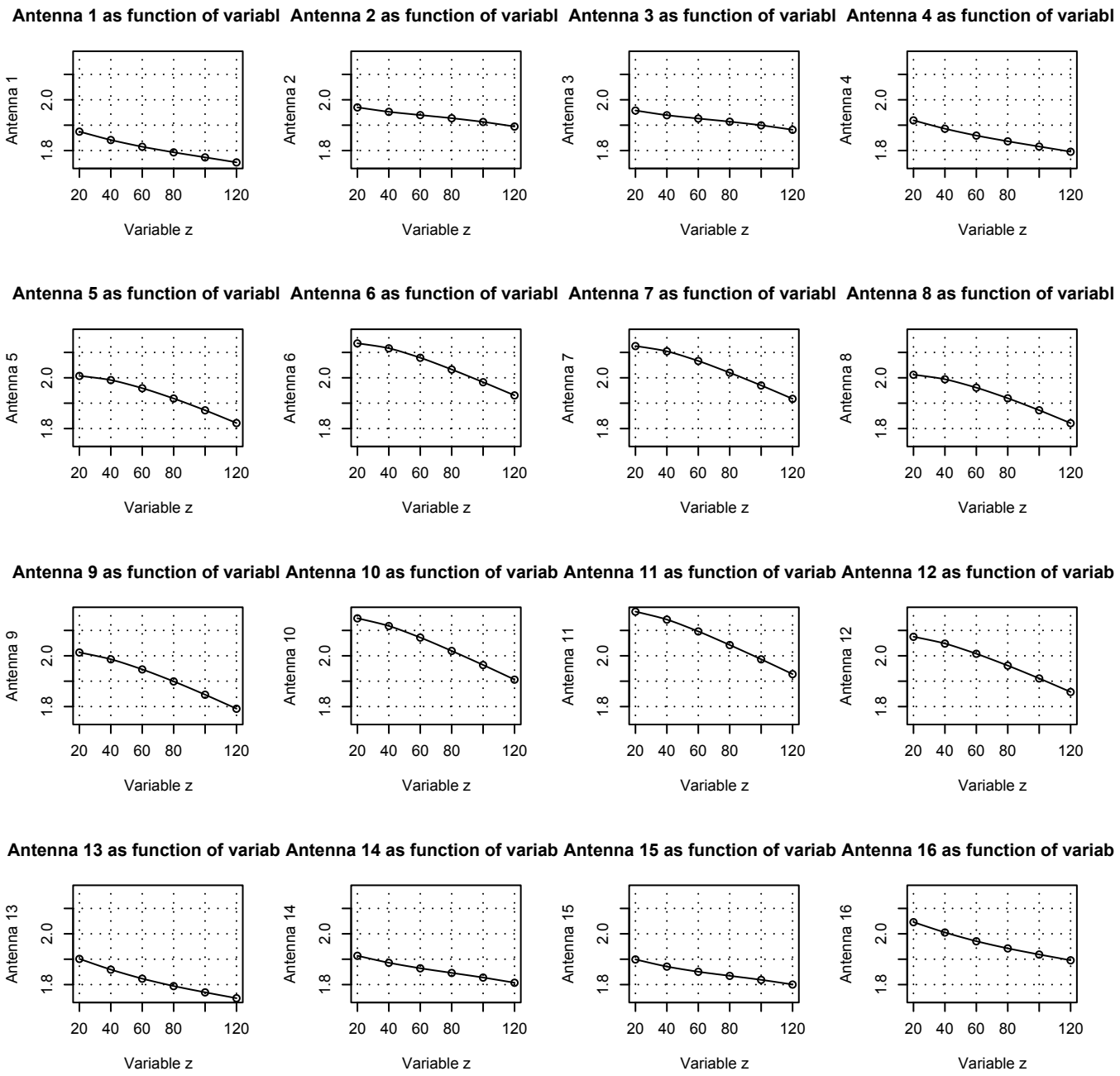
Antenna 1 as function of variabl
Antenna 2 as function of variabl
Antenna 3 as function of variabl
Antenna 4 as function of variabl
Antenna 5 as function of variabl
Antenna 6 as function of variabl
Antenna 7 as function of variabl
Antenna 8 as function of variabl
Antenna 9 as function of variabl
Antenna 10 as function of variab
Antenna 11 as function of variab
Antenna 12 as function of variab
Antenna 13 as function of variab
Antenna 14 as function of variab
Antenna 15 as function of variab
Antenna 16 as function of variab
Antenna 1
Antenna 2
Antenna 3
Antenna 4
Antenna 5
Antenna 6
Antenna 7
Antenna 8
Antenna 9
Antenna 10
Antenna 11
Antenna 12
Antenna 13
Antenna 14
Antenna 15
Antenna 16
1.8
2.0
20 40 60 80 120
Variable z

Antenna 1 as function of variable

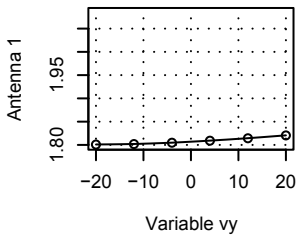

Antenna 2 as function of variable

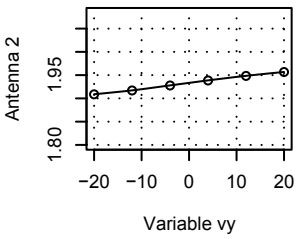

Antenna 3 as function of variable

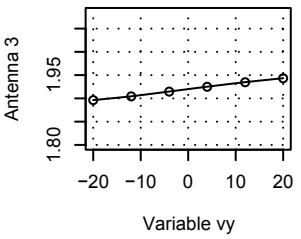

Antenna 4 as function of variable

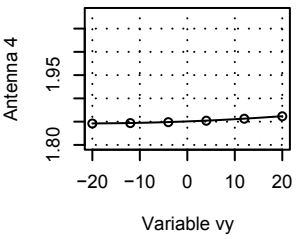

Antenna 5 as function of variable

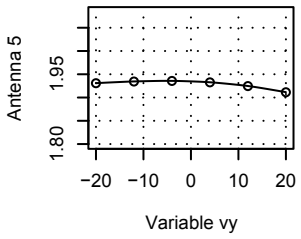

Antenna 6 as function of variable

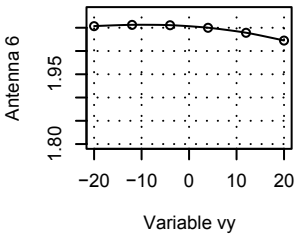

Antenna 7 as function of variable

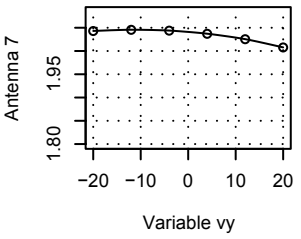

Antenna 8 as function of variable

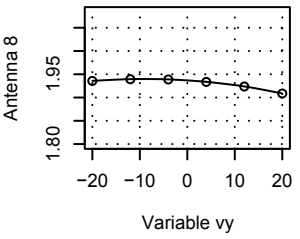

Antenna 9 as function of variable

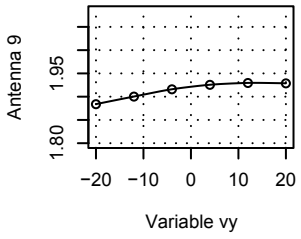

Antenna 10 as function of variabl

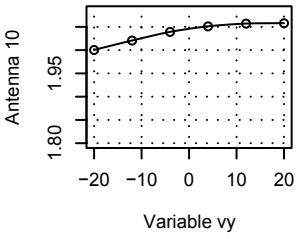

Antenna 11 as function of variabl

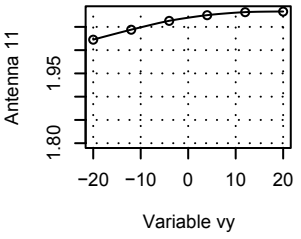

Antenna 12 as function of variabl

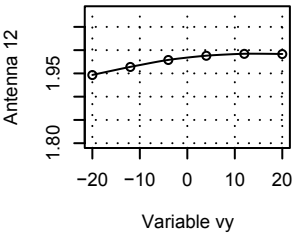

Antenna 13 as function of variabl

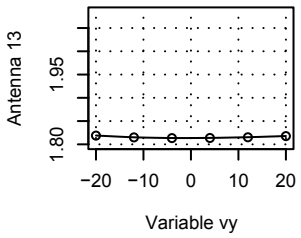

Antenna 14 as function of variabl

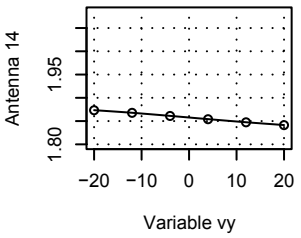

Antenna 15 as function of variabl

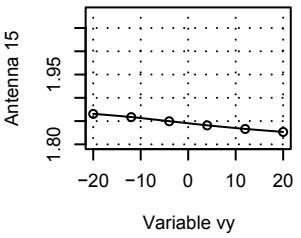

Antenna 16 as function of variabl

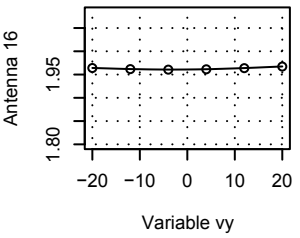

Antenna 1 as function of variable

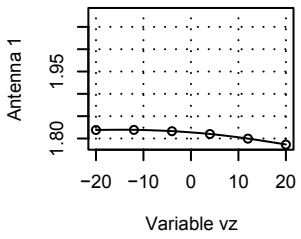

Antenna 2 as function of variable

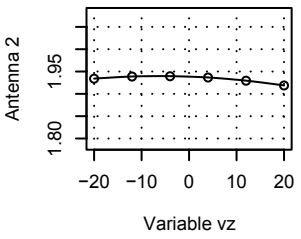

Antenna 3 as function of variable

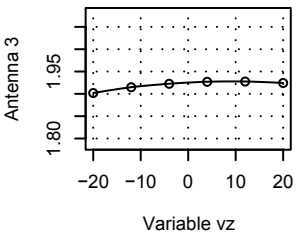

Antenna 4 as function of variable

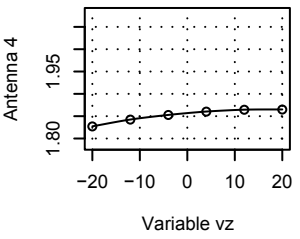

Antenna 5 as function of variable

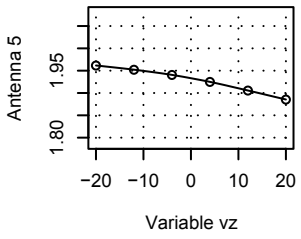

Antenna 6 as function of variable

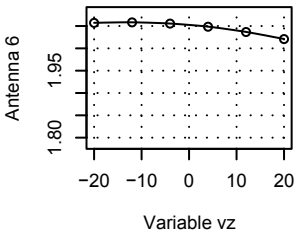

Antenna 7 as function of variable

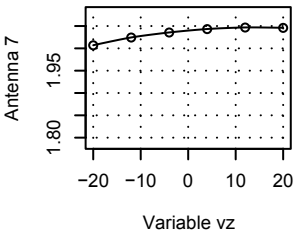

Antenna 8 as function of variable

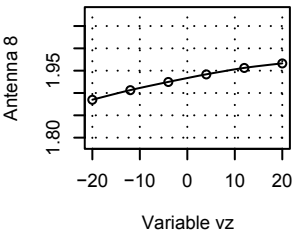

Antenna 9 as function of variable

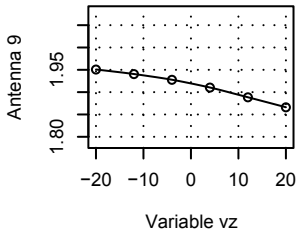

Antenna 10 as function of variabl

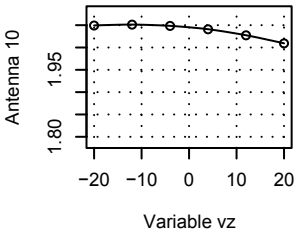

Antenna 11 as function of variabl

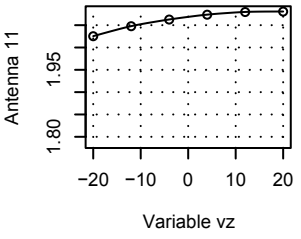

Antenna 12 as function of variabl

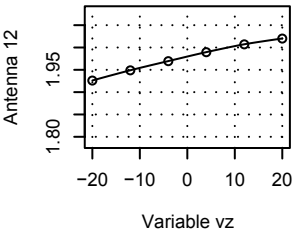

Antenna 13 as function of variabl

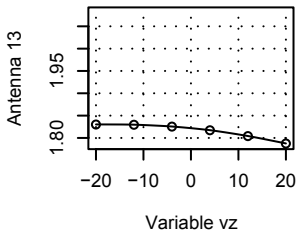

Antenna 14 as function of variabl

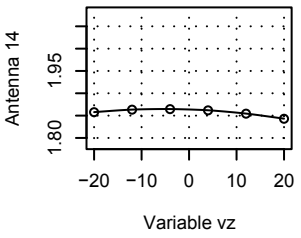

Antenna 15 as function of variabl

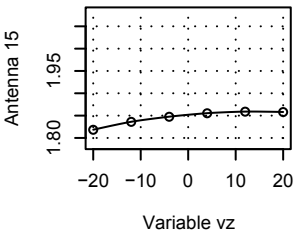

Antenna 16 as function of variabl

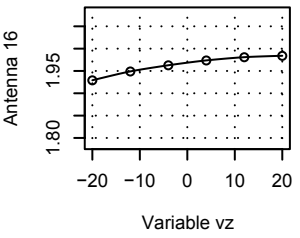

A3.2 DBA005, 3D-antenna coil 3

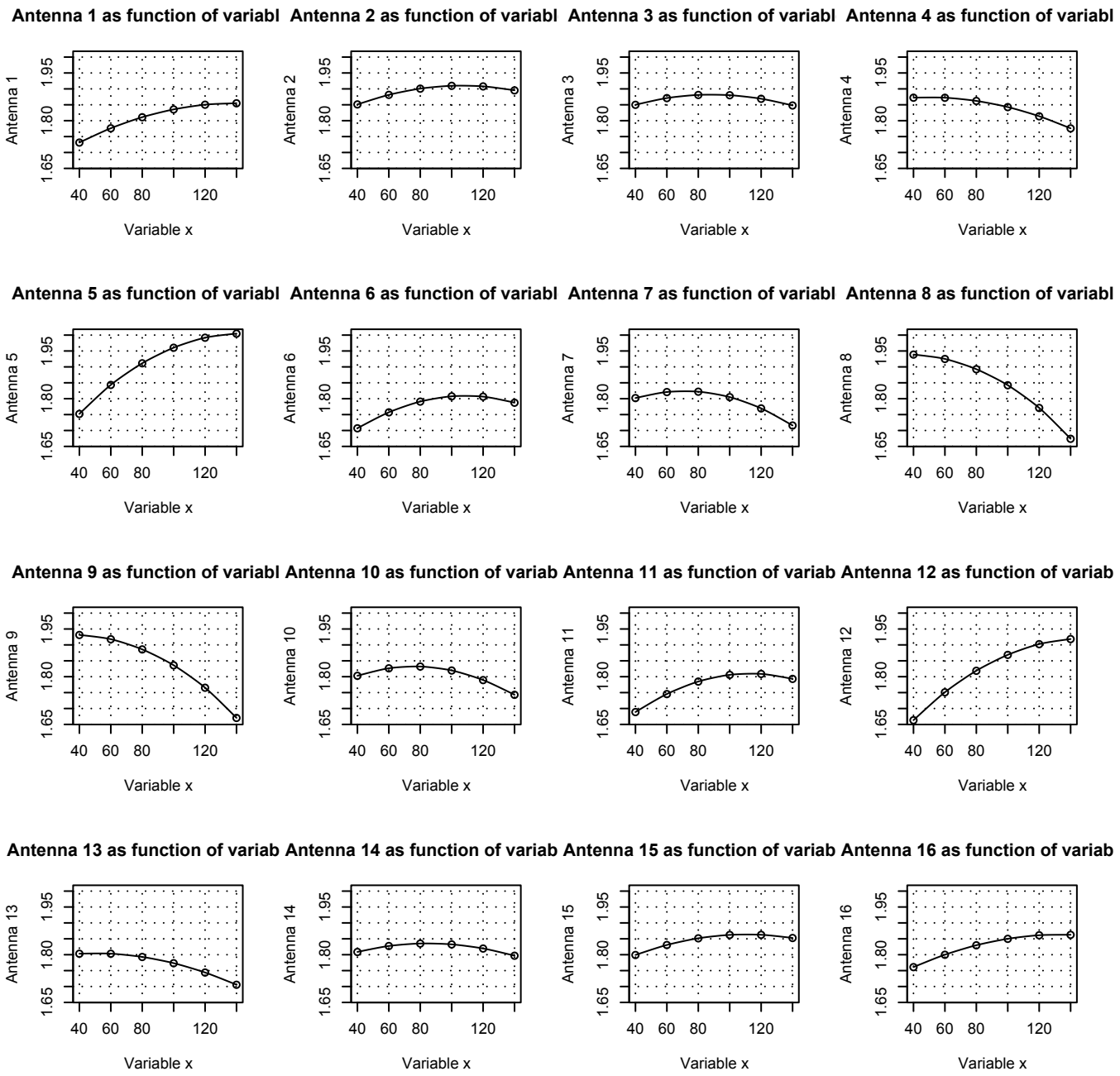

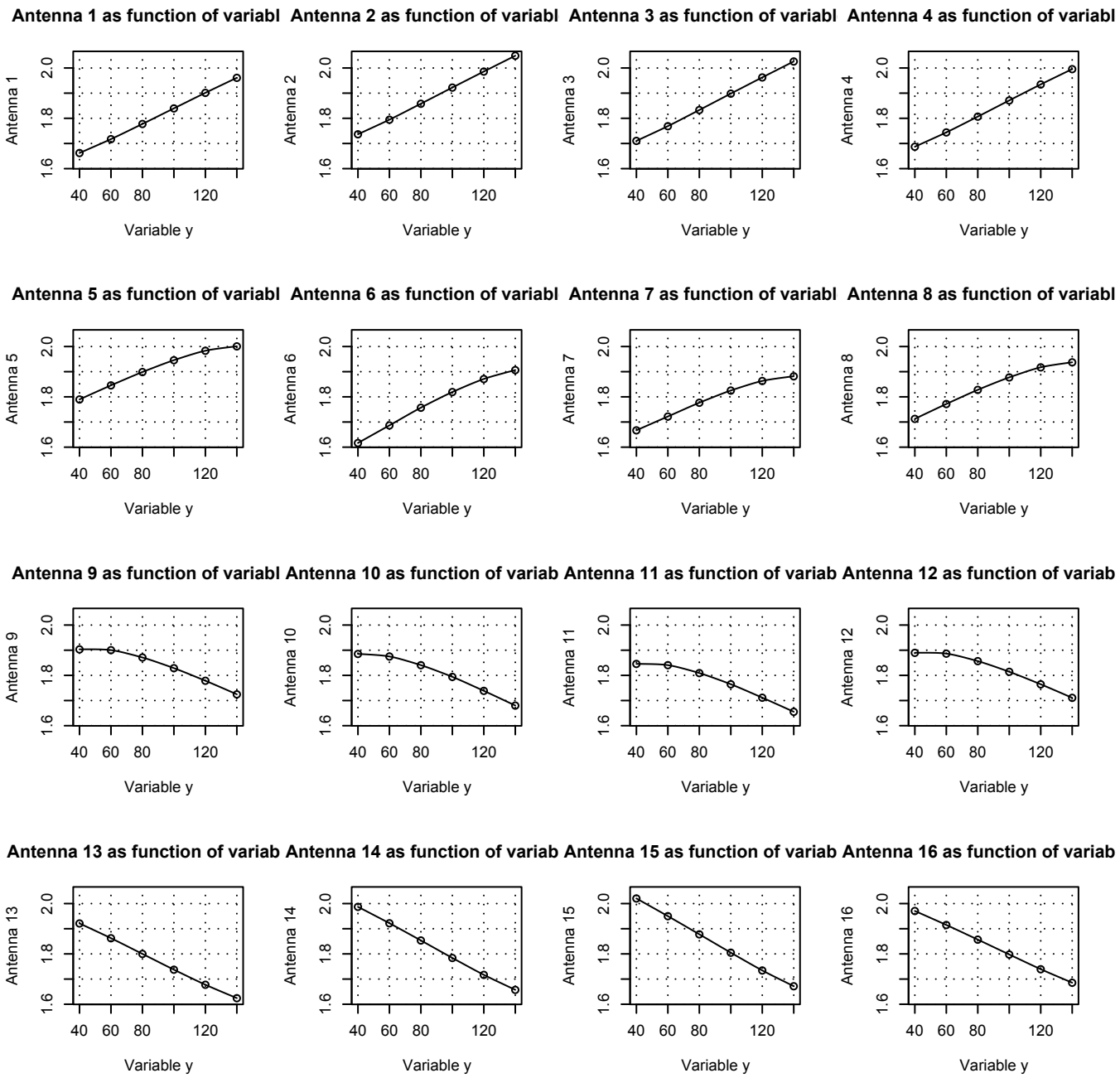
Antenna 1 as function of variabl
Antenna 2 as function of variabl
Antenna 3 as function of variabl
Antenna 4 as function of variabl
Antenna 5 as function of variabl
Antenna 6 as function of variabl
Antenna 7 as function of variabl
Antenna 8 as function of variabl
Antenna 9 as function of variabl
Antenna 10 as function of variab
Antenna 11 as function of variab
Antenna 12 as function of variab
Antenna 13 as function of variab
Antenna 14 as function of variab
Antenna 15 as function of variab
Antenna 16 as function of variab
Antenna 1
Antenna 2
Antenna 3
Antenna 4
Antenna 5
Antenna 6
Antenna 7
Antenna 8
Antenna 9
Antenna 10
Antenna 11
Antenna 12
Antenna 13
Antenna 14
Antenna 15
Antenna 16
1.6
1.8
2.0
40
60
80
120
Variable y

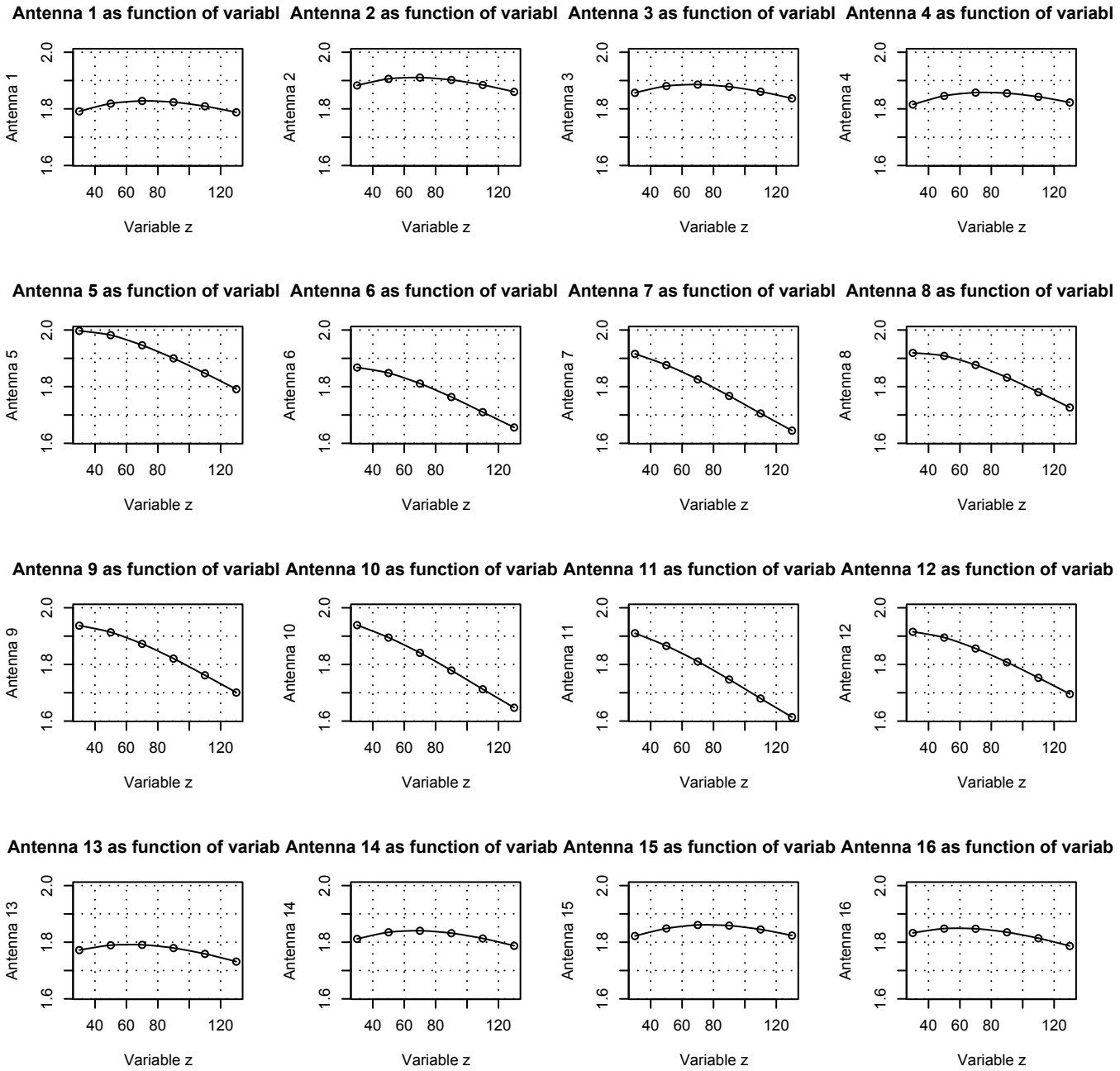
Antenna 1 as function of variabl
Antenna 2 as function of variabl
Antenna 3 as function of variabl
Antenna 4 as function of variabl
Antenna 5 as function of variabl
Antenna 6 as function of variabl
Antenna 7 as function of variabl
Antenna 8 as function of variabl
Antenna 9 as function of variabl
Antenna 10 as function of variab
Antenna 11 as function of variab
Antenna 12 as function of variab
Antenna 13 as function of variab
Antenna 14 as function of variab
Antenna 15 as function of variab
Antenna 16 as function of variab
Antenna 1
Antenna 2
Antenna 3
Antenna 4
Antenna 5
Antenna 6
Antenna 7
Antenna 8
Antenna 9
Antenna 10
Antenna 11
Antenna 12
Antenna 13
Antenna 14
Antenna 15
Antenna 16
1.6
1.8
2.0
40
60
80
120
Variable z

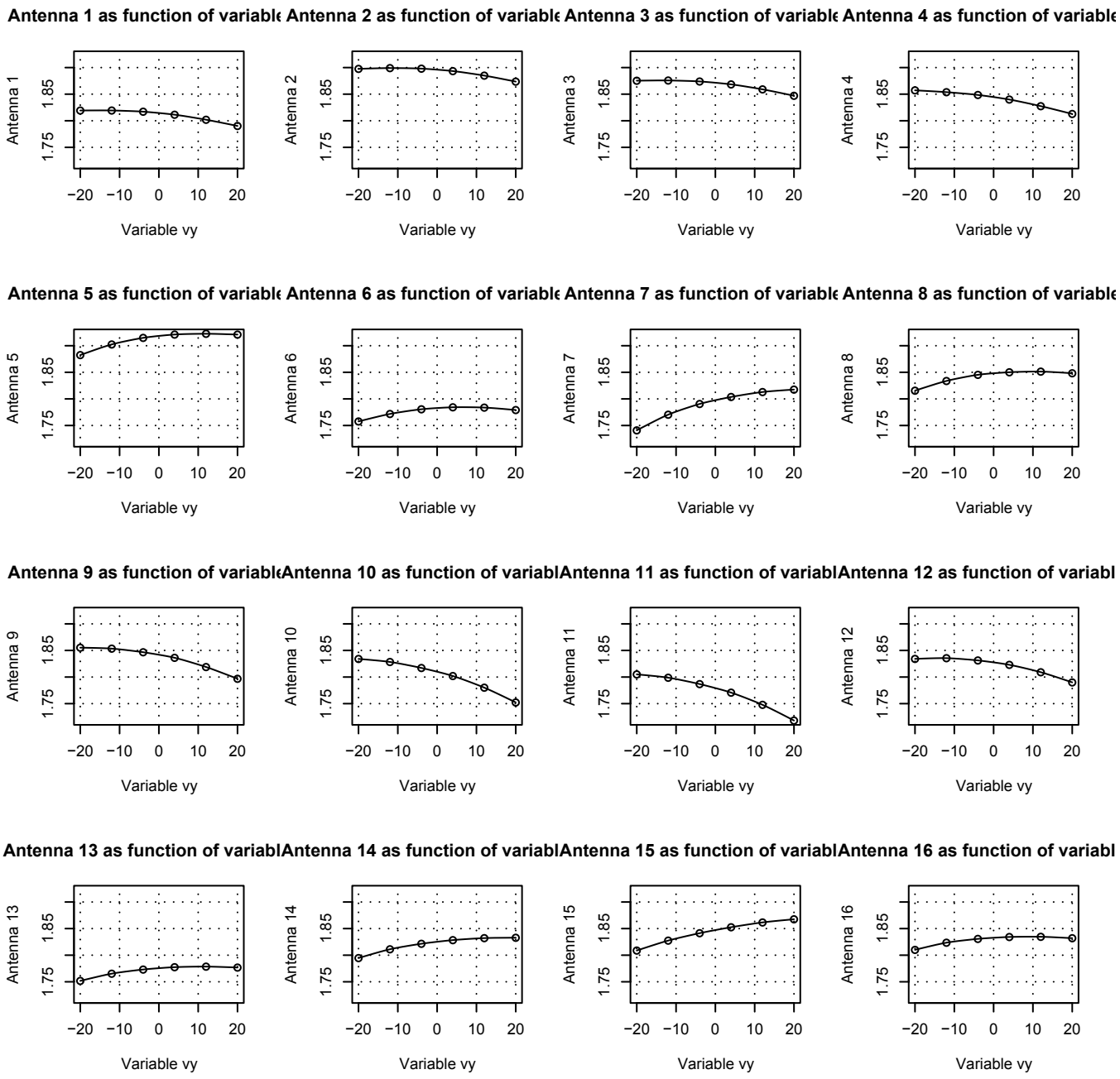
Antenna 1 as function of variable
Antenna 2 as function of variable
Antenna 3 as function of variable
Antenna 4 as function of variable
Antenna 5 as function of variable
Antenna 6 as function of variable
Antenna 7 as function of variable
Antenna 8 as function of variable
Antenna 9 as function of variable
Antenna 10 as function of variabl
Antenna 11 as function of variabl
Antenna 12 as function of variabl
Antenna 13 as function of variabl
Antenna 14 as function of variabl
Antenna 15 as function of variabl
Antenna 16 as function of variabl
Antenna 1
Antenna 2
Antenna 3
Antenna 4
Antenna 5
Antenna 6
Antenna 7
Antenna 8
Antenna 9
Antenna 10
Antenna 11
Antenna 12
Antenna 13
Antenna 14
Antenna 15
Antenna 16
1.75
1.85
−20 −10 0 10 20
Variable vy

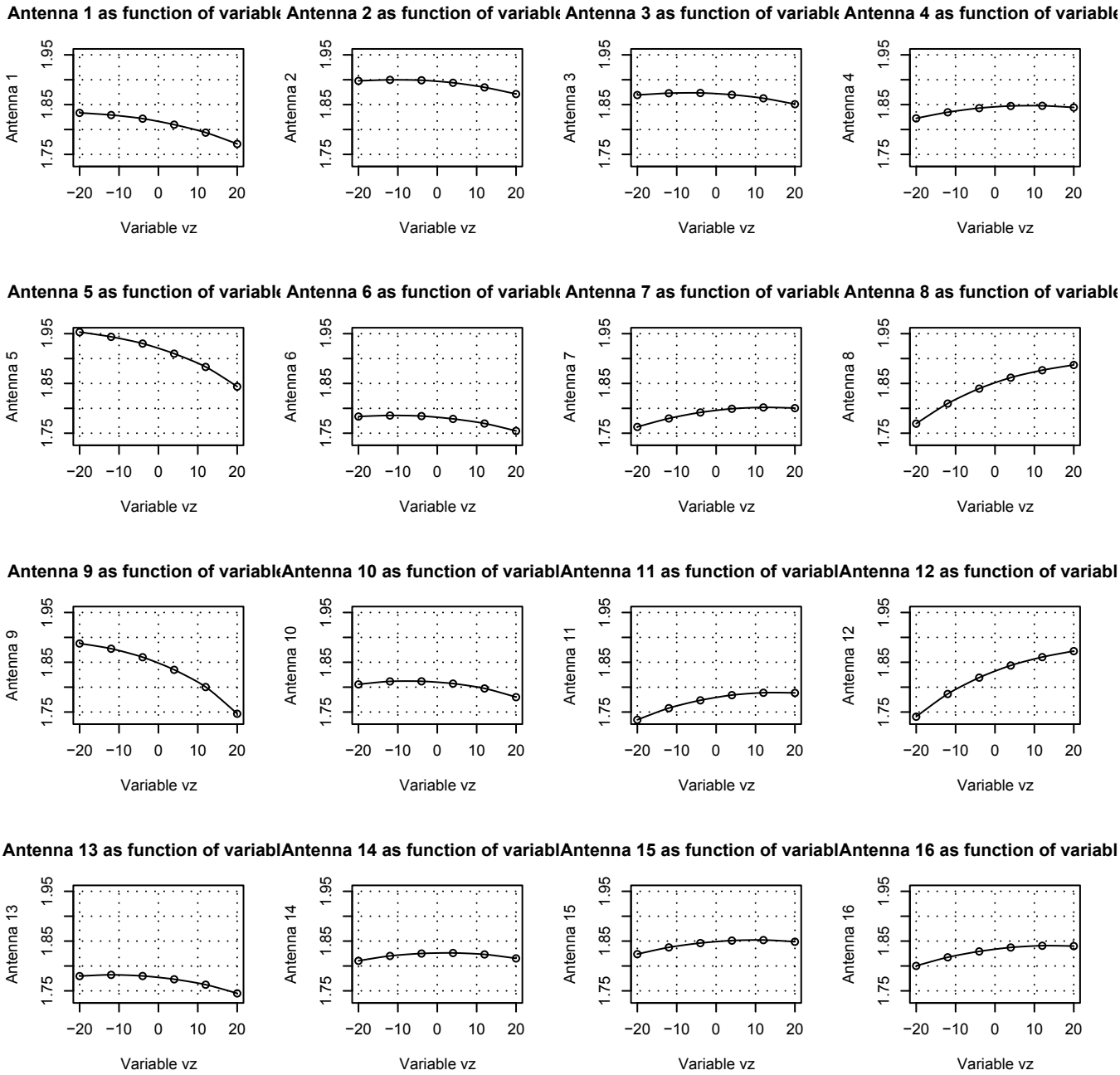
Antenna 1 as function of variable
Antenna 2 as function of variable
Antenna 3 as function of variable
Antenna 4 as function of variable
Antenna 5 as function of variable
Antenna 6 as function of variable
Antenna 7 as function of variable
Antenna 8 as function of variable
Antenna 9 as function of variable
Antenna 10 as function of variabl
Antenna 11 as function of variabl
Antenna 12 as function of variabl
Antenna 13 as function of variabl
Antenna 14 as function of variabl
Antenna 15 as function of variabl
Antenna 16 as function of variabl
Antenna 1
Antenna 2
Antenna 3
Antenna 4
Antenna 5
Antenna 6
Antenna 7
Antenna 8
Antenna 9
Antenna 10
Antenna 11
Antenna 12
Antenna 13
Antenna 14
Antenna 15
Antenna 16
1.75
1.85
1.95
−20
−10
0
10
20
Variable vz

A3.3 DBA014, 3D-antenna coil 1

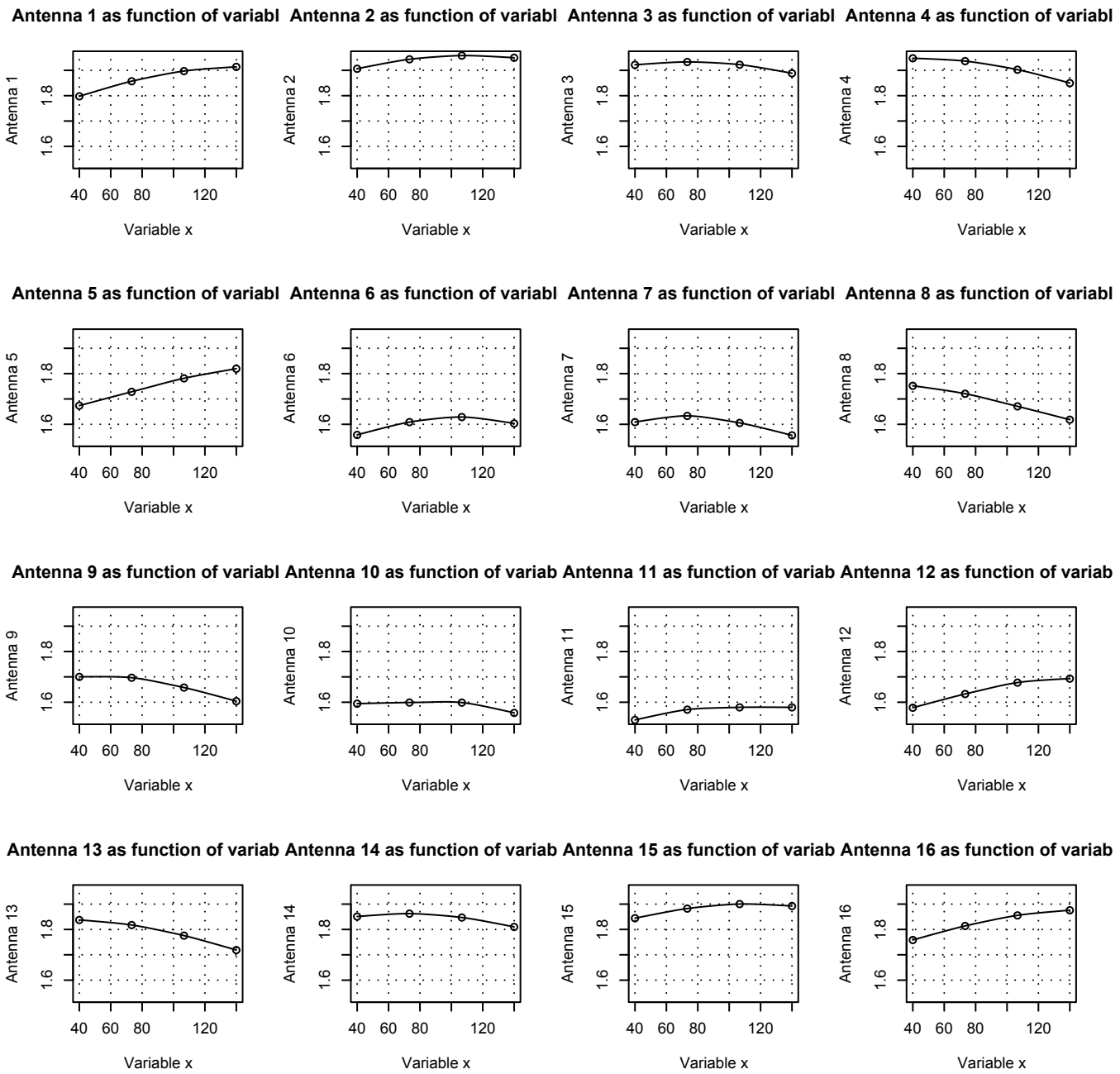

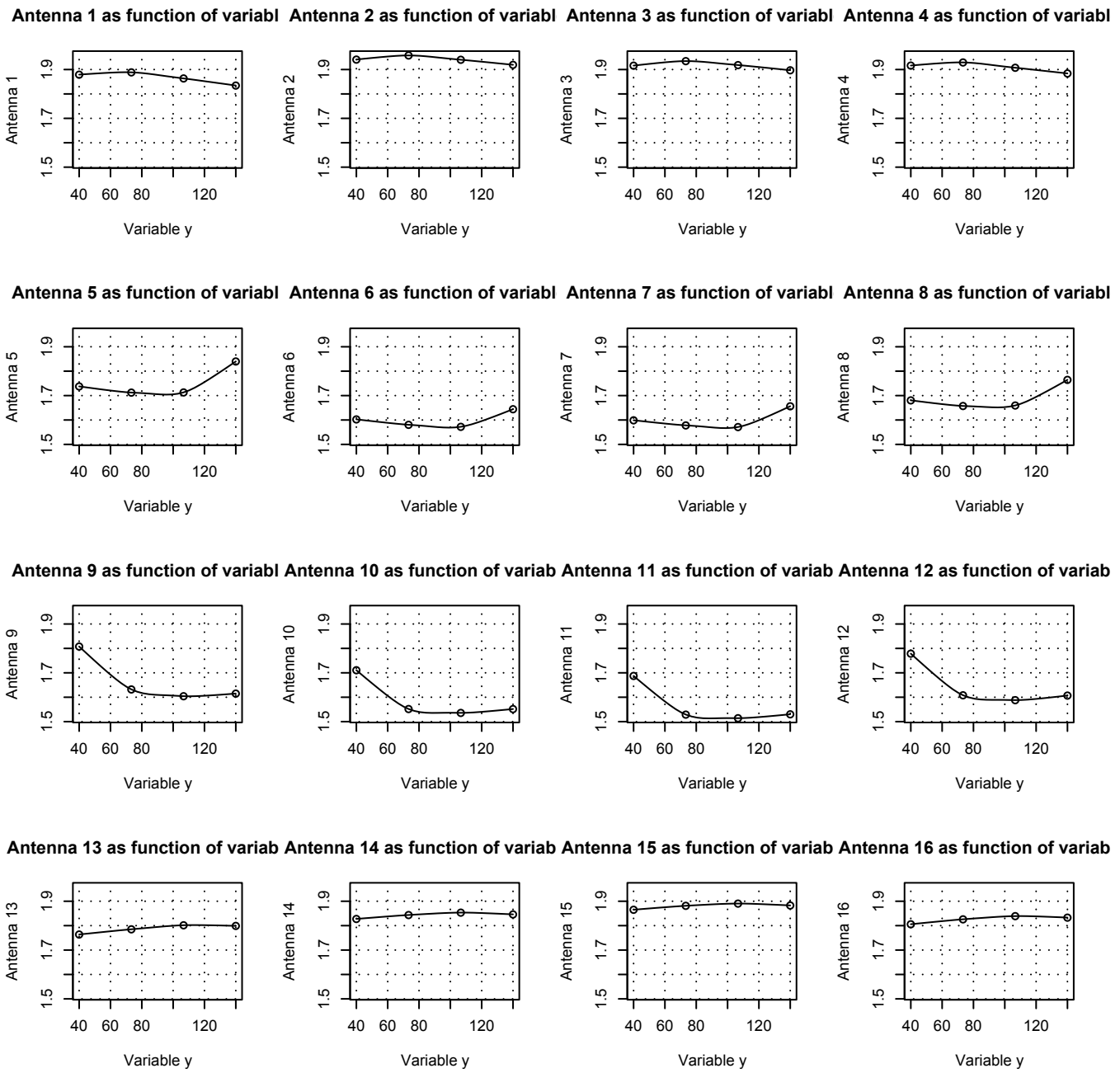
Antenna 1 as function of variabl
Antenna 2 as function of variabl
Antenna 3 as function of variabl
Antenna 4 as function of variabl
Antenna 5 as function of variabl
Antenna 6 as function of variabl
Antenna 7 as function of variabl
Antenna 8 as function of variabl
Antenna 9 as function of variabl
Antenna 10 as function of variab
Antenna 11 as function of variab
Antenna 12 as function of variab
Antenna 13 as function of variab
Antenna 14 as function of variab
Antenna 15 as function of variab
Antenna 16 as function of variab
Antenna 1
Antenna 2
Antenna 3
Antenna 4
Antenna 5
Antenna 6
Antenna 7
Antenna 8
Antenna 9
Antenna 10
Antenna 11
Antenna 12
Antenna 13
Antenna 14
Antenna 15
Antenna 16
1.5
1.7
1.9
40
60
80
120
Variable y

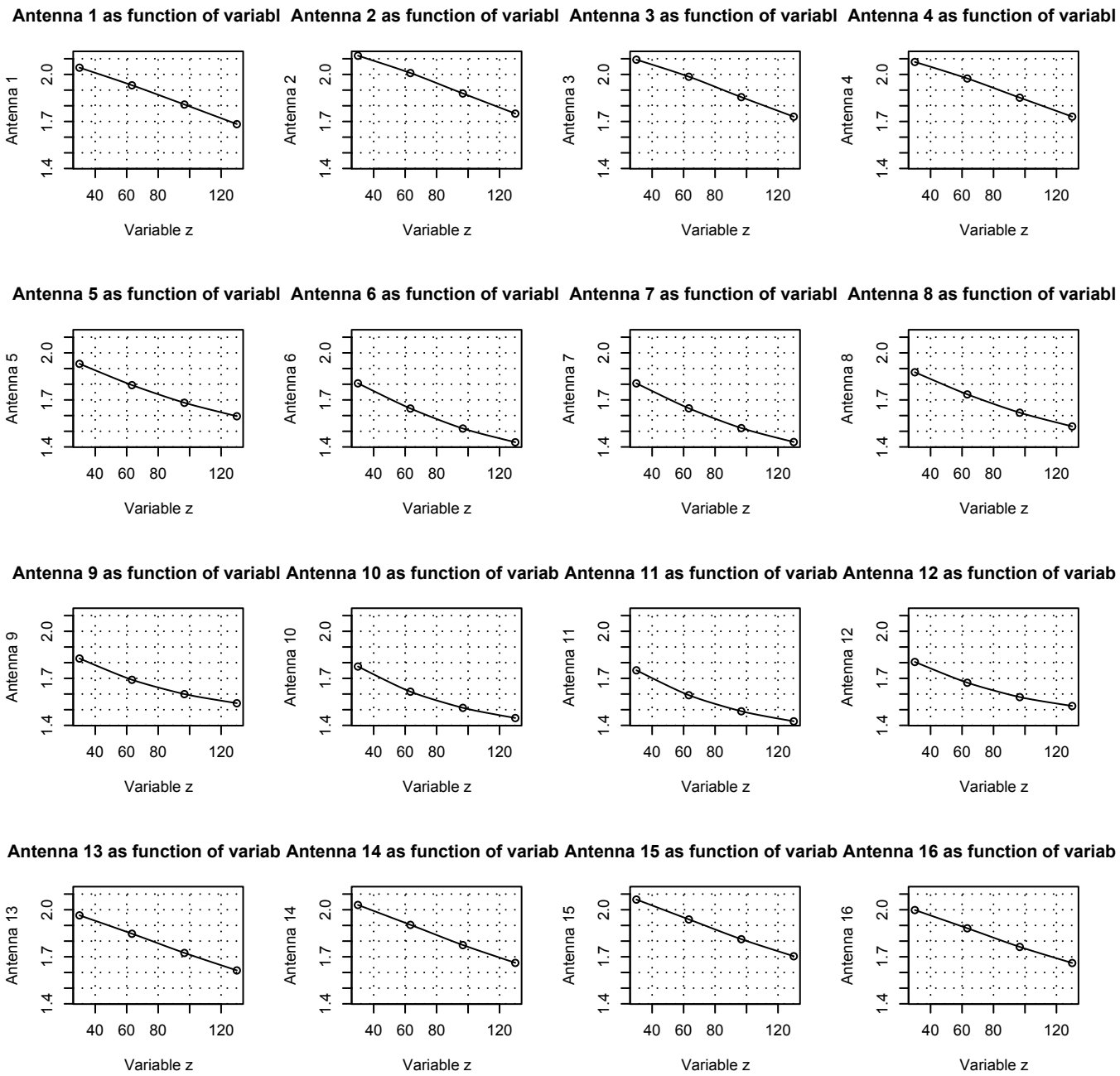
Antenna 1 as function of variabl
Antenna 2 as function of variabl
Antenna 3 as function of variabl
Antenna 4 as function of variabl
Antenna 5 as function of variabl
Antenna 6 as function of variabl
Antenna 7 as function of variabl
Antenna 8 as function of variabl
Antenna 9 as function of variabl
Antenna 10 as function of variab
Antenna 11 as function of variab
Antenna 12 as function of variab
Antenna 13 as function of variab
Antenna 14 as function of variab
Antenna 15 as function of variab
Antenna 16 as function of variab
Antenna 1
Antenna 2
Antenna 3
Antenna 4
Antenna 5
Antenna 6
Antenna 7
Antenna 8
Antenna 9
Antenna 10
Antenna 11
Antenna 12
Antenna 13
Antenna 14
Antenna 15
Antenna 16
1.4
1.7
2.0
40
60
80
120
Variable z

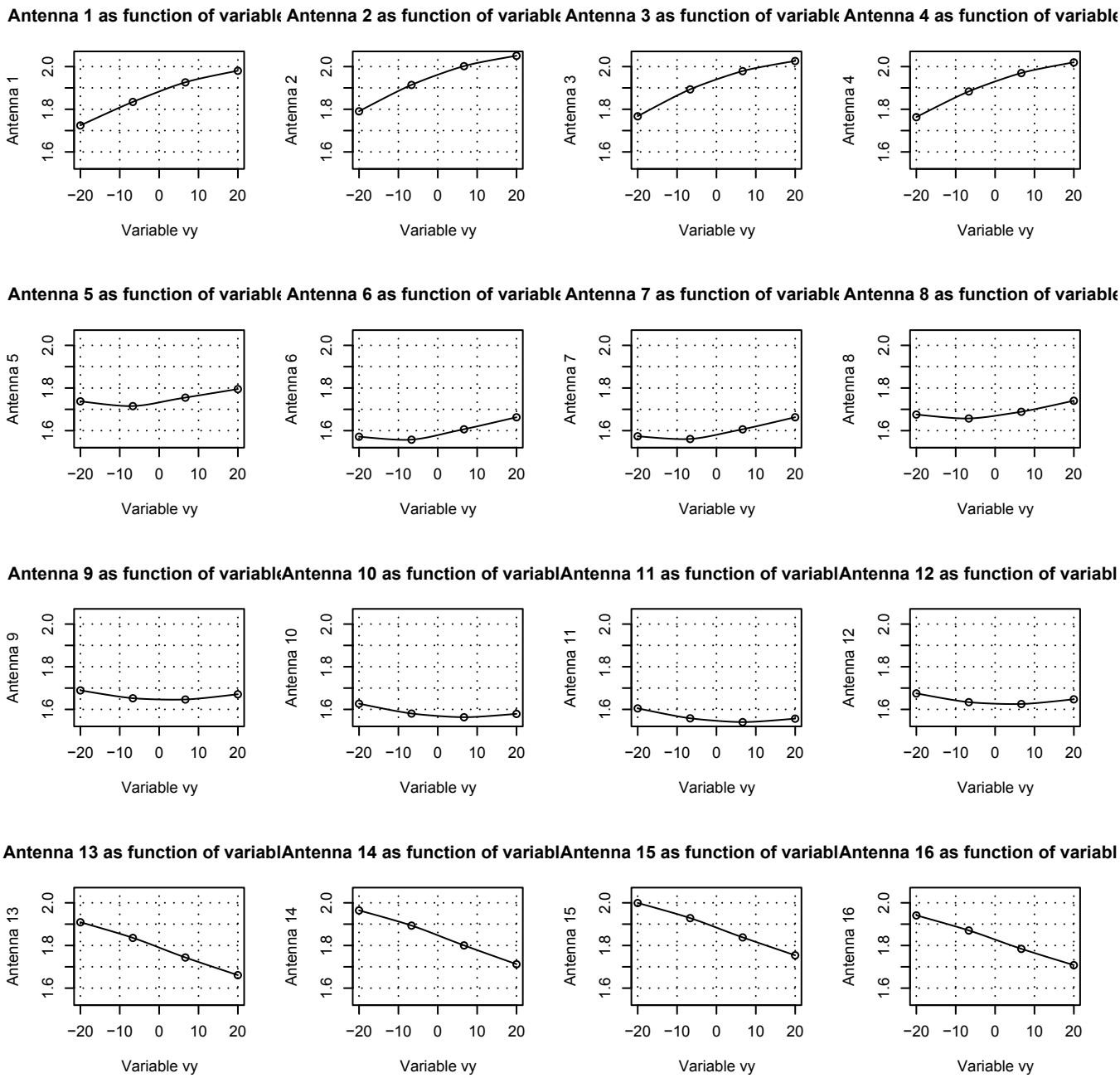
Antenna 1 as function of variable
Antenna 2 as function of variable
Antenna 3 as function of variable
Antenna 4 as function of variable
Antenna 5 as function of variable
Antenna 6 as function of variable
Antenna 7 as function of variable
Antenna 8 as function of variable
Antenna 9 as function of variable
Antenna 10 as function of variabl
Antenna 11 as function of variabl
Antenna 12 as function of variabl
Antenna 13 as function of variabl
Antenna 14 as function of variabl
Antenna 15 as function of variabl
Antenna 16 as function of variabl
Antenna 1
Antenna 2
Antenna 3
Antenna 4
Antenna 5
Antenna 6
Antenna 7
Antenna 8
Antenna 9
Antenna 10
Antenna 11
Antenna 12
Antenna 13
Antenna 14
Antenna 15
Antenna 16
1.6
1.8
2.0
−20
−10
0
10
20
Variable vy

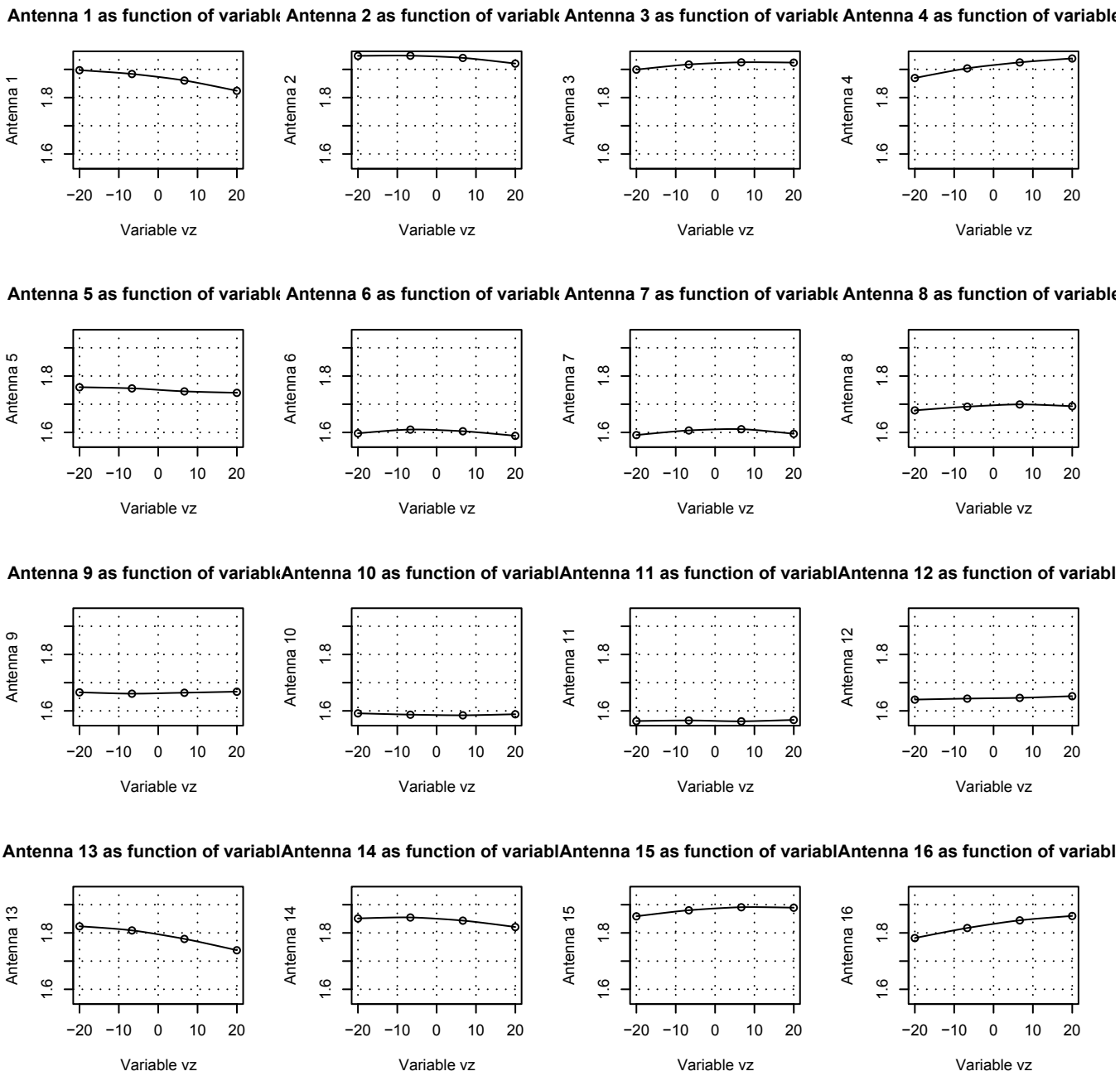
Antenna 1 as function of variable
Antenna 2 as function of variable
Antenna 3 as function of variable
Antenna 4 as function of variable
Antenna 5 as function of variable
Antenna 6 as function of variable
Antenna 7 as function of variable
Antenna 8 as function of variable
Antenna 9 as function of variable
Antenna 10 as function of variabl
Antenna 11 as function of variabl
Antenna 12 as function of variabl
Antenna 13 as function of variabl
Antenna 14 as function of variabl
Antenna 15 as function of variabl
Antenna 16 as function of variabl
Antenna 1
Antenna 2
Antenna 3
Antenna 4
Antenna 5
Antenna 6
Antenna 7
Antenna 8
Antenna 9
Antenna 10
Antenna 11
Antenna 12
Antenna 13
Antenna 14
Antenna 15
Antenna 16
1.6
1.8
−20 −10 0 10 20
Variable vz

A3.4 DBA017, 3D-antenna coil 2

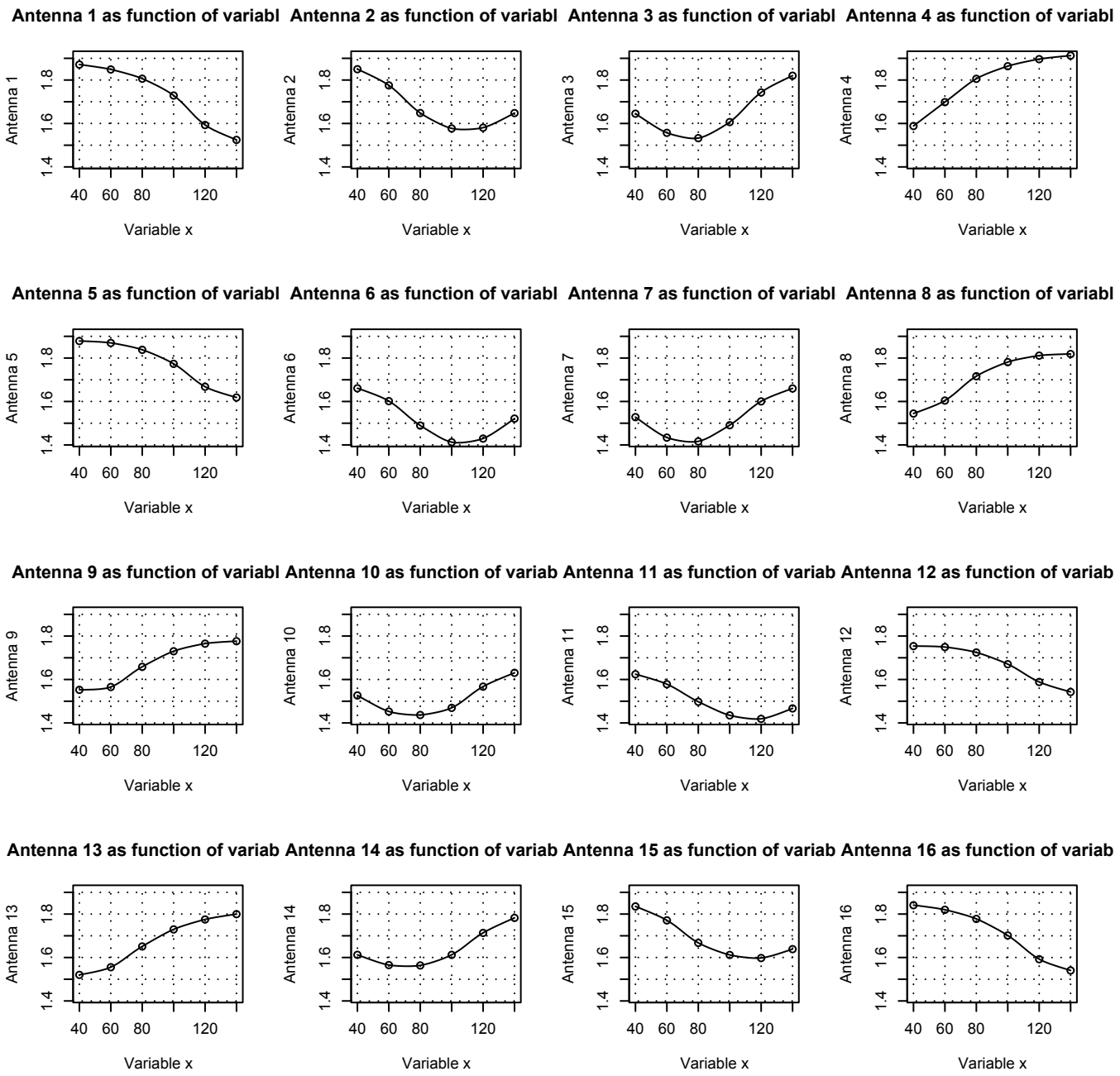

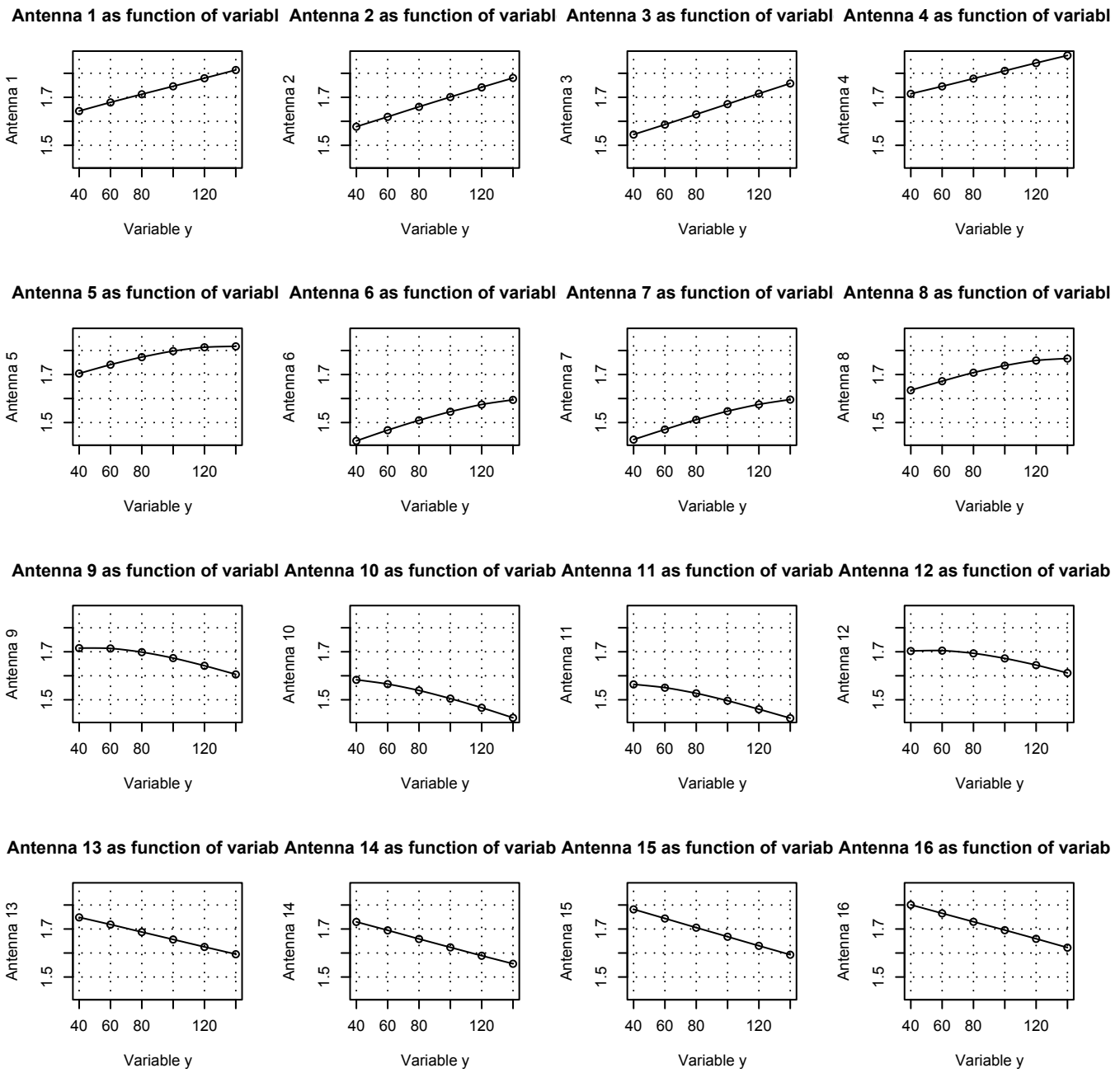
Antenna 1 as function of variabl
Antenna 2 as function of variabl
Antenna 3 as function of variabl
Antenna 4 as function of variabl
Antenna 5 as function of variabl
Antenna 6 as function of variabl
Antenna 7 as function of variabl
Antenna 8 as function of variabl
Antenna 9 as function of variabl
Antenna 10 as function of variab
Antenna 11 as function of variab
Antenna 12 as function of variab
Antenna 13 as function of variab
Antenna 14 as function of variab
Antenna 15 as function of variab
Antenna 16 as function of variab
Antenna 1
Antenna 2
Antenna 3
Antenna 4
Antenna 5
Antenna 6
Antenna 7
Antenna 8
Antenna 9
Antenna 10
Antenna 11
Antenna 12
Antenna 13
Antenna 14
Antenna 15
Antenna 16
1.5
1.7
40
60
80
120
Variable y

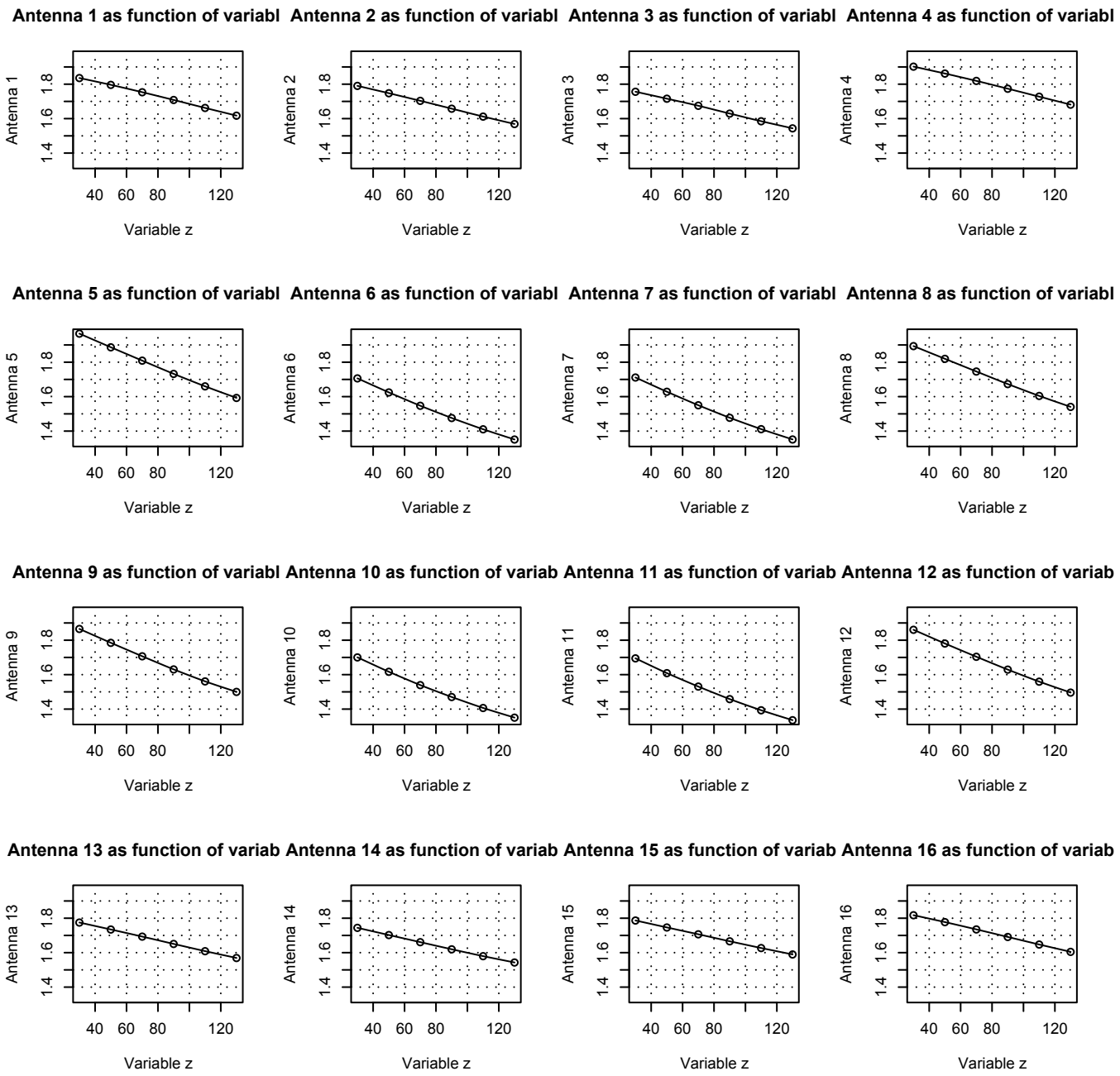
Antenna 1 as function of variabl
Antenna 2 as function of variabl
Antenna 3 as function of variabl
Antenna 4 as function of variabl
Antenna 5 as function of variabl
Antenna 6 as function of variabl
Antenna 7 as function of variabl
Antenna 8 as function of variabl
Antenna 9 as function of variabl
Antenna 10 as function of variab
Antenna 11 as function of variab
Antenna 12 as function of variab
Antenna 13 as function of variab
Antenna 14 as function of variab
Antenna 15 as function of variab
Antenna 16 as function of variab
Antenna 1
Antenna 2
Antenna 3
Antenna 4
Antenna 5
Antenna 6
Antenna 7
Antenna 8
Antenna 9
Antenna 10
Antenna 11
Antenna 12
Antenna 13
Antenna 14
Antenna 15
Antenna 16
1.4 1.6 1.8
40 60 80 120
Variable z

Antenna 1 as function of variable

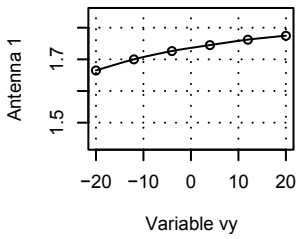

Antenna 2 as function of variable

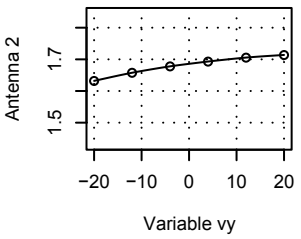

Antenna 3 as function of variable

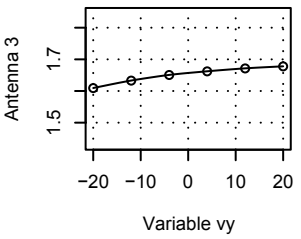

Antenna 4 as function of variable

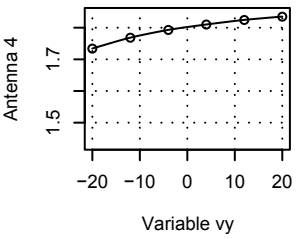

Antenna 5 as function of variable

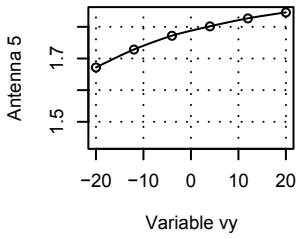

Antenna 6 as function of variable

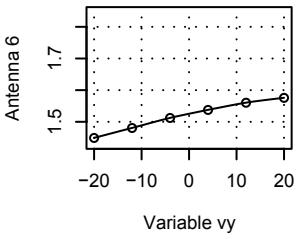

Antenna 7 as function of variable

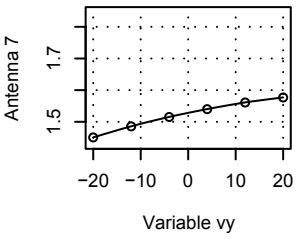

Antenna 8 as function of variable

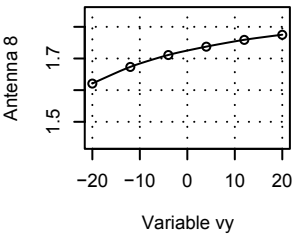

Antenna 9 as function of variable

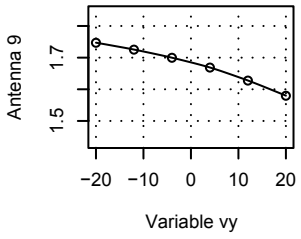

Antenna 10 as function of variabl

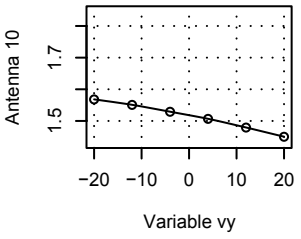

Antenna 11 as function of variabl

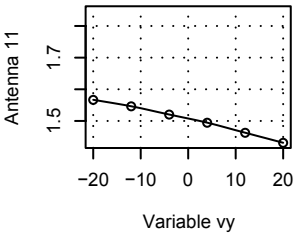

Antenna 12 as function of variabl

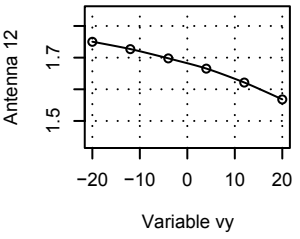

Antenna 13 as function of variabl

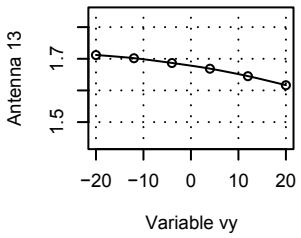

Antenna 14 as function of variabl

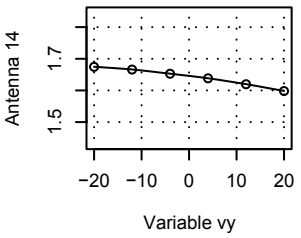

Antenna 15 as function of variabl

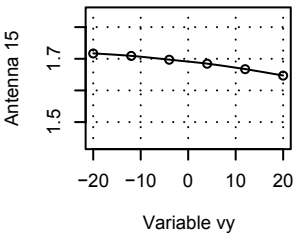

Antenna 16 as function of variabl

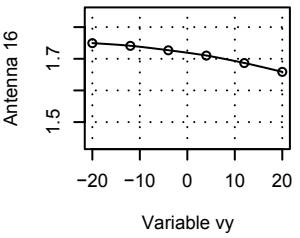

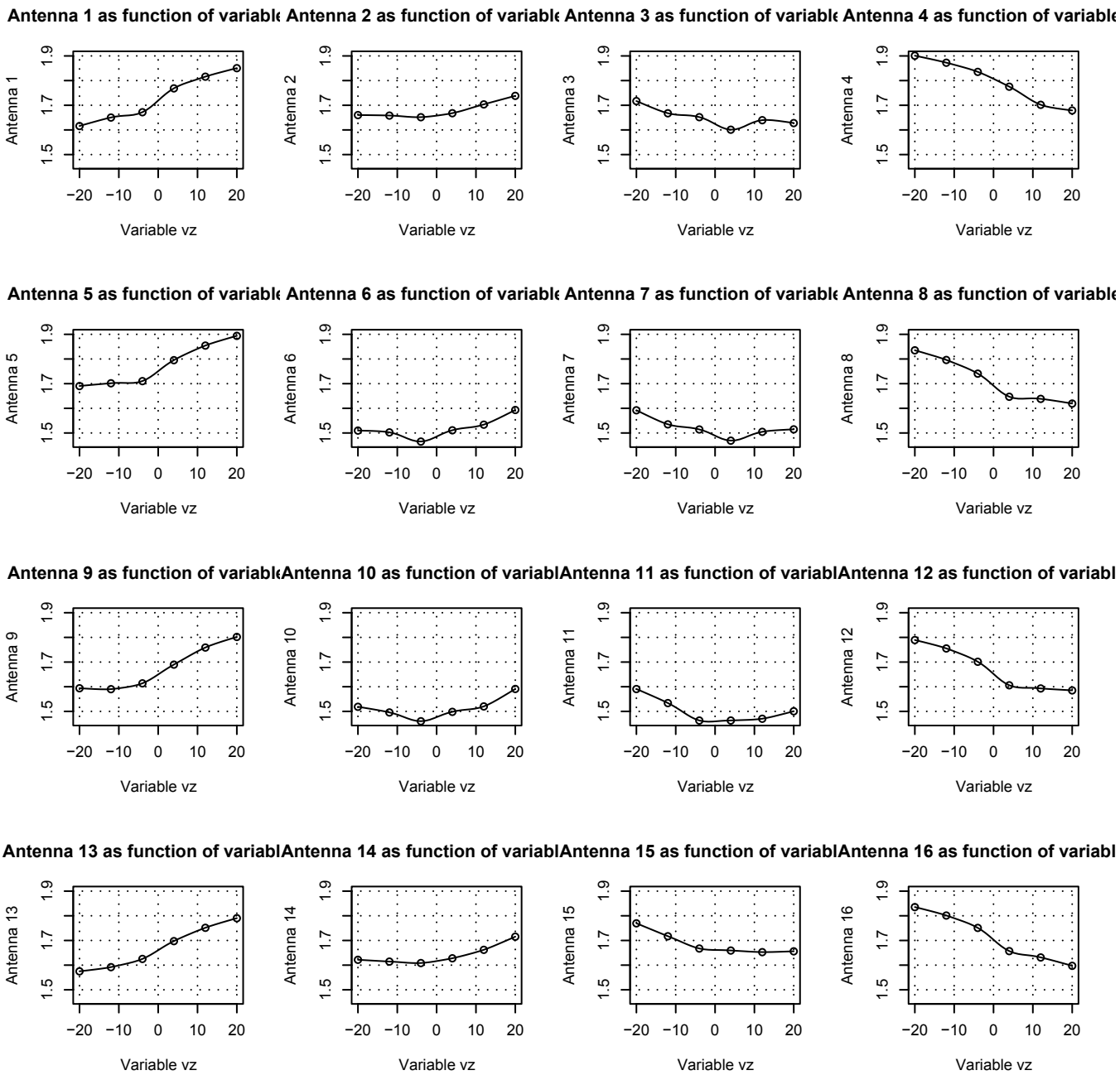
Antenna 1 as function of variable
Antenna 2 as function of variable
Antenna 3 as function of variable
Antenna 4 as function of variable
Antenna 5 as function of variable
Antenna 6 as function of variable
Antenna 7 as function of variable
Antenna 8 as function of variable
Antenna 9 as function of variable
Antenna 10 as function of variabl
Antenna 11 as function of variabl
Antenna 12 as function of variabl
Antenna 13 as function of variabl
Antenna 14 as function of variabl
Antenna 15 as function of variabl
Antenna 16 as function of variabl
Antenna 1
Antenna 2
Antenna 3
Antenna 4
Antenna 5
Antenna 6
Antenna 7
Antenna 8
Antenna 9
Antenna 10
Antenna 11
Antenna 12
Antenna 13
Antenna 14
Antenna 15
Antenna 16
1.5
1.7
1.9
−20
−10
0
10
20
Variable vz